Distribution of fat, selenium, mercury, cadmium, arsenic, and persistent organic pollutants in Atlantic Bluefin Tuna (*Thunnus thynnus*) and implications for sampling and food safety

By

Sigurd Øyan

Master thesis in environmental chemistry

Department of Chemistry

University of Bergen

&

Institute of Marine Research

2021

Distribution of fat, selenium, mercury, cadmium, arsenic, and persistent organic pollutants in Atlantic Bluefin Tuna (*Thunnus thynnus*) and implications for sampling and food safety.

Sigurd Øyan

http://bora.uib.no/

Abstract

The Atlantic bluefin tuna (ABFT)(*Thunnus thynnus*) has for a long time been absent off the Norwegian coast, but has started reappearing increasingly in the last decade. The ABFT has both high economic and cultural values, and is a large predatory pelagic fish at the top of the food chain known to accumulate high concentrations of contaminants. Eleven adult and wild ABFT (ranging from 230 to 307 cm straight fork length) caught along the Norwegian coast in the years 2018, 2019 and 2020 were sampled to investigate the content of fat, selenium, mercury, cadmium, arsenic and selected persistent organic pollutants. Ten cuts were sampled from edible tissue of each fish, including fillet, neck, tail, and fat samples. The levels and distributions of the analytes were used to suggest a reasonable and representative sampling procedure in ABFT and to assess food safety. Some samples provided challenges during homogenization. A cryo-mill was successfully used to improve the homogeneity, resulting in visually more homogenous samples and a decrease in the analytical relative standard deviations between parallels.

The concentrations and distributions of the investigated substances were mostly following the fat content, with strong negative correlation between fat and mercury (R^2=-0.45). The persistent organic pollutants were even stronger positively correlated with fat (R^2=0.56). The concentrations of the investigated persistent organic pollutants were high, with PCDD/F ranging from 1.2 ± 1.1 pg/g to 2.9 ± 2.3 pg/g, PCDD/F + dl-PCBs from 8.0 ± 8.4 to 23 ± 15 pg/g and PCB6 from 310 ± 21 to 100 ± 12 ng/g, highlights the importance of the present study. The concentrations of the trace elements ranged from 0.19 ± 0.090 mg/kg to 1.4 ± 0.50 mg/kg, 0.0093 ± 0.0043 mg/kg to 0.042 ± 0.022 mg/kg and 1.3 ± 0.33 mg/kg to 5.3 ± 0.86 mg/kg for mercury, cadmium and arsenic, respectively. A tail sample, cut five, could be shown to be representative for largest part of the fillet of the ABFT with respect to the investigated contaminants. Sampling an aggregate fat sample (cut one), tail sample (cut five) and lean red sample (cut ten) is suggested to investigate the contaminants in ABFT. Mercury and persistent organic pollutants are the two main contaminants limiting the consumption of ABFT muscle/fillet. For the tail sample, an intake of 136 grams and 37 grams would lead to an exceedance of the tolerable weekly intake (TWI) for mercury and PCDD/F + dl-PCBs, respectively. This same sample exceeded the maximum level set for trade in 36% of the fish for mercury and 17% of the fish for PCDD/F +dl-PCBs. However, a large variation in the investigated contaminants between fatty, lean and red muscle was found.

Acknowledgements

This master thesis in environmental chemistry was done at the University of Bergen (UiB) and at the Institute of Marine Research (IMR). The laboratory work was conducted at the IMR and I am grateful to the people responsible for the different labs who scheduled time for me, making this possible.

I would first and foremost like to thank my two supervisors Stig Valdersnes and Martin Wiech. You have both been very knowledgeable, enthusiastic, and accessible, making writing this thesis engaging.

For help with sample preparation, thank you to everyone at the sample reception laboratory. Thank you to André Marcel Bienfait for help with using the cryo-mill. For training with the metal & element and methylmercury determination, I would like to thank Berit Solli and Nina Margrethe Steinsvik. For training and help with total fat determination, thank you to Nawaraj Gautam and Georg Olsen. For good ideas in programming in R, thank you to Are Sæle Bruvold.

I would also like to extend my gratitude to everyone I have met while sampling fish through the recreational fishing project for their help, interest, and friendliness.

Last but not least, I would like to thank Peder Jakob Reksten for proof-reading and being a great friend, my fiancée Inga Rullestad for always being sympathetic and caring, and my parents for being supportive.

Terms

ABFT…….Atlantic Bluefin Tuna

AIC…….Akaike Information Criterion

ANOVA……..Analysis of Variance

ASQ……...American Society for Quality

BW……..…….Body Weight

CDC……..…Centers for Disease Control and Prevention

CONTAM……..…….Panel on the contaminants in the food chain

dl……...……Dioxin-Like

EC…….European Commission

ECoS…….…..Eberly College of Science

EFSA…….European Food Safety Authority

EPA…….…...Environmental Protection Agency

FAO……...Food and Agriculture Organization of the United Nations

Fiskeridirektoratet…….Norwegian Directorate of Fisheries

ICCAT…….……International Commission for the Conservation of Atlantic Tunas

ICP-MS……Inductively Coupled Plasma Mass Spectroscopy

IMR…….……...…….Institute of Marine Research

ISO……..International Organization for Standardization

JECFA..……Joint FAO/WHO Expert Committee on Food Additives

JHSPH…….…Johns Hopkins Bloomberg School of Public Health

LoD…….....….Limit of Detection

LoQ……..……...….Limit of Quantification

MeHg……..……...…...Methylmercury

ML…….……..Maximum level

MU……..….....Measurement Uncertainty

ndl……..…….....Non Dioxin-Like

NHS…….....National Health Services

NMKL……..Nordisk Metodikkomité for Næringsmidler

NOAA……...…National Oceanic and Atmospheric Administration

NRC…….. National Research Council

OIML……..…International Organization of Legal Metrology

PCB…….....……Polychlorinated Biphenyls

PCDD…….……...Polychlorinated Dibenzodioxins

PCDF……...Polychlorinated Dibenzofurans

POPs……..……...……..Persistent Organic Pollutants

RSD……...…….Relative Standard Deviation

SBFT…….…...Southern Bluefin Tuna

TEF……...…Toxicity Equivalency Factor

TEQ…….……..Toxic Equivalent

TWI……..……...…….……..…Tolerable Weekly Intake

UVA……..University of Virginia

WHO…….……World Health Organization

WW……...……..……..….Wet Weight

Table of Contents

1 Introduction

1.1 Background

The Atlantic bluefin tuna (ABFT) (*Thunnus thynnus* L) is a magnificent fish desired by fish-enjoyers and fishermen alike due to its uniquely rich taste, status and exclusivity. It is highly sought after particularly in Japanese sushi-sashimi cooking. However, even though the ABFT is a fish loved by many as a seafood-dish it is not without risk, and potential contaminants are of concern. Since the ABFT has a long lifespan and may reach substantial lengths and masses it can accumulate significant levels of contaminants(Annibaldi et al., 2019; Block et al., 2001; Chapman et al., 2011). Due to bioaccumulation and biomagnification, ABFT may pose a threat to human health. The maximum levels for trade in the EU are set by the European Commission and adapted by Norway. In this case, in commission regulation number 1881/2006, maximum limits are given in mg contaminant per kg wet weight (WW) edible tissue. For mercury, the standard maximum level is 0.5 mg/kg WW, for tuna however, (*Thunnus species, Euthynnus species* and *Katsuwonus Pelamis*) it has been set to 1 mg/kg WW (EC, 2006). Such maximum levels (ML) for trade may be set following assessments made by the European Food Safety Authority (EFSA) and their estimation of tolerable weekly intakes (TWI) that focus on the health aspect for a given contaminant (CONTAM, 2012).

In this work the contaminants of main concern are mercury, cadmium and persistent organic pollutants (POPs), which are frequently seen in high levels in fish and other seafood. These contaminants were investigated in ten muscle samples of edible tuna tissue taken from different parts of the fish including the belly, neck, back and tail. In 2018, the IMR conducted a limited preliminary investigation on contaminants in a few tuna-samples. Results from 2018 confirmed suspicions that ABFT may exceed given MLs for trade for certain contaminants in select samples (unpublished results).

1.2 Aim of the study

This study's overarching aim was to investigate the distribution of contaminants as well as fat and selenium in individual ABFTs. This information is important to evaluate if ABFT is safe for

consumption. In addition, it was desirable to investigate if it was possible to develop a future sensible sampling protocol that could be both representative for the entire fish while also being economically sound.

2 Theory

2.1 The Atlantic bluefin tuna

The Atlantic bluefin tuna is a pelagic fish and the largest of all tuna species. Tunas have fins with rays, making them part of the Actinopterygii class, also belonging to the order Scombriformes and are a subgroup of the mackerel family (*Scombridae*). The ABFT has very advanced traits, including but not limited to: two dorsal fins very anteriorly placed pelvic fins and fins with rays. The ABFT possesses remarkable traits such as the ability to reach masses of 700 kg, growing to up to 3 meters long and with a possible lifespan of more than 25 years (Block et al., 2001; Chapman et al., 2011). The ABFT is an exceptionally strong swimmer and it has been theorized to reach staggering velocities of 80 km/h (Wardle et al., 1989), and being able to dive to depths of around one kilometer (Block et al., 2001). In addition to the raw size and power of the fish, it possesses a unique trait in being endothermic, meaning it utilizes metabolic heat to elevate its body temperature up to more than 10°C above the temperature of the surrounding water (Carey, 1973; Graham & Dickson, 2001). Because of this raise in body temperature, the muscles can function at a higher capacity. The increased temperature allows the tuna to swim faster, farther and dive to the depths previously mentioned, in contrast to ectotherms (cold species). Being a large pelagic fish built for speed and activity, the ABFT (Figure 2.1.1) exhibits extensive migratory behavior.

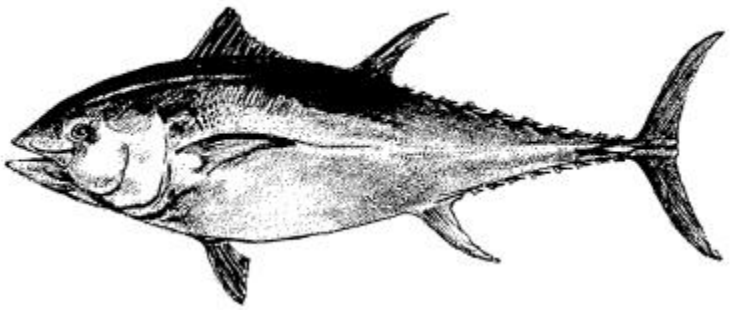

Figure 2.1.1 Illustration of an Atlantic bluefin tuna (*Thunnus thynnus*)(Mather et al., 1995).

Another interesting trait the tuna is thought to possess based on its migration patterns is naval homing, which describes the behavior of it migrating to specific areas for spawning (Fromentin & Powers, 2005). However, it is argued that this behavior in tunas is more akin to repeat homing which is related to spatial learning rather than imprinting (Fromentin & Powers, 2005).

The population of the ABFT is distributed throughout the Atlantic Ocean. It spans from the Gulf of Mexico and the east coast of the USA to the west coast of Africa all the way up to the Norwegian shoreline (Fromentin & Powers, 2005; Taylor et al., 2011). The international commission for the conservation of Atlantic tunas (ICCAT) has defined two separate stocks of ABFT based on the parameters: homing behavior, spawning site fidelity, genetic differentiation, and differing ages for reaching sexual maturity. These two stocks are the Eastern and Western Atlantic stock, separated by a 45°W meridian (Rodriguez-Marin et al., 2015). This is the operating model for the ABFT stock. The eastern stock is estimated to be larger by an approximate factor of ten, and more stable than the western one (Rodríguez-Ezpeleta et al., 2019; Rooker et al., 2007). It is important to note that this two-stock model has been criticized as it does not account for stock-mixing or perhaps the presence of more distinct stocks (Galuardi et al., 2010). Figure 2.1.2 shows Geographical distribution of ABFT with data from 1997 to 2014.

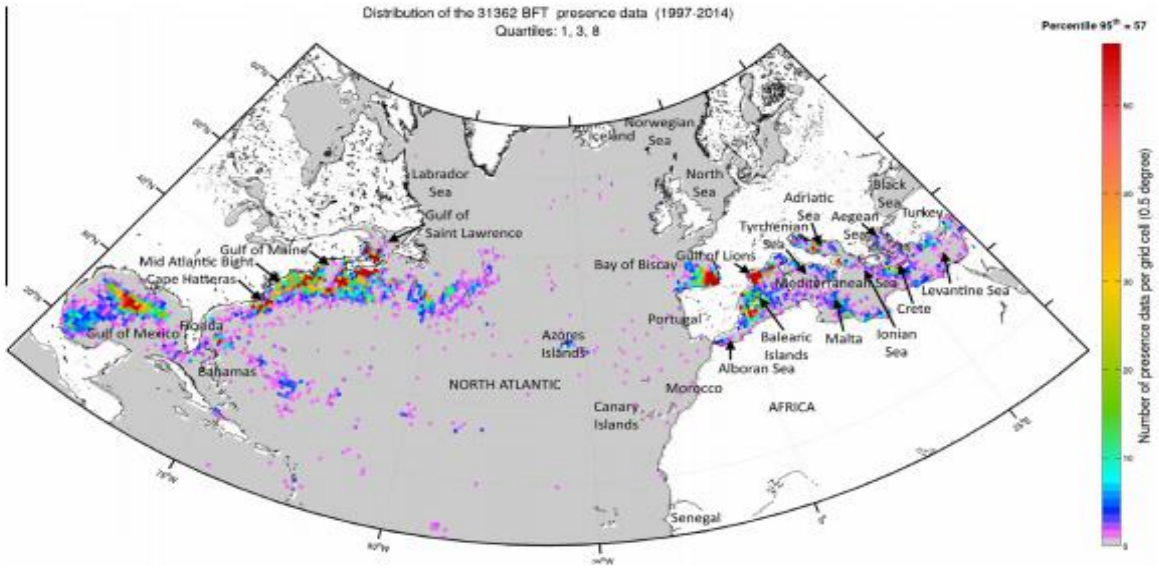

Figure 2.1.2 Geographical distribution of all Atlantic bluefin tuna (*Thunnus thynnus*) presence data (including data without weight information) collected in the period 1997 to 2014 (in number of observations by 0.5° grid cells) (Druon et al., 2016).

The ABFT has increased its financial importance over the last half century, as the value has gone up significantly. This began when Japanese food gained a lot of global attention starting in the 70's in the USA, followed by the rest of the world somewhat later. This is said to be caused by Japanese food being associated as "health-food" (Endo, 2013). In the 1980's exploitation of ABFT was made even more profitable with the rise of the sushi-sashimi, which commonly uses the bluefin tuna (Fromentin et al., 2014; Fromentin & Ravier, 2005). The current market value is very high, where one individual ABFT was sold for around 174,000 USD in 2001 in Tokyo (Fromentin & Powers, 2005), which at 202kg equates to around 861 USD per kilogram (ABCNews, 2006). The average price taken from marunaka (MARUNAKA, 2020) for *T. thynnus* from Japan was 3,080 Yen / kg which equals 27.88 USD / kg at the current rate.

2.2 Historical fishing of ABFT

The ABFT has been fished for a very long time. Archaeological excavations have shown that fishing of ABFT ranges back to as early as the 7th millennium BC, in the Mediterranean area. At early stages of ABFT-fishing (approximately 400 BCE) the equipment in use was mainly hand lines, harpoons, and seines, particularly beach seines (Figure 2.2.1). The catches yielded by this gear were at a relatively small scale (Fromentin & Powers, 2005; Mather et al., 1995).

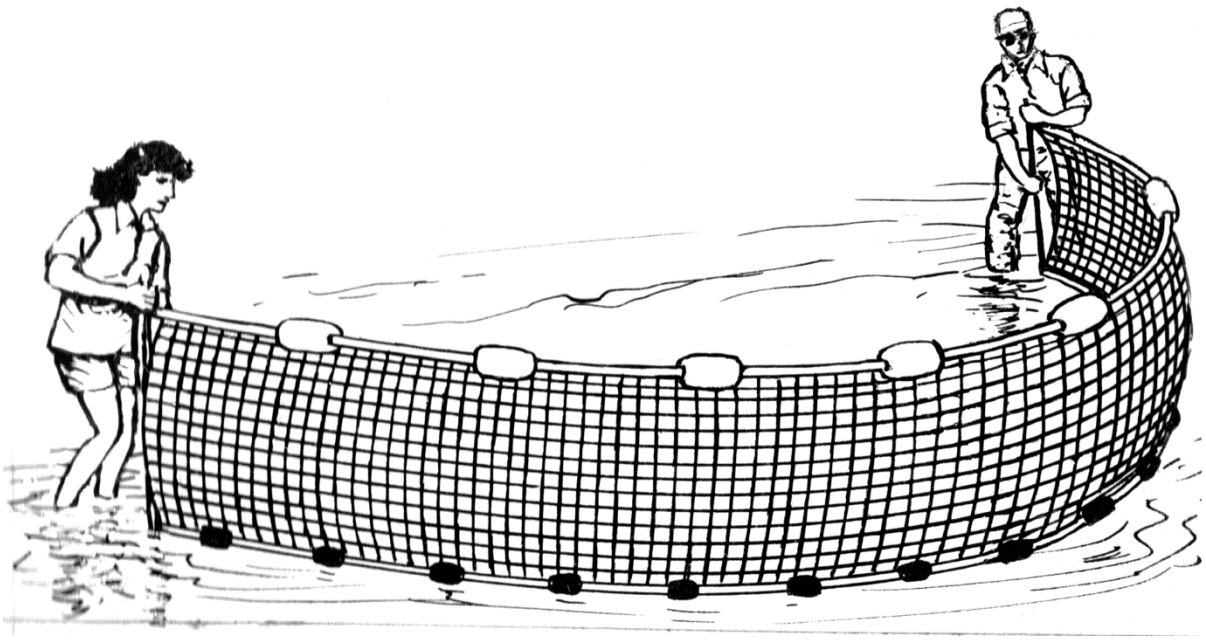

Figure 2.2.1 Illustration of basic seine net (Pearson-Scott-Foresman, 2010).

The historical evolution of ABFT fishery since the start has gone from hand seines and beach seines to traps (Figure 2.2.2), mainly during the period between the 16th and the 19th century (Fromentin & Powers, 2005; Ravier & Fromentin, 2001).

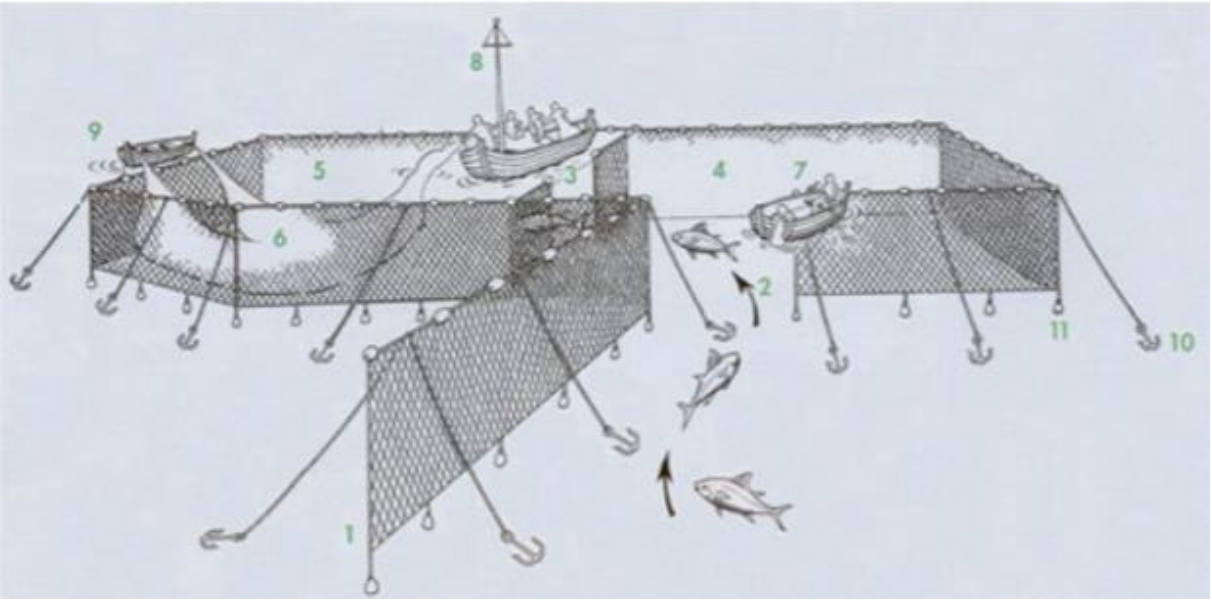

Figure 2.2.2 Illustration of small static tuna trap (Cattaneo-Vietti et al., 2015).

The biggest difference in seine, handline, and harpoon fishing compared to using traps is the operation-requirement by the fishermen. Where the aforementioned methods require a very hands-on approach, the traps can be set to passively catch fish. The estimated efficiency of traps given in annual average yield was 15,000 tons, fluctuating between 7,000 and 30,000 tons (Fromentin & Powers, 2005). The next big technological advance was seen after the second world war, namely in the introduction of three much more productive methods than the previously used ones in; live-bait, pelagic longline and purse seine (Figure 2.2.3) (Mather et al., 1995).

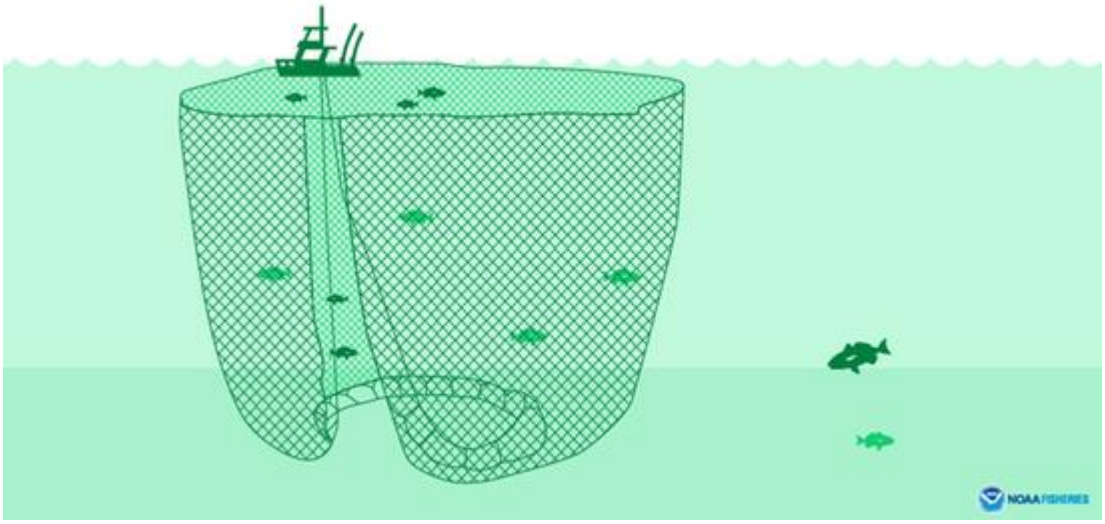

Figure 2.2.3 Illustration of purse seine vessel (NOAA, 2019).

In light of these changes, the French catch for example, increased from 600 tons in 1948 to 1,900-3,500 tons in the years 1950-1959. The catches however, declined the following decade to 400-1,600 tons (Mather et al., 1995). The Japanese longline fishery, which entered the Atlantic in 1956, had a rapid expansion, with an initial yearly catch of below 7,000 fish per year in the period 1956 to 1961. This grew to 53,000-67,000 fish per year in the years 1962-1965 (Mather et al., 1995).

Norway has a hundred-year-old history of fishing ABFT. A commercial tuna fishery was attempted established in 1920's, with little success. With the introduction of the purse seine in the late 1940's Norway became the number one ABFT fishing nation in Europe, catching up to 16,000 tons each year during the 1950's. This comprised around 80% of the total Nordic catch (Fromentin & Powers, 2005; Tangen, 2009). However, this new efficiency in ABFT fishing brought with it the issue of over-fishing and by 1970 the catches were significantly reduced with catches around 12,000 tons (Fromentin & Powers, 2005), and after 1987 the species were virtually gone from the Norwegian coast (Tangen, 2009).

During the 1990's and 2000's the fishing efficiency and capacity of fleets rose, especially in the Mediterranean Sea. In this period a new farming technique was introduced as well, which is called "fattening". In this technique a school of tuna is caught using purse seine vessels and are thereafter transported to floating cages where they are fed oily pelagic fish. This is mainly motivated by the rise of Japanese interest in the fish due to their sushi-sashimi industry as previously mentioned

(FAO, 2021). Lastly the storage capacity for ABFT also rose in this period, which in addition to the other factors mentioned resulted in critical overexploitation of the fish (Fromentin et al., 2014; Fromentin & Ravier, 2005).

2.3 Regulations and fishing now

Because the bluefin holds both cultural and monetary value it is of great interest to both map out and properly regulate it for a healthy and sustainable fishery. The extent of overfishing has been the focus of several studies. A study that produced a model to estimate historical populations of ABFT postulates that populations of the western and eastern stocks have fallen to 17% and 33% of their 1950 spawning stock biomass, respectively (Taylor et al., 2011). This is a critical drop in the amount of tuna available in the Atlantic. To mitigate this overexploitation, the International Commission for the Conservation of Atlantic Tunas (ICCAT) was established (LOVDATA, 1969). ICCAT desires to co-operate in maintaining the populations of tuna and tuna-like fishes found in the Atlantic ocean, at levels which will yield the maximum sustainable catch for food and other purposes (ICCAT, 2017). The scientific body of ICCAT raised serious concern about the ABFT stock since the early 90's and estimated it to be overexploited by 1996. From 1998 and onwards a total allowable catches (TAC), together with size limit regulations and time/area closures, were progressively implemented. From the late 90's to 2008 however, ICCAT recommended a TAC higher than the scientific recommendation (Fromentin et al., 2014).

By 2007 the stocks were officially recognized as overexploited by International Commission for the Conservation of Atlantic Tunas (ICCAT, 2008, 2010) which resulted in more restrictions on fisheries: fishing season was shortened, minimum weight was increased from 10kg to 30kg and a more effective monitoring control was implemented (Fromentin et al., 2014). Rebuilding quotas were also introduced, which logically are quotas that allow for the stock to rebuild without subsiding to catch the fish. The quotas set are 1,750 and 12,900 tons for the western and eastern Atlantic respectively (Taylor et al., 2011). The 2008 plan reinforced the previous plan, but set the TAC two to three times higher than scientific advice which lead to the eastern stock of bluefin tuna's nomination for protection under the Convention on International Trade in Endangered Species of flora and fauna (CITES) in 2009 (Webster, 2011). Rebuilding quotas were set as a result of this nomination. Some of the issues regarding stock management are illegal, unreported and

unregulated (IUU) catches and bycatches. The main source of ABFT bycatch of the western stock is the pelagic longline in the Gulf of Mexico. This longline fishing targets other species such as yellowfin tuna and swordfish (Teo & Block, 2010). Figure 2.3.1 shows the reported catches, total allowable catches, IUU catches and scientific advice for the eastern stock of ABFT from the years 1992 to 2012. This provides an interesting look at the strength of the stock and regulations set in place as well as the scientific opinion on the matter.

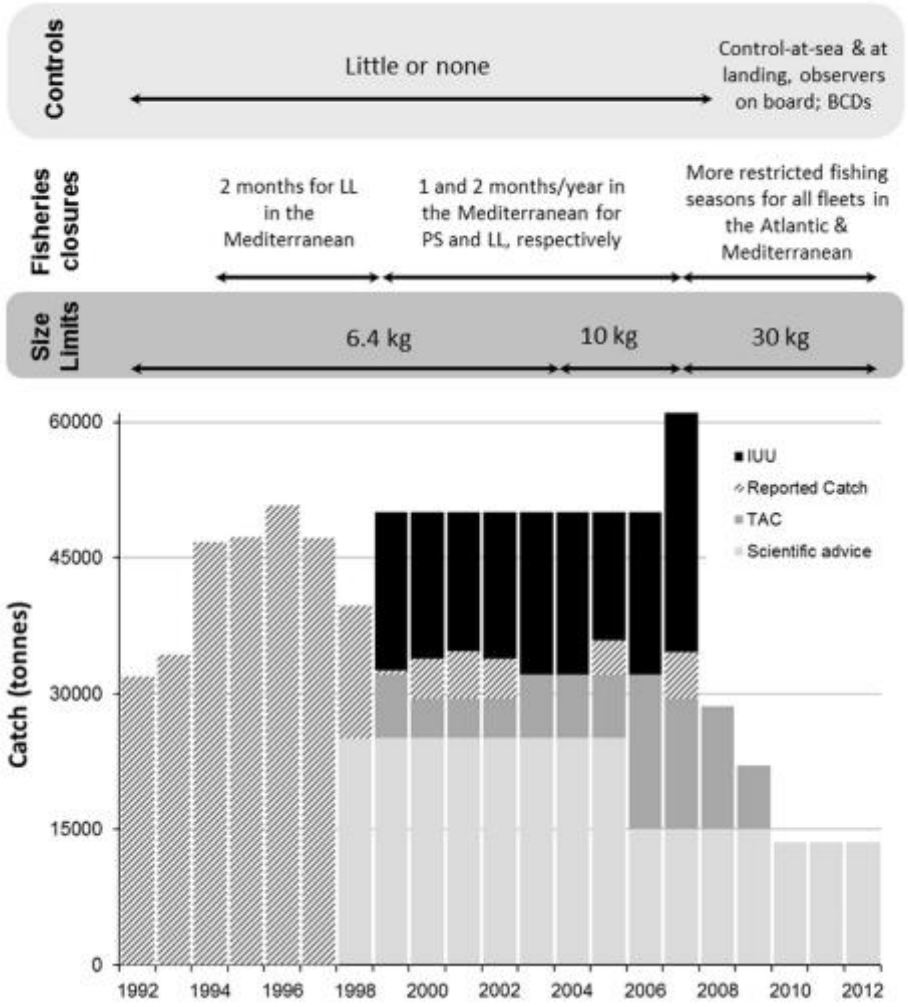

Figure 2.3.1 Catch levels of Atlantic bluefin tuna (*Thunnus thynnus*) recommended by the ICCAT scientific community, Total allowable Catches (TAC) decided by ICCAT reported catches, and the illegal unreported unregulated (IUU) catches from 1992 to 2012 for the eastern stock (Fromentin et al., 2014).

2.4 Recreational fishing project

The cuts taken in this study are large and many, making it unviable to sample from fish sold to the food industry as they want the carcass intact. Taken the price per kilogram and size of an individual ABFT into account, it was not reasonable to purchase several fish for the purpose of performing this study.

In 2020, 24 approved recreational fishing teams in Norway got a license from the Norwegian Directorate of Fisheries (Fiskeridirektoratet) to harvest 1 tuna per season, and anglers were asked to provide meat samples for the present study. Five tons of Norway's 2020 quota of 3012 tons was allocated to this project.

2.5 Analytes

As mentioned before there is great interest in preserving and maintaining ABFT for a healthy and sustainable fishery. On the other hand there are concerns related to the presence of harmful substances in ABFT that might have an impact on food safety. These harmful substances are called contaminants and can exist in very small amounts in all food. EU defines a contaminant as "any substance not intentionally added to food which is present in such food as a result of the production (including operations carried out in crop husbandry, animal husbandry and veterinary medicine), manufacture, processing, preparation, treatment, packing, packaging, transport or holding of such food, or as a result of environmental contamination. Extraneous matter, such as, for example, insect fragments, animal hair, etc, is not covered by this definition" (EC, 1993). Contaminants addressed in the present study are trace elements and persistent organic pollutants (POPs).

The definition of a trace element in analytical chemistry is "any element having an average concentration of less than about 100 parts per million atoms (ppma) or less than 100 µg/g" (Chavoshani et al., 2020). Some elements are essential in trace amounts, and the American Chemical Society defines them as follows: "An element is considered essential when a deficient intake produces an impairment of function and when restoration of physiological levels of that element relieves the impaired function or prevents impairment. The organism can neither grow nor complete its life cycle without the element in question. The element should have a direct influence on the organism and be involved in its metabolism. The effect of the essential element cannot be

wholly replaced by any other element" (Frieden, 1985). An important aspect to consider when discussing essential elements is that they have an inherent toxic effect either when in deficit, but also when in too high doses (Figure 2.5.1).

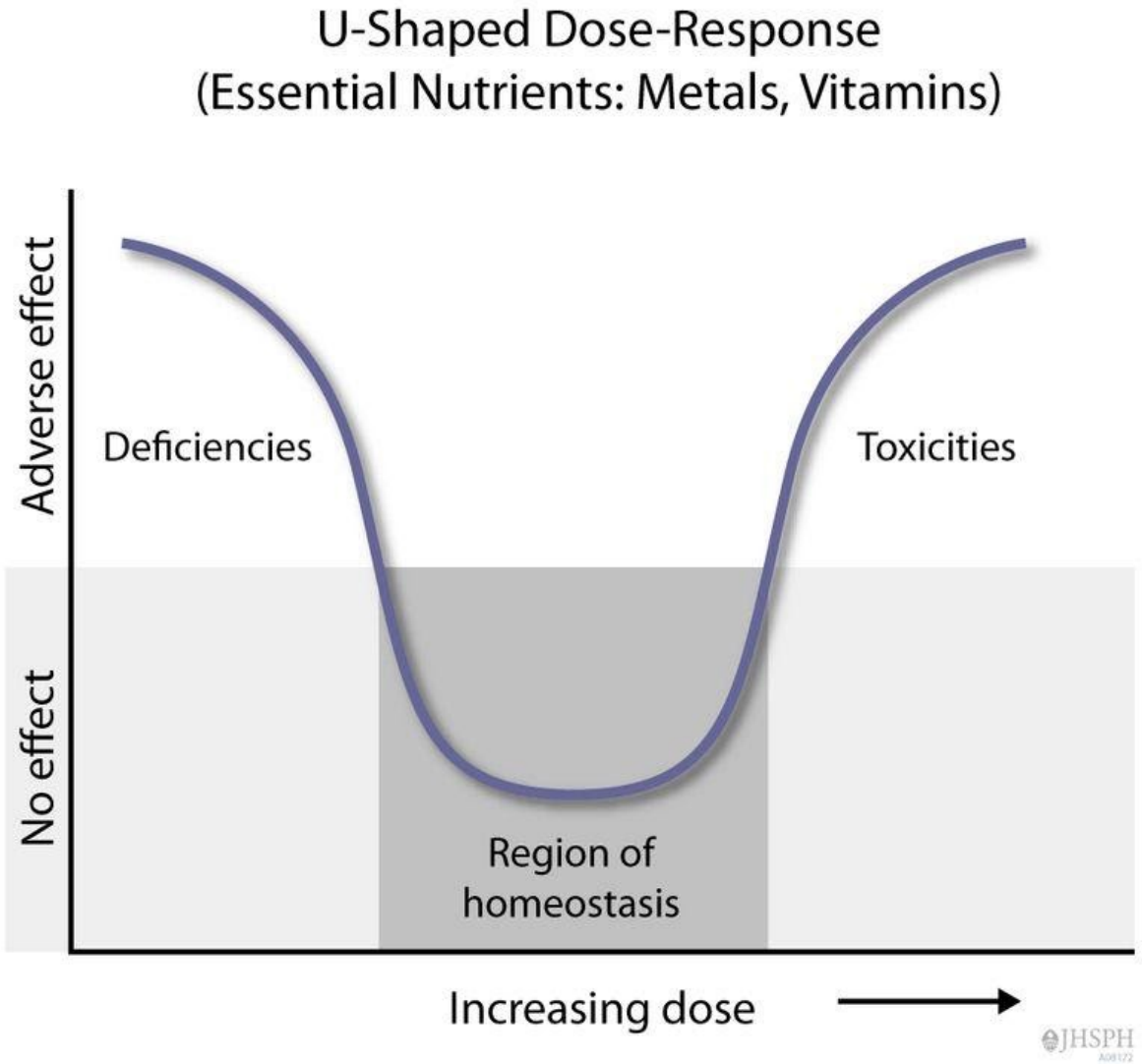

Figure 2.5.1 U-shaped dose response curve regarding essential nutrients such as metals and vitamins (JHSPH, 2021).

2.5.1 Fat content

Fat content was included as an analyte to investigate its relationship to the different contaminants in the edible tissue of ABFT. It is well known that mercury accumulates in protein rich tissue, and POPs accumulates in lipid-rich tissue. Moreover, fatty tuna tissue containing poly-unsaturated fatty acids, and a high ratio of omega-3 to omega-6 fatty acids, are beneficial to human health (Albert et al., 2002; Økland et al., 2005; Truzzi et al., 2018).

2.5.2 Selenium

Selenium (atomic number 34) is a nonmetal/metalloid found in the p-block and is an essential element in humans as it is incorporated in many pleiotropic effects (producing/having multiple effects from a single gene) ranging from antioxidant and anti-inflammatory effects to the production of active thyroid hormone (Rayman, 2012). Regarding contaminants, selenium is of special interest due to its interaction with mercury, where it is known that selenium can counteract the toxicity presented by mercury. The protective effect of selenium to mercury toxicity is not completely ascertained, and several reasons have been suggested (Azad et al., 2019). The most likely mechanism is the high binding affinity of mercury to selenium, where methylmercury covalently binds to selenium in the active sites of selenium dependent enzymes, inhibiting their activity (Ralston et al., 2008). It is possible to numerically assess selenium's protective effect by calculating the molar ratio of selenium to mercury (Se:Hg), where under the assumption that all Hg is bound by Se, values over 1:1 are suggested to be protective (Kljaković-Gašpić & Tičina, 2021). The molar ratio of selenium to mercury was calculated by dividing their concentrations in mg/kg by their atomic weights of 200.59 g/mol and 78.96 g/mol, respectively.

However, some trace elements can also have an exclusively toxic effect depending on their species, and the most common of these substances are the focal points of this study. A toxic trace element is an element that can elicit a toxic effect even in trace amounts. In this study the levels of the toxic trace elements of mercury (and the more toxic specie methylmercury), cadmium, lead and arsenic are investigated. These trace elements have caused major human health problems in several parts of the world (Hutton & Meema, 1987).

2.5.3 Mercury

Mercury (atomic number 80), also known as quicksilver, is a heavy metal located in the d-block in the periodic table. Elemental mercury is a shiny silver-white odorless liquid and becomes a colorless and odorless gas when heated (Jaishankar et al., 2014). Mercury is a metallic element that occurs naturally in the environment and is also introduced by anthropogenic activities e.g. mining and burning of coal. There are three primary categories of mercury and its compounds: elemental/metallic mercury (Hg^0), inorganic mercury (I-Hg) and organic mercury compounds,

primarily methyl mercury (Me-Hg) (Guzzi & La Porta, 2008). Elemental Hg that enters our oceans, lakes and rivers is first oxidized to inorganic mercury by combining with other elements such as sulfur or oxygen, to form compounds or salts (CDC, 2009). The inorganic salts are methylated to MeHg by aquatic biota and photo-methylation, and further bioaccumulates in aquatic food webs (Figure 2.5.3.1) (Lehnherr et al., 2011).

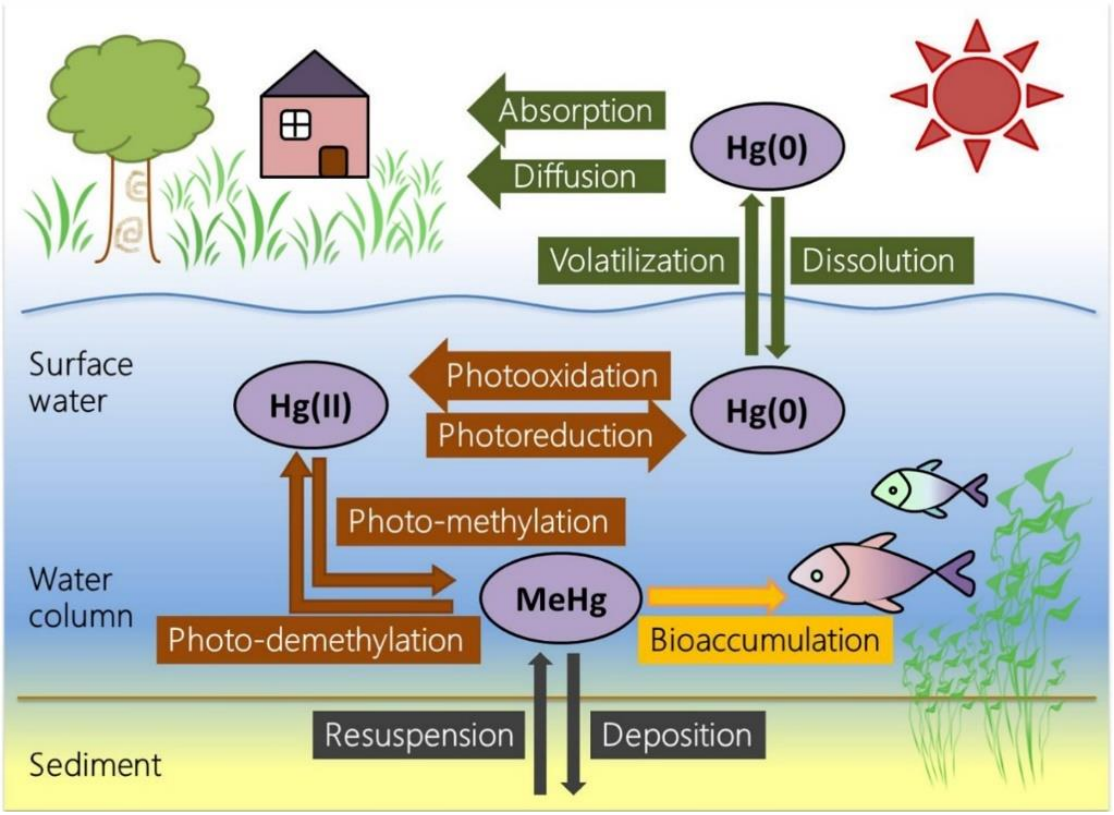

Figure 2.5.3.1 Illustration of mercury's fate in into and in the aquatic environment (Luo et al., 2020).

MeHg is the mercury specie that bioaccumulates and biomagnifies, and is the most toxic (Hong et al., 2012). Humans and wildlife are exposed to MeHg primarily through the consumption of contaminated fish, particularly large predatory fish such as tuna and swordfish (Fisher, 2003; NRC, 2000). Making mercury the most relevant toxic trace element of this study. The clinical manifestations of mercury poisoning are varied and mimic many other conditions. One symptom is central nervous system toxicity, which includes inability to concentrate, encephalopathy, peripheral neuropathy, parkinsonian symptoms, tremors, ataxia, impaired hearing (ototoxicity),

among others. There are also a range of symptoms regarding renal, gastrointestinal and dermal toxicity (Hyman, 2004). The specific mechanism of this toxicity is primarily focused on the brain. However, mercury can impair any organ and lead to malfunctioning of nerves, muscles or organs, like kidney. Mercury can also disrupt cellular membrane potential and the calcium homeostasis. In addition to the above mentioned affinity to selenium, mercury has a particular affinity for sulfhydryl (thiol; -SH) (Ajsuvakova et al., 2020). When methyl mercury binds to selenohydryl and sulfhydryl group creating RSeHgMe and RSHgMe, respectively, it is capable of damaging tertiary and quaternary proteins structures, hampering the cellular structure. The processes of translation and transcription of genes is also affected potentially leading to the disappearance of ribosomes and eradication of endoplasmic reticulum as well as the activity of natural killer cells. The cellular integrity is impacted, leading to the formation of free radicals, which is known to lead to an increase in oxidative stress experienced by the body (Figure 2.5.4.1) (Jaishankar et al., 2014).

2.5.4 Lead

Lead (atomic number 82) is found in the p-block in the periodic table, appearing in elemental form as a solid, soft and malleable metal at standard temperature and pressure (Mason et al., 2014). Lead is one of the most ubiquitous heavy metals and has been detected in virtually all phases of the environment. Lead is introduced into the environment naturally through volcanic explosions and forest fires. Non-natural, anthropogenic sources mainly include emissions from the industry and transportation (Zhang et al., 2015). The toxic effects of lead may involve several organ systems within the body and vary from subtle biochemical effects to overt effects such as lead poisoning (Juberg et al., 1997). The major health effects manifest itself in three organ systems: hematological system, central nervous system and renal system (Hutton & Meema, 1987). Specifically, like one of the mechanisms for toxicity by mercury, lead can also lead to the formation of free radicals. This increases the oxidative stress, potentially damaging the cell, or in the worst case leading to apoptosis (cell death) (Figure 2.5.4.1).

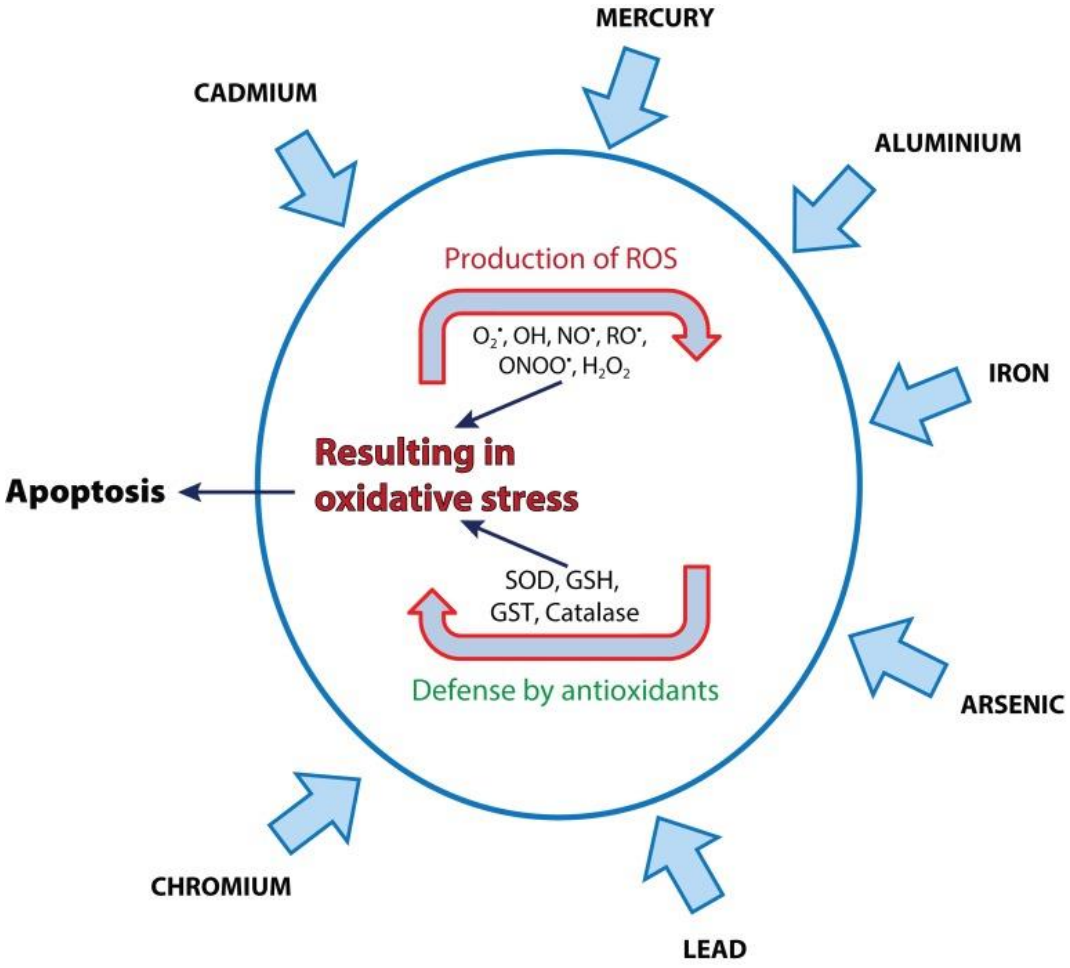

Figure 2.5.4.1 Attack of several heavy metals on a cell resulting in the increase of reactive oxygen species and defense presented by antioxidants (Jaishankar et al., 2014).

2.5.5 Cadmium

Cadmium (atomic number 48) is in its elemental form a silvery-white, soft and ductile metal (Sharma et al., 2015) found in the d-block on the periodic table. Volcanic action is considered to be the major natural source of cadmium in the atmosphere. This is related to the very large quantities of particle matter emitted, together with the high enrichment of cadmium in volcanic aerosols (Hutton, 1983). Nonferrous metal mines, particularly those which exploit lead-zinc ore fields, are a significant source of environmental cadmium (Hutton, 1983). Cadmium is used in things like Ni-Cd batteries, pigments for plastics, ceramics and glasses (Faroon et al., 2013). It is also widely used in industrial processes as an anticorrosive agent (Godt et al., 2006). Cadmium exposure can result in a variety of adverse effects, such as renal and hepatic dysfunction,

pulmonary edema, testicular damage, osteomalacia, and damage to the adrenals and hemopoietic system (Genchi et al., 2020). The kidney is the critical organ of intoxication after long-term exposure to cadmium, with one of the initial signs as increased urinary excretion of proteins (Hutton & Meema, 1987). Similarly to mercury, cadmium's critical targets are the thiol groups (-SH) of cysteines present in proteins (Genchi et al., 2020). Long term exposures to cadmium may cause carcinogenic effects in humans, where normal epithelial cells transform into malignant cells inhibiting biosynthesis of DNA, RNA and proteins (Sharma et al., 2015; Waalkes, 2003). Cadmium is classified as the seventh most toxic heavy metal per ATSDR (Agency for Toxic Substances and Disease Registry) ranking (Jaishankar et al., 2014).

2.5.6 Arsenic

Arsenic (atomic number 33) is found in the p-block in the periodic table. Arsenic is classified chemically as a metalloid, having both properties of a metal and nonmetal. Elemental arsenic is a grey solid metal. However, arsenic is usually found in the environment combined with other elements such as oxygen, chlorine, and sulfur. These combinations with arsenic are called inorganic arsenic. Arsenic combined with carbon is organic arsenic. Most inorganic and organic compounds are white or colorless powders, and odorless that do not evaporate (Chou & Harper, 2007). Like lead, it is also is ubiquitous in nature, and humans are exposed to it via air, ground water and food sources. Arsenic occurs naturally in soil and minerals, occurring as a major constituent in more than 200 minerals including elemental arsenic, arsenides, sulfides, oxides, arsenates and arsenites (Chou & Harper, 2007; Garelick et al., 2009). The toxicity of arsenic compounds varies widely depending on chemical form of the element. Inorganic forms of arsenic such as arsenite (As(III)) and arsenite (As(V)) are highly toxic to humans and animals (Donohue & Abernathy, 1999). The largest portion of arsenic in seafood is, however, usually present as arsenobetaine, which is an organic form considered to be non-toxic (Francesconi & Kuehnelt, 2004). In fish filet, the fraction of inorganic arsenic has been reported very low (usually <1% of total arsenic) (Julshamn et al., 2012). The inorganic forms are highly carcinogenic and can cause cancer of the lungs, liver, bladder and skin (Jaishankar et al., 2014). Chronic arsenic toxicity is termed arsenicosis, which mainly focuses on skin manifestations. The specific symptoms indicating chronic arsenic toxicity are pigmentation and keratosis of the skin (Jaishankar et al., 2014; Martin & Griswold, 2009).

2.5.7 Persistent organic pollutants

The last group of foreign substances looked at in this study are persistent organic pollutants (POPs). POPs are a group containing very many substances, one characteristic they share is that they have long half lives in soils sediments, air and biota (Jones & De Voogt, 1999), and are hence characterized as persistent. Most POPs are also generally lipophilic and tend to avoid water. This means that in aquatic systems and soils they partition strongly to solids, notably organic matter. In an individual organism they partition into the lipids and become stored in fatty tissue (Jones & De Voogt, 1999). In this work the POPs investigated were polychlorinated dibenzodioxins (PCDD), polychlorinated dibenzofurans (PCDF), dioxin-like polychlorinated biphenyls (dl-PCBs), non-dioxin-like polychlorinated biphenyls (ndl-PCBs) and polybrominated diphenyl-ethers (PBDE). In total there are 7 PCDDs, 10 PCDFs and 12 dl-PCBs which are considered dioxins or dioxin-likes by the World Health Organization (WHO) (Van den Berg et al., 2006). The United States Environmental Protection Agency states that POPs include substances that are either intentionally produced for agriculture, disease control manufacturing or industrial processes, or unintentional products of industry. The intentional group contains for example polychlorinated biphenyls (PCBs), used in electrical transformers and large capacitors, as hydraulic and heat exchange fluids, and as additives to paints and lubricants. The unintentional group contains dioxins that result from industrial processes and combustion, like municipal and medical waste incineration and backyard burning of trash (EPA, 2009).

Dioxins

The group of chemicals denoted as dioxins are all derived from 1,4 dioxin (Figure 2.5.7.1).

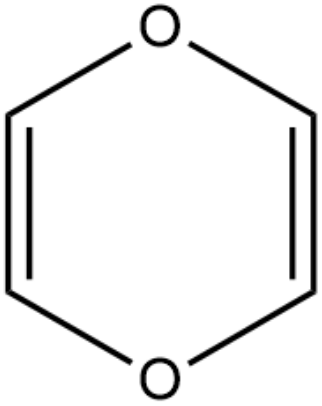

Figure 2.5.7.1 Structure of 1,4 dioxin. Created using ChemDraw®.

The term dioxins however, generally refers to the family of chemicals known as polychlorinated dibenzodioxins (PCDDs) (Figure 2.5.7.2). When the term dioxin is used in singular it often refers to the most toxic PCDD called 2,3,7,8-Tetrachlorodibenzodioxin (TCDD) having the general form as PCDD, with a tetra-substitution of chlorine atoms.

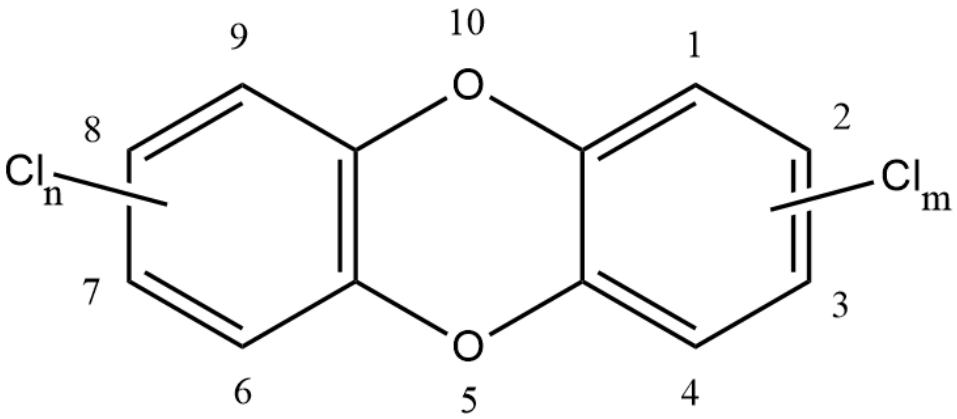

Figure 2.5.7.2 General structure of polychlorinated dibenzodioxins (PCDDs). Created using ChemDraw®.

Furans

The group denoted as furans contain the base structure of furan (Figure 2.5.7.3).

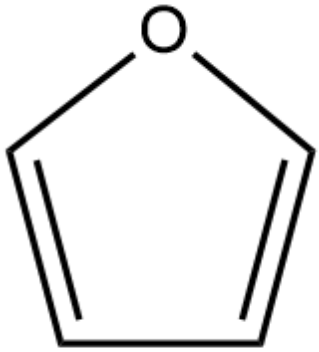

Figure 2.5.7.3 Structure of furan. Created using ChemDraw®.

The group polychlorinated dibenzofurans (PCDFs) denote the substances with the general structure shown in Figure 2.5.7.4.

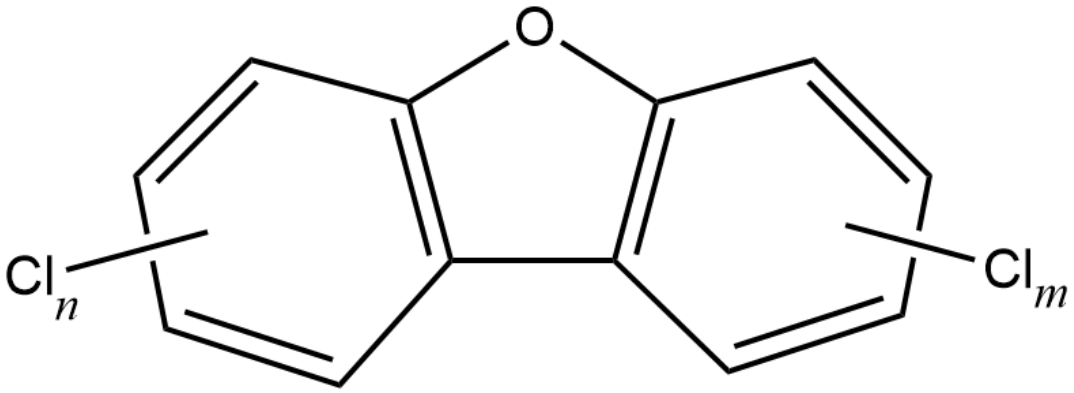

Figure 2.5.7.4 General structure of polychlorinated dibenzofurans (PCDF). Created using ChemDraw®.

Polychlorinated biphenyls (PCBs)

PCBs are a large family of 209 possible congeners, where 12 congeners are considered dioxin-like, and the remaining are non dioxin-like. General structure of PCBs is shown in figure 2.5.7.5.

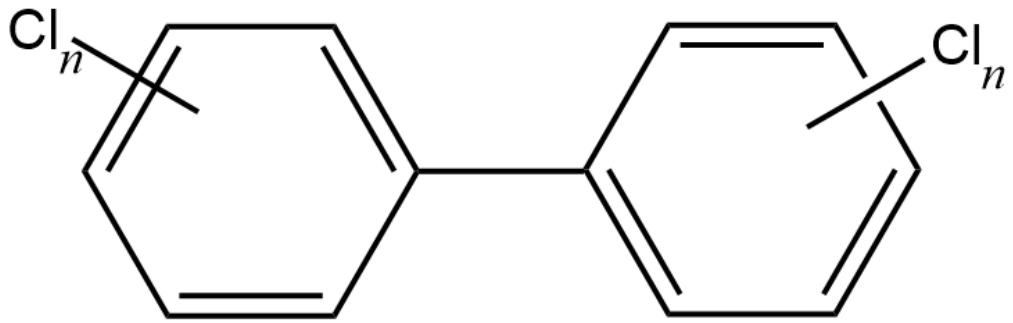

Figure 2.5.7.5 General structure of polychlorinated biphenyls (PCBs). Created using ChemDraw®.

Given the fact that the two rings are connected by a single bond the planarity of the different PCB congeners vary. This is based on the substitution pattern of chlorine atoms on the rings, as steric effects will orient the rings in a way that gives the least amount of stress on the molecule. The toxicity of the PCBs are affected by their shape, conformation and specifically, planarity. The PCBs which can achieve a planar conformation resemble dioxins in stereochemistry and dioxin effect on the human body and they are therefore called dioxin like-PCBs (dl-PCBs). The dl-PCBs are the mono-ortho and non-ortho substituted PCBs. The PCBs that cannot achieve planar conformation are consequently called non dioxin like-PCBs (ndl-PCBS). Figure 2.5.7.6 illustrates planarity based on chlorine substitution.

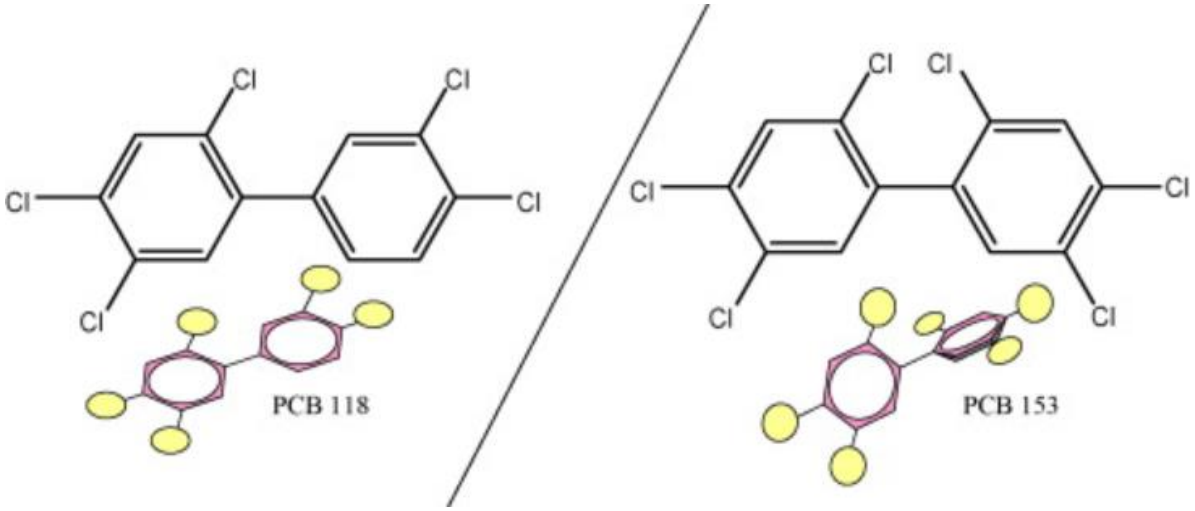

Figure 2.5.7.6 Comparison of the dioxin-like PCB 118 and the non dioxin-like PCB 153, showing different substitution and its effect on planarity (Gutleb et al., 2010).

The main mechanism of action by dioxins and dl-PCBs is the activation of the Aryl hydrocarbon Receptor (AhR) which is a ligand-based cellular transcription factor (White & Birnbaum, 2009). In humans dioxin exposure may cause cardiovascular disease, diabetes, cancer, porphyria, endometriosis and early menopause among other things (White & Birnbaum, 2009).

Polybrominated diphenyl ethers (PBDEs)'s general structure is shown in figure 2.5.7.7. The concentrations of PBDEs have not been assessed as there is no maximum level or tolerable weekly intake set.

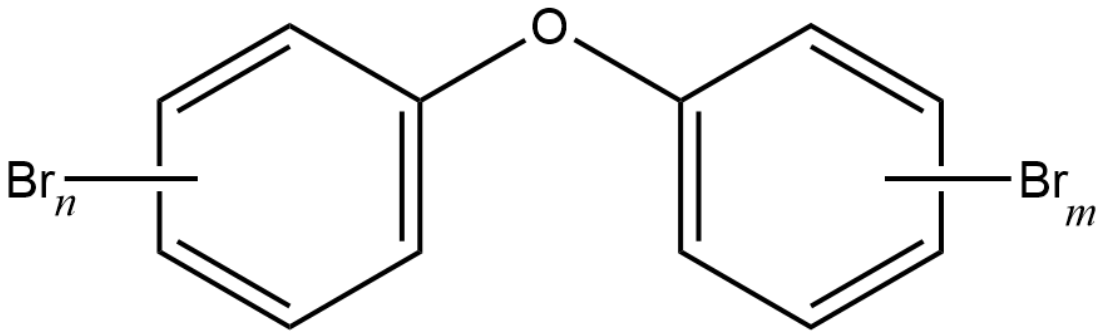

Figure 2.5.5.7 General structure of polybrominated diphenyl ethers (PBDEs). Created using ChemDraw®.

2.6 Risk assessment and risk management

This study focuses on the food safety of ABFT. One possibility to assess this is by measuring the different contaminants' mass fractions and compare them to existing maximum levels (ML) for the specific substances. An ML is the highest level of substance that is legally tolerated in food given by an authority. Setting maximum levels is a rather involved process starting with data collection, followed by risk assessment and risk management. Formally, the process starts with a request from political authorities to risk assessment organizations. Initially, data on occurrence and intake are gathered to conduct an assessment on the specific substance. A principle applied in this process is "as low as reasonably achievable" ALARA, stating that even if it is a small dose, if receiving that dose has no direct benefit, you should try to avoid it (CDC, 2015). The data obtained on contaminants' mass fractions is then used to calculate exposure and tolerable weekly intake (TWI). Some of the organizations responsible for these risk assessments are the Joint Expert Committee on Food Additives (JECFA), the European Food Safety Authority (EFSA) and Norwegian Scientific Committee for Food and environment (VKM), on a global, European and Norwegian level, respectively. Tolerable weekly intake (TWI) is a measure of dietary exposure to a certain contaminant that can be ingested weekly over a lifetime without appreciable health risk (Horiguchi et al., 2004). This is usually given in weight (µg) contaminant per weight (kg) bodyweight. TWI is not to be confused with AWI (acceptable weekly intake), where TWI is used for substances that are not deliberately added (contaminants) and AWI for substances deliberately added (additives).

When the exposure and tolerable weekly intake have been assessed, the management part of the process starts. Several organizations are in charge of reviewing the assessments made in addition to actively managing the risks associated with the substances. These organizations are Codex, the European commission and the Norwegian Food Safety Authority, at global, European and Norwegian levels, respectively. The management may consist of giving dietary advice or setting the maximum allowed levels for certain additives/contaminants in foodstuffs. An example of a document regarding maximum levels for contaminants in foodstuffs in Europe is Commission Regulation (EC) 1881/2006 (EC, 2006). These maximum levels are often given in weight (µg) contaminant per wet weight (kg) food. After the content of a certain contaminant has been determined in a foodstuff it is desirable to compare this value to its maximum level. Thus, the

results from analytical methods serve as basis of objectively determining whether the tuna is fit for human consumption and if so, further assess how much an individual of a given bodyweight safely can consume per week.

2.7 Sampling, sample preparation and analyses

2.7.1 Sampling

Representative tissue sampling of ABFT and other large tuna species can be challenging. Different studies have done this in different ways. Most studies that sample large tuna fish are mainly concerned with mercury determination. Kljaković-Gašpić et. al. presented a study similar to the present one: "Investigating mercury and selenium levels in archived samples of wild Atlantic bluefin tuna from the Mediterranean Sea" (Kljaković-Gašpić & Tičina, 2021). The samples taken were from the liver, gills, white muscle from behind the head, white muscle form middle dorsal part, white muscle from the tail and red muscle from the middle. This totaled in two organ samples and four muscle samples. A study from the Italian Journal of Food safety from 2020 by Piras et. al. aimed to verify the effective uneven distribution of mercury in various muscles and also identify the sites representative of the entire carcass (Piras et al., 2020). This study took seven samples from the entire carcass (Figure 2.7.1.1).

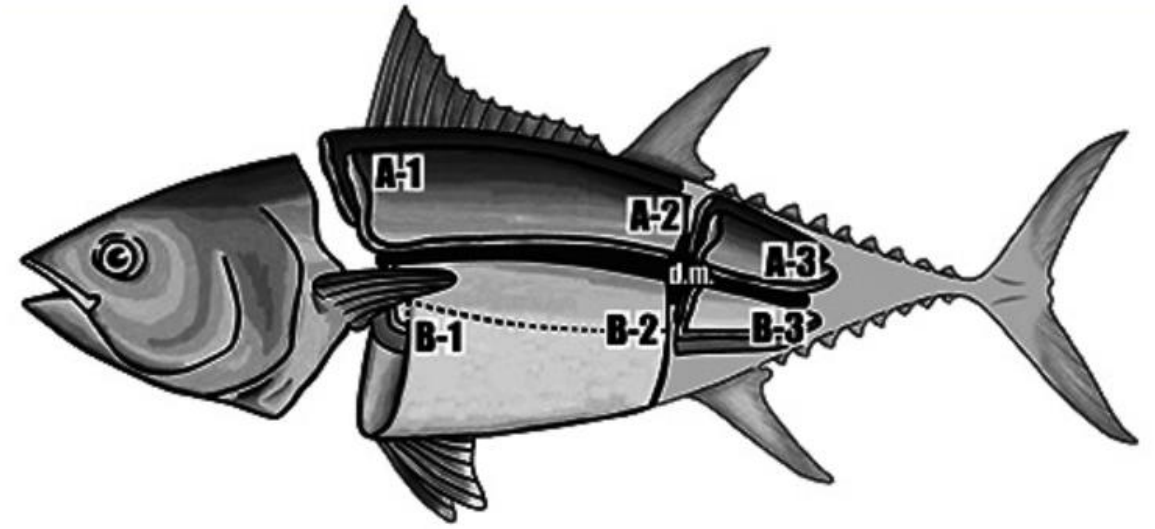

Figure 2.7.1.1 Scheme of the sampling points selected for the analysis of Hg in bluefin tuna caught by traditional static tuna traps in the Mediterranean. With "A" is indicated the upper loin points (epaxial muscles), with "B" the full-thickness lower loin points (all hypaxial muscles, including belly flap) and with "d.m." the dark muscle (Piras et al., 2020).

Similar studies have also been carried out on different, but related tuna species, such as Balshaw et. al. on the southern bluefin tuna (SBFT) *Thunnus maccoyii* (Mercury distribution in the muscular tissue of farmed SBFT (*Thunnus maccoyii*) is inversely related to the lipid content of the tissue) (Balshaw et al., 2008) and Bosch et.al. on Yellowfin tuna *Thunnus albacares* (Mercury accumulation in Yellowfin tuna (*Thunnus albaraes*) with regards to muscle type, position and fish size) (Bosch et al., 2016). Balshaw investigated samples as shown in figure 2.7.1.2, and further divided the samples into akami portions from cuts 1-6, chu-toro from 1-6 and o-toro from 4-5. Cross section showing akami, chu-toro and o-toro given in figure 2.7.1.3.

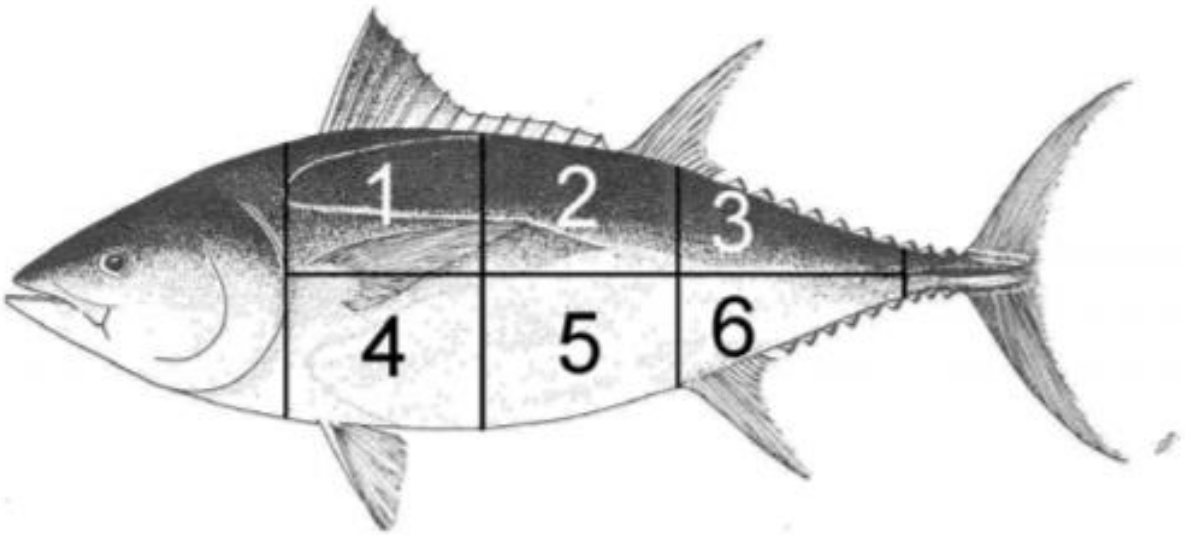

Figure 2.7.1.2 Schematic diagram of the SBFT (*Thunnus maccoyii*), with the 6 cuts used to produce the whole tissue composite and the tissue group composites (Balshaw et al., 2008).

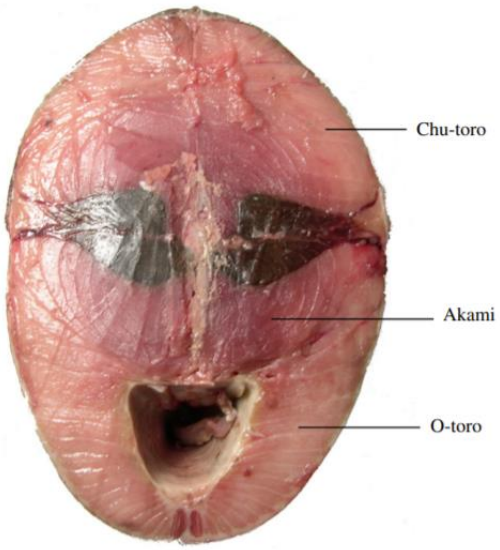

Figure 2.7.1.3 cross section of farmed SBFT (*Thunnus maccoyii*), indicating each of the tissue cuts (akami , chu-toro and o-toro) (Balshaw et al., 2008).

Bosch's study on yellowfin tuna investigated six samples as shown in figure 2.7.1.4.

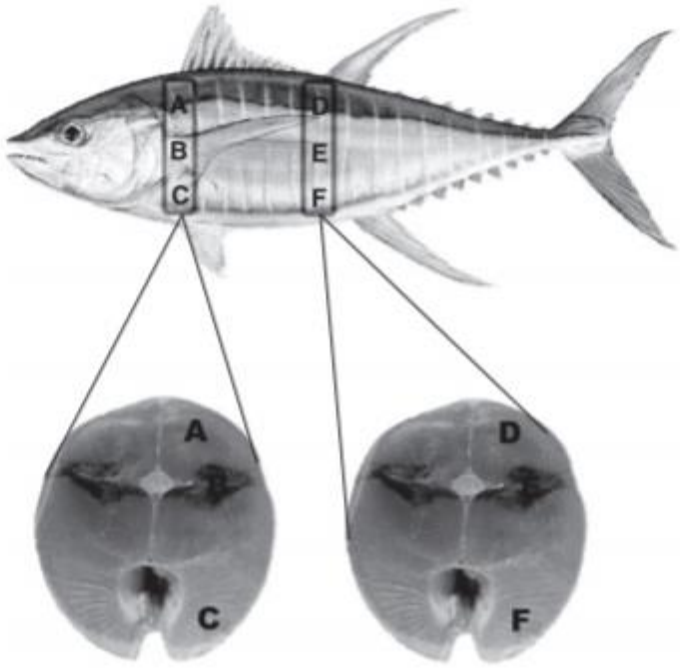

Figure 2.7.1.4 Transverse section of yellowfin tuna (*Thunnus albaraes*) carcass indicating position of white (A, C, D and F) and dark (B and E) muscle. Letters A-F indicate sampling location (Bosch et al., 2016).

Lastly, a Japanese study by Ando et. al. “Trial for Quality Control in Mercury Contents by Using Tail Muscle of Full-Cycle cultured Pacific bluefin tuna (*Thunnus orientalis*)” (Ando et al., 2008) sampled very similarly to Balshaw shown in figure 2.7.1.5.

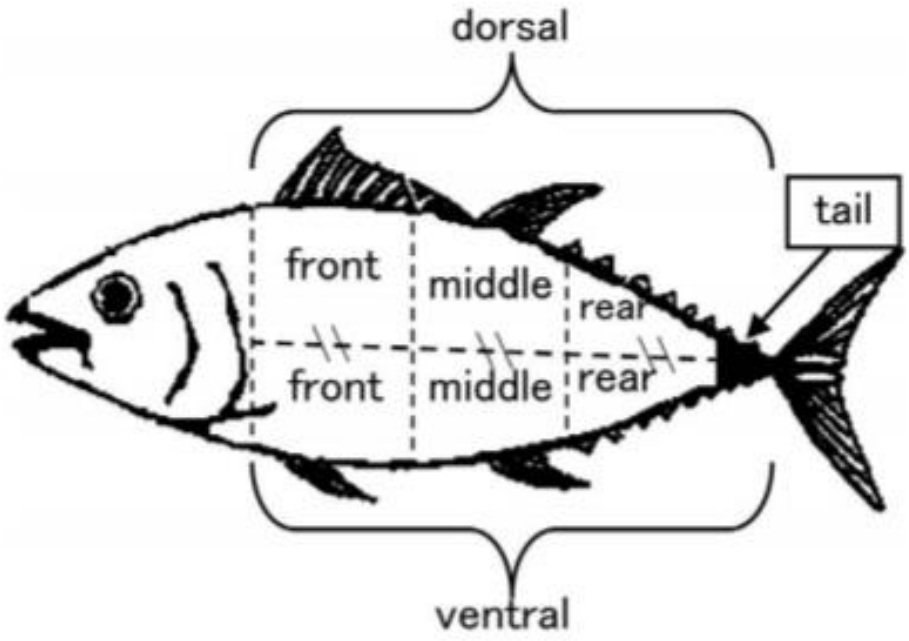

Figure 2.7.1.5 The seven muscle parts used for comparing mercury concentrations deployed by Ando et. al.. Red muscle was completely removed from each part except tail before analysis (Ando et al., 2008).

2.7.2 Sample preparation

Often, the first step when preparing samples of fish muscle is homogenization by food processor. For most sample matrices this step is sufficient to obtain a homogenous paste. Pictures taken of a sample before and after processing by food processor provided in figure 2.7.2.1.

Figure 2.7.2.1 Sample before (left panel) and after (right panel) homogenization by food processor.

Homogenization by food processor is often followed by freeze-drying (lyophilization). Freeze-drying has several benefits, like increasing concentration of analytes, improving the ease of storage for samples, increasing homogeneity and making samples easier to work with in smaller quantities**.** For fatty samples that may boil under vacuum, and ruin the sample e.g. liver samples, mackerel and herring, it is not recommended to lyophilize, which also applies to fatty samples like tuna (IMR, 2020d).

Another way to homogenize difficult samples is cryo-milling. This method utilizes two steps to homogenize the samples at low temperatures. The first step is cooling the sample substantially. In this case liquid nitrogen (LN) was used as it is an inert cryogenic fluid with a temperature of -196°C (Mindess, 2019). The sample is placed in a tube, together with the metallic milling rod. The tube is then placed inside a chamber on the mill's hatch, which is subsequently lowered into a bath of LN (Figure 2.7.2.2 and figure 2.7.2.3).

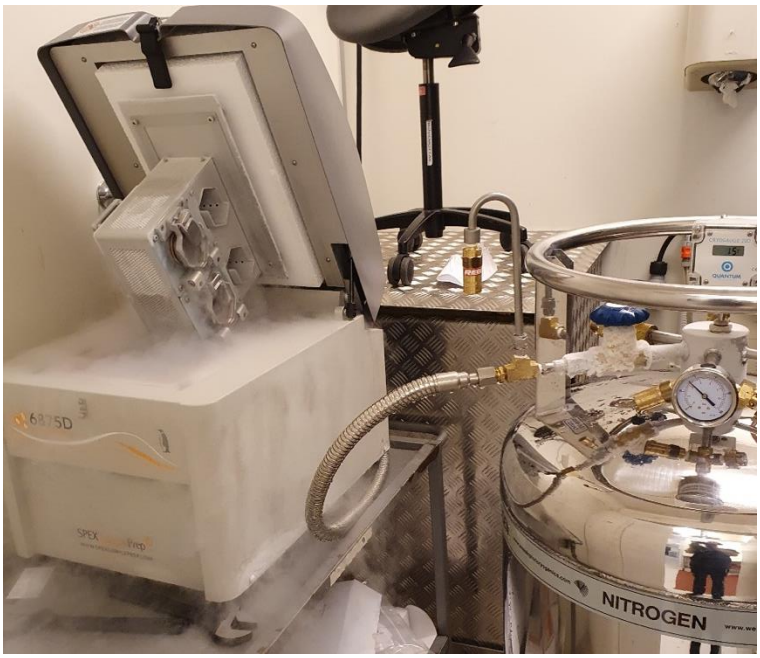

Figure 2.7.2.2 Cryo-mill with its hatch open after a finished sequence.

Figure 2.7.2.3 Picture of two tubes with samples inside and the rods outside, before processing with cryo-mill.

The second step is the mechanical milling of the cooled sample. This is achieved by the steel rod placed inside the tube with the sample. The metallic rod is moved by a solenoid, which is a cylindrical coil of wire which acts as a magnet when an electric current is applied to it, making the metal rod the only moving part of the system. The fact that there are so few moving parts makes this setup very robust. Cryo-milling is a very reliable process which produces fine powders of sample matrices that can be very hard to process by conventional homogenization methods. The

supplier, SPEX®SamplePrep boasts great homogenization of many matrices in their brochure for the machine used in this study (6875D) ranging from plastic toys and hair to beef lung and dog treats.

2.7.3 Total fat determination

Total fat determination is done gravimetrically by extracting the fat content from a sample with a solvent, placing a weighed amount of extract in an evaporation dish of known weight, and evaporating the solvent before weighing the dish again. The difference between the first and second weighing of the evaporation dish is defined as fat. The solvent used for fat extraction in this work is ethyl acetate (EA). What this method determines is defined as total fat which is a mixture of all substances soluble in ethyl acetate present in the sample. This makes the method defining, meaning that there are potentially some fats that would be better extracted with other solvents. Codex defines a defining method as follows: A method which determines a value that can only be arrived at in terms of the method per se and serves by definition as the only method for establishing the accepted value of the item measured (Codex, 2007). Results from this analysis are therefore best compared to results from the same analysis. Other methods could have comparable results, like in this case using methyl acetate as a solvent. However, the important part is to be cognizant of the comparability of results. The total defined by the method normally includes all lipids such as triacylglycerols (usually more than 90% of crude fat sample), diglycerides, monoglycerides, phospholipids, and steroids among other substances. The weight of the sample at the end of the procedure is used to obtain the total fat% of sample by dividing by the initial sample weight and multiplying by 100, formulated in formula 1.

$$\%fat_{fish\ sample} = \frac{Crude\ fat\ weight(g)}{Fish\ sample\ weight\ (g)} * 100 \quad \textbf{Formula 1}$$

This method is validated for concentrations over 0,1g/100g fat in wet samples, in the sample matrices of foodstuffs, feed, tissue and tissue fluids (IMR, 2020a).

2.7.4 Multielement determination

Elements were determined using an inductively coupled plasma mass spectrometer (ICP-MS). The ICP-MS has several components working together to produce a result. The mass spectrometer of

the instrument displays the number of ions detected at each value of mass to charge ratio (m/z). To obtain this mass spectrum, the sample needs to be atomized and ionized. This is done by plasma. Figure 2.7.4.1 shows general schematic of ICP-MS.

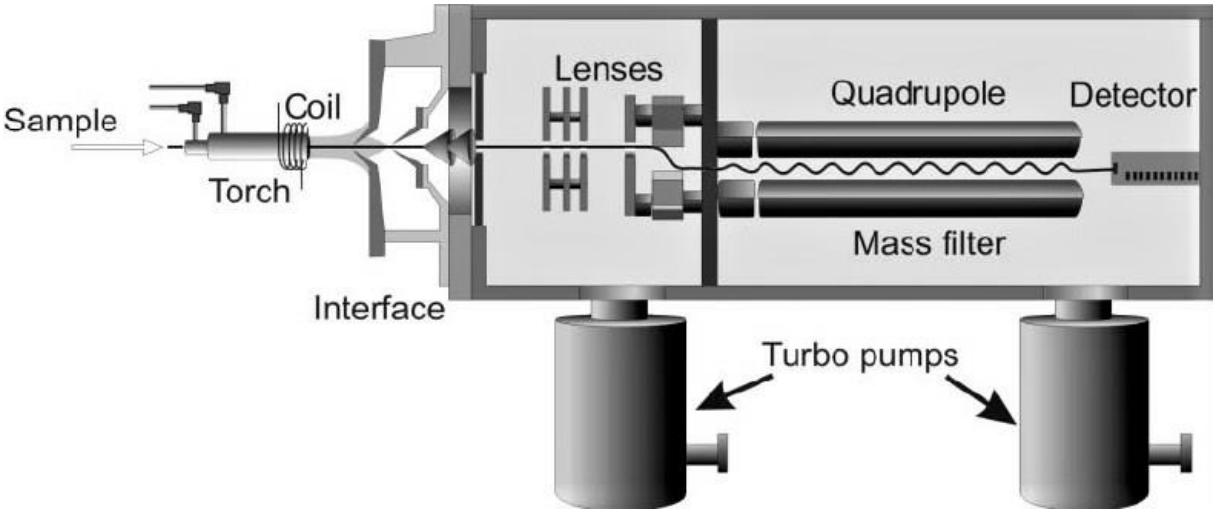

Figure 2.7.4.1 Illustration of general schematic of ICP-MS (Wilschefski & Baxter, 2019).

Due to the ICP-MS requiring samples to be in the liquid state and of low viscosity a necessary step in sample preparation is acid digestion (IMR, 2021)**.** Acid digestion is the chemical decomposition of a sample through exposure to strong acids, such as nitric, sulfuric or perchloric acid. This process can be accelerated using heat. In this study micro-wave heating is used to aid the decomposition process. The use of micro-wave assisted heating for decomposition of organic and inorganic samples was first introduced in 1975 (Abu-Samra et al., 1975). Another useful tool in the decomposition process, is closed vessels. These have a higher pressure than the open vessels due to vapor pressure being contained. This increase in pressure allows the content of the vessel to reach higher temperatures, which is very useful for difficult matrices (Sandroni & Smith, 2002). In this study nitric acid is used, being the recommended acid for micro-wave assisted digestion by the Environmental Protection Agency (EPA) (EPA, 2007). Microwaves are a form of electromagnetic radiation of frequencies between radio waves and visible light, specifically in the range of 300 MHz to 300 GHz (Hitchcock, 2004). The metallic ions will reflect the microwaves and are therefore not eligible for energy transfer from the oven. Conversely, water is a good medium for this energy, being able to absorb the energy from the radiation as the long microwaves penetrate the water efficiently. The energy transfer happens via two mechanisms. Firstly, the water

molecules, being permanent electric dipoles, will rotate in the changing electric field and collide with other molecules. These collisions increase the kinetic energy and thereby increase the temperature of the solution. The other mechanism is dissolved ions “wandering” in the electric field and collide with molecules around them, also causing an increase in temperature (IMR, 2021).

After the sample has been digested, it is ready to be introduced to the ICP-MS. The first step is an injection of a certain amount of the sample onto the system by an autosampler. Once the sample is injected onto the system it is converted from its liquid state to a mist by a nebulizer. The nebulizer also functions as a sort of filter as it does not allow the larger droplets to enter the torch (PerkinElmer, 2011). The nebulized sample is then introduced to the plasma. The plasma torch holds a very high temperature, reaching about 10,000K. The sample molecules moving through it experience around 8,000K (Lajunen, 2007). To produce the plasma a gas is required. In this work, argon is used because it is abundant, and because it has a higher first ionization energy than all the other elements except helium, fluorine and neon. This makes the ionization of the sample more favorable than the ionization of the plasma gas, ensuring the sample is ionized first. The high temperatures of the plasma torch are surrounding it with an induction coil which radio frequencies are being applied to. This creates an intense oscillating magnetic field around the coil. The magnetic field makes seed electrons introduced into the coil by a tesla discharge start oscillating within the field, producing the actual plasma (Figure 2.7.4.2).

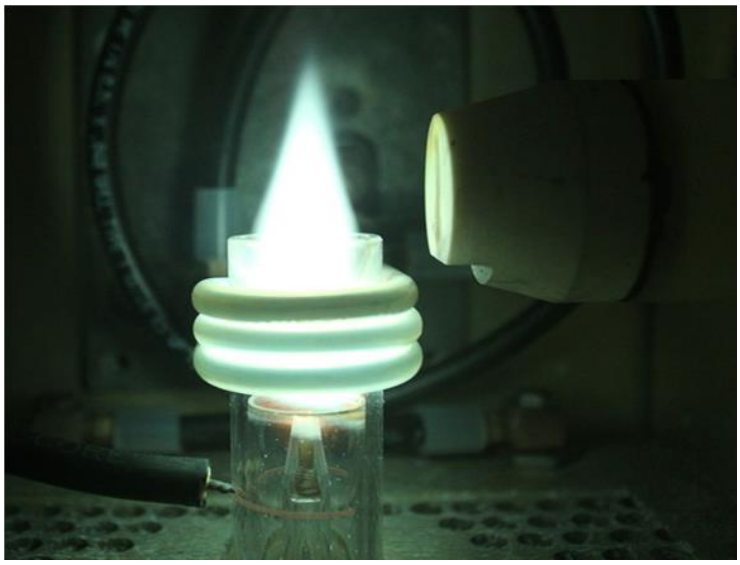

Figure 2.7.4.2 Picture of plasma coil surrounded by induction coil. Picture cropped from (Blanchard, 2011).

The sample, when introduced to the plasma is first dried to a solid and then heated to a gas. After being atomized more energy is absorbed, and the atoms release one electron to become singly charged ions. The sample exits the plasma in this atomic and ionic state.

The plasma torch operates at very different physical conditions than other parts of the system. Due to its very high temperature and atmospheric pressure compared to the vacuum of the ion lens and MS-parts of the system, an interface is required. The interface traditionally consists of two inverted funnel-like devices called cones. The ion optics are located directly following the interface region. The ion optics are made up of a series of metallic plates, barrels or cylinders that have a high voltage placed on them. The lenses' main objective is to focus the ion beam into the mass analyzer. The ion optics also remove unwanted particles from the injected samples (e.g. neutral species and photons) (Thomas, 2001). By adjusting instrument settings such as RF power, nebulization gas flow rate and sampling position within the plasma, interferences such as oxides and double charged ions can be minimized (Wilschefski & Baxter, 2019).

The mass analyzer used was a quadrupole mass analyzer. These quadrupoles are made up of four cylindrical rods of the same length and diameter oriented parallel to each other. The basic principle for how these quadrupoles select masses based on their mass to charge ratio is by applying a direct current on one pair of the rods, and radio frequency field on the opposing pair (Thomas, 2001). This allows the analyzer to let ions of selected mass pass through to the detector, while unwanted ions are ejected. The values for mass to charge can change quickly, either in succession of discrete hops or continuously (Artioli & Angelini, 2010). After ions have been selected by the mass selector they are registered by the detector as hits per second. The mass fraction of the element is then given by the computer software in µg/g. This is done through an external standard curve which is a part of the computational software (Figure 2.7.4.3).

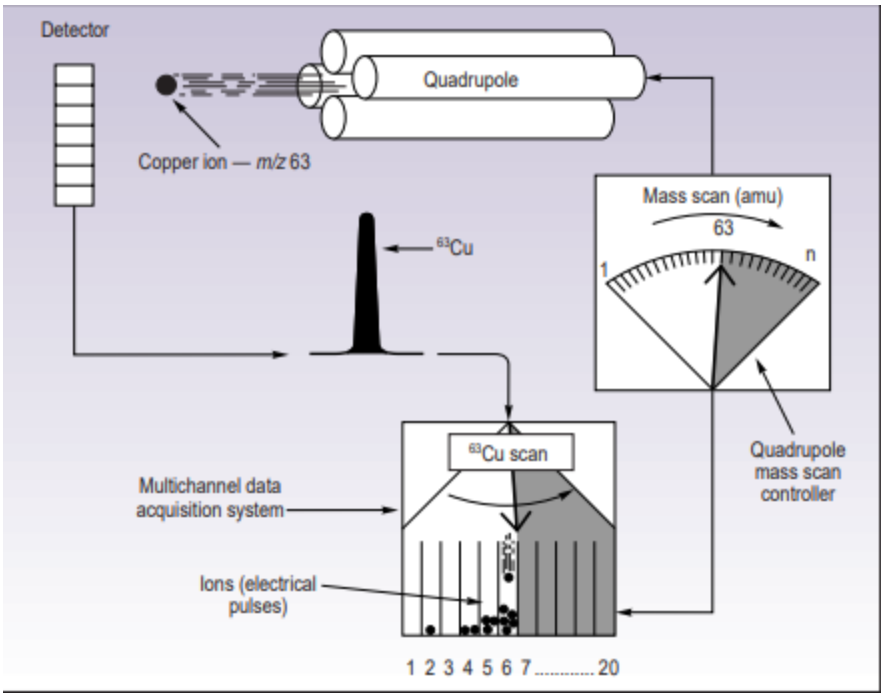

Figure 2.7.4.3 Schematic representation of how profiles of different masses are acquired by the data system following an ICP-MS analysis (Thomas, 2001).

The use of standard curve is a common way of establishing a relationship between measured quantity and response in analyzed quantity. To observe internal drift in the instrument an internal standard is used, usually rhodium, germanium, indium or thallium.

The range of accredited values, in the sample matrices of foodstuffs, feed, tissue and tissue fluids, for given elements for this method is given in table 2.7.4.1 (IMR, 2020b).

Table 2.7.4.1 Range of accredited values for given elements given in mg/kg dry weight for the ICP-MS method (IMR, 2020b).

As (mg/kg DW)	Cd (mg/kg DW)	Cu (mg/kg DW)	Zn (mg/kg DW)	Hg (mg/kg DW)	Se (mg/kg DW)	Pb (mg/kg DW)
0.01-420	0.005-27	0.1-275	0.5-1400	0.005-5	0.01-8	0.03-11

2.7.5 Determination of MeHg

Determination of MeHg is done by gas chromatography-inductively coupled- mass spectrometry (GC-ICP-MS). Before the sample can be analyzed it initially has to be spiked with isotope enriched Hg then solved in a strong base, in this case tetramethyl ammonium hydroxide. The technique of spiking is the method of adding a solution of a known concentration to the sample, so that when the sample is analyzed it has a known reference point. The spiking of the sample is crucial to the analysis of methyl mercury as the concentration of MeHg is calculated from the ratios of Hg-isotopes 200/201 and 202/201, given in formula 2, where C_S is concentration of analyte in sample (ng/g), C_{Sp} is concentration of analyte in spike solution (ng/g), m_S is weight sample (g), m_{Sp} is weight of spike added (g), M_S is molar mass of analyte in sample (g/mol), M_{Sp} is molar mass of analyte in spike solution (g/mol), A^a_S is percent of reference isotope a (200 or 202) in sample, A^b_{Sp} is percent of reference isotope b (201) in spike solution, R_S is ratio of isotope a and b in sample, R_{Sp} is ratio of isotope a and b in spike solution and R_m is determined ratio of isotope a and b in sample.

$$C_S = C_{Sp} \frac{m_{Sp}}{m_S} \frac{M_S}{M_{Sp}} \frac{A^b_{Sp}}{A^a_S} \left(\frac{R_m - R_{Sp}}{1 - R_m * R_S} \right) \quad \textbf{Formula 2}$$

Following dissolution in the base the sample is pH-adjusted to 5. The next step is treatment with a derivatization reagent (sodium tetraethyl borate), which derivatizes methyl mercury in the sample to ethyl methyl mercury and inorganic mercury present to diethyl mercury. The derivatized mercury compounds are then extracted out of the dissolved sample using hexane.

Gas chromatography is the first part of the instrument analysis in this method and it is an example of partition chromatography, where the compounds being analyzed adsorb on the stationary phase, consisting of a non-volatile liquid, usually a polymer with a high boiling point. The mobile phase is an inert gas, usually helium or nitrogen (Mohrig et al., 2010). The underlying chemical principle for separation is difference in interaction with the liquid and the stationary phase. This partitioning of a substance between the liquid and gas phases depends on both its attraction to the liquid phase and its vapor pressure. This means that thousands of liquid-gas equilibria take place as the substances travel through the column. A more volatile compound spends more time in the gas

phase than a less volatile one (Mohrig et al., 2010). Schematic of a GC-setup is shown in figure 2.7.5.1.

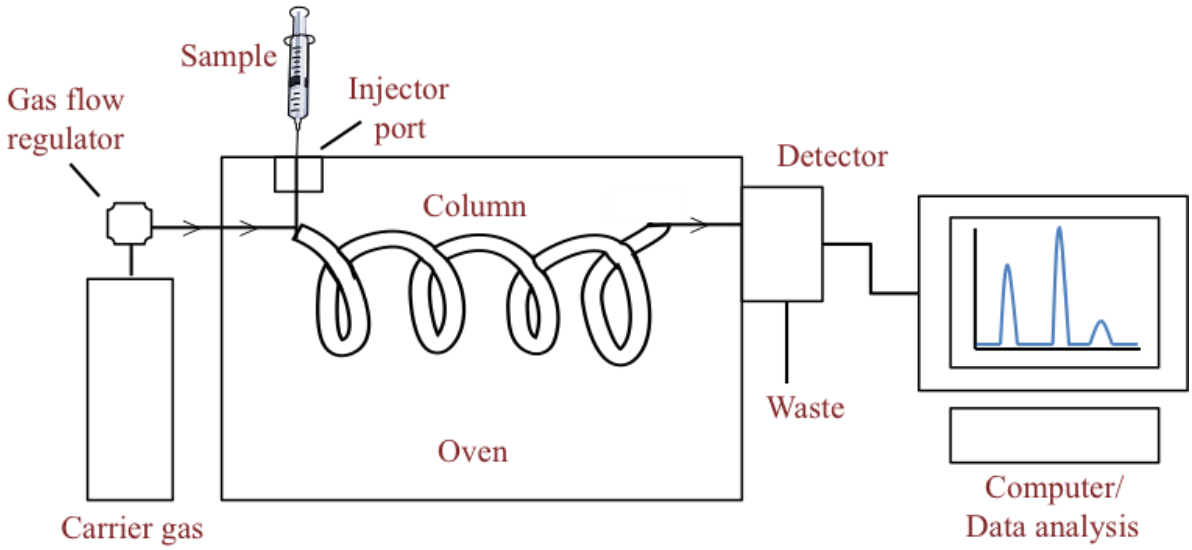

Figure 2.7.5.1 Schematic of a GC-setup (BiteSizeBio, 2016).

After the sample has been through the GC part of the system it is introduced to the ICP-MS. Theory for ICP-MS is outlined in the previous section on multielement determination.

This method is validated in the range 3-5300 ng/g for dry material in the sample matrices of fish muscle, fish liver and shells (IMR, 2020e).

2.7.6 Determination of Dioxins/PCDD, Furans/PCDF, PCBs and PBDEs

Determination of POPs is done by a variety of analytical methods. These are all combinations with gas spectroscopy, like high resolution gas chromatography high resolution mass spectrometry (HRGC-HRMS), or combinations like GC-MS/MS and GC-MS, depending on the analyte in question. The chemical process is started by adding hydromatrix and internal standard for PCDD, PCDF, PCBs and PBDEs. Samples are then extracted with hexane using an accelerated solvent extraction (ASE) system. The ASE system uses high temperature and pressure, reducing the time the extraction requires, hence the name. The extract is then cleaned chromatographically with two

columns on GO-HT (Figure 2.7.6.2). The GO-HT system is a system that automates extraction sample preparation for dioxin and PCB analyses (DSP-Systems, 2021).

Figure 2.7.6.2 Picture of a GO-6HT system (DSP-Systems, 2021).

Two fractions are then collected from the GO-HT. The first fraction contains mono-ortho PCBs, non dioxin-like PCBs (two or more ortho substitutions) and PBDEs. The second fraction contains dioxins, furans and non-ortho PCBs. Dioxins, furans and non-ortho PCBS are analyzed on HRGC/HRMS and is quantified using isotope dilution/internal standard method. Mono-ortho PCBs, non dioxin-like PCBS and tri-hepta PBDEs are analyzed on GC-MSMS also quantified using isotope dilution/internal standard method lastly, okta-deka PBDEs are analyzed on GC-MS, quantified in the same way as the two previously mentioned groups of analytes.

Using a wide variety of analysis instrument configurations allows for the determination of a large range of analytes (Table 2.7.6.1), as it detects many of the congeners discussed in the POPs section (section 2.5.7). The difference between high resolution and low resolution MS is the ability to determine the amount of analyte to a greater precision with the high resolution technique, allowing detection of analytes to the nearest 0.001 atomic mass units (Cook-Botelho et al., 2017).

Table 2.7.6.1 Table of analytes and configuration of instruments used to determine them, used in the persistent organic pollutants determination at the IMR (IMR, 2020c).

Analysis intstruments	HRGC-HRMS			GC-MS/MS		GC-MS/MS	GC-MS (NCI)
Analytes	Dioxins	Furans	Non-ortho PCB	Mono-ortho PCB	Non dioxin-like PCB	PBDE	PBDE

In some methods multiple MS's are combined in the same instrument. This technique of multiple MS-analyzers in succession is called tandem mass spectrometry. This can for example be done to achieve separation of mother molecules by weight by the first mass spectrometer, then fragment them, and then identify them on the basis of their daughter fragments by a second mass spectrometer (Vockley, 2013), allowing for a more selective process.

This method is accredited for polychlorinated dibenzodioxins (PCDD), polychlorinated dibenzofurans (PCDF) dioxin-like polychlorinated biphenyls (dl-PCBs), non dioxin-like polychlorinated biphenyls (ndl-PCBS) and polybrominated diphenyl ethers (PBDEs) in seafood including liver, oil, feed and feed ingredients (IMR, 2020c).

2.8 Quality assurance

To ensure that the results produced by the analytical methods are trustworthy it is important that the chemical analyses maintain high quality. The term quality in regard to a chemical analysis usually refers to fitness for purpose. This means that it should satisfy the customers' needs while also being as efficient as possible for the laboratory, this can be a hard balance to strike and is a very important aspect to consider when reviewing analyses. A vital step in this quality assurance process is accreditation of said analyses to given quality standards. Accreditation is defined as the formal procedure carried out by the relevant authority, which confers to formal recognition that a laboratory is competent to carry out certain tasks (Prichard & Barwick, 2007). In this case the methods are accredited in accordance to ISO 17025 (ISO, 2017) this is a very important step as it greatly increases the weight the analytical result gives both internally and internationally. ISO (international organization for standardization) is an organization that develops and publishes

international standards. A standard can be everything from a unit of measurement to a guiding document.

In the case of ISO 17025 it is a rather involved document containing overarching guidelines for many processes from leadership to methods, to ensure quality. In this case, where food safety is considered, it is very important to detect possible harmful substances, and if they are above a certain maximum level as previously discussed. The process of accrediting a method requires certain parameters to be established. These parameters include, but are not limited to; selectivity, precision, trueness, limits of detection and quantification, measurement uncertainty and robustness. Selectivity is defined as capability of a measuring system, using a specified measurement procedure, to provide measurement results for two or more quantities of the same kind involving different components in a system undergoing measurement, without interference from each other or from other quantities in the same system (ISO, 2004). Precision is defined closeness of agreement between quantity values obtained by replicate measurements of a quantity, under specified conditions (ISO, 2004). Precision is thus the measure of random error. Random error is the error present in the analysis that can be accredited to random fluctuations/differences that differ in an unpredictable way, such as temperature and meniscus in glassware between parallels. The precision of an analysis is usually evaluated by assessing the variation through standard deviation between parallels. Trueness is defined as closeness of agreement between the average that would ensue from an infinite number of quantity values obtained under specified measurement conditions and the true value of the measurand (ISO, 2004). Trueness is thus the measure of systematic error. Systematic error is the deviation from the “true” value, often described as a bias. This differs in a predictable way, as opposed to the random error. A systematic error can be caused by a weight not being completely levelled, which may give e.g. a slightly higher reading every time it is used. Precision and trueness are components of accuracy, which represents the total error of the method. Accuracy is often numerically described as the

measurement uncertainty of an analytical result. The relationship between these three quantities is given in figure 2.8.1.

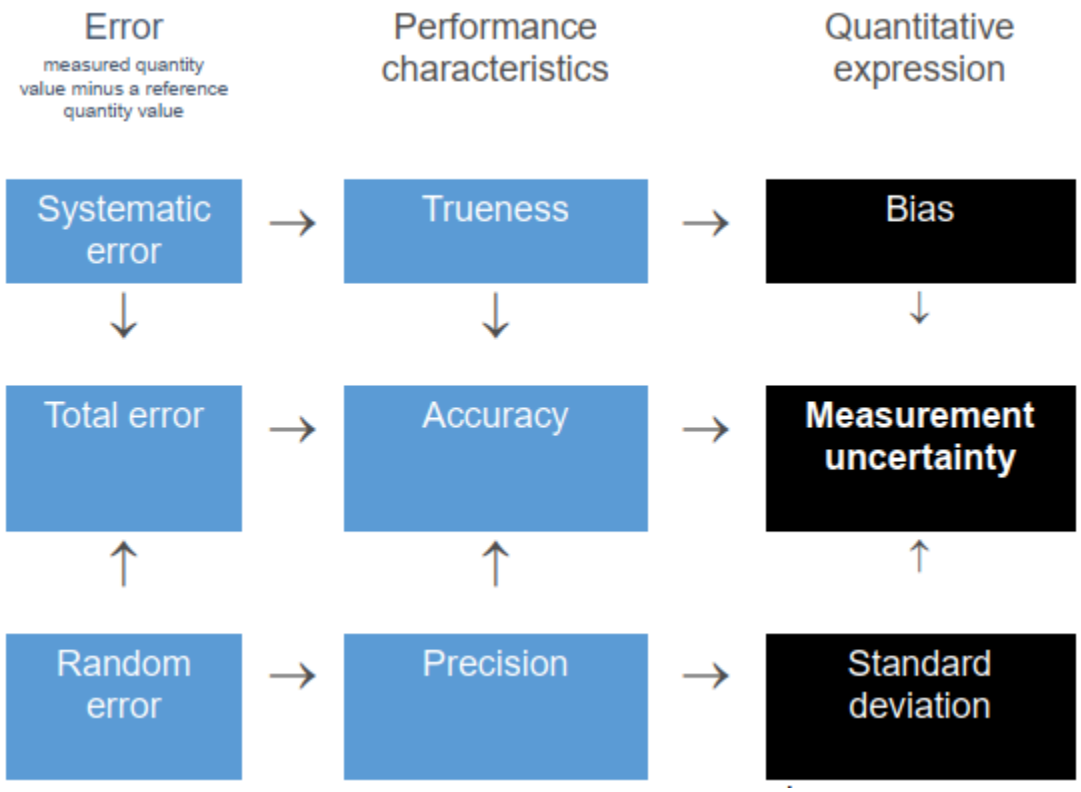

Figure 2.8.1 Flow chart of relationship between random, systematic and total error, (NMKL, 2007b).

The International Union of Pure and Applied Chemistry (IUPAC) defines limit of detection (LoD) expressed as the concentration, c_L, or the quantity, q_L, is derived from the smallest measure, x_L, that can be detected with reasonable certainty for a given analytical procedure. The value of x_L is given by formula 3, where x_{bi} is the mean of the blank measures, s_{bi} is the standard deviation of the blank measures, and k is a numerical factor chosen according to the confidence level desired (Inczédy et al., 1997).

$$x_L = x_{bi} + ks_{bi}$$ ……...**Formula 3**

The experimental determination of LoD is usually accepted as three times the standard deviation (σ) for blind samples (n≥20), this is formulated in formula 4 (Eurachem, 2014).

$$LoD = 3 * \sigma$$ ……...……**Formula 4**

The limit of quantification (LoQ), defined by Eurachem's guide on the fitness for purpose of analytical methods, is the lowest level at which the performance is acceptable for a typical application (Eurachem, 2014). Experimentally the LoQ is accepted as ten times the standard deviation (σ) for blind samples (n≥20), this is formulated in formula 5 (Eurachem, 2014). Alternatively, it is possible to multiply the LoD by 3.

$$LoQ = 10 * \sigma$$ .....**Formula 5**

As different analysis methods have different sensitivities and other properties the determination of LoQ/LoD might have to be looked at closer than the general assumptions given above to provide a more accurate value.

The use of control charts is a good tool to measure internal drift of various analyses. The control charts plot how a process changes over time (Figure 2.8.2). It is common to use a control material in each batch of analyses and to plot the result in the chart. These charts contain a lot of valuable information about the trend of an analysis. These charts may give indications of unwanted phenomena occurring within the analyses. An example of this is a datapoint being more than 3 standard deviations away from mean, meaning that one sample is highly out of control. Another example might be that six or more data points in a row are steadily increasing or decreasing meaning there is a trend present.

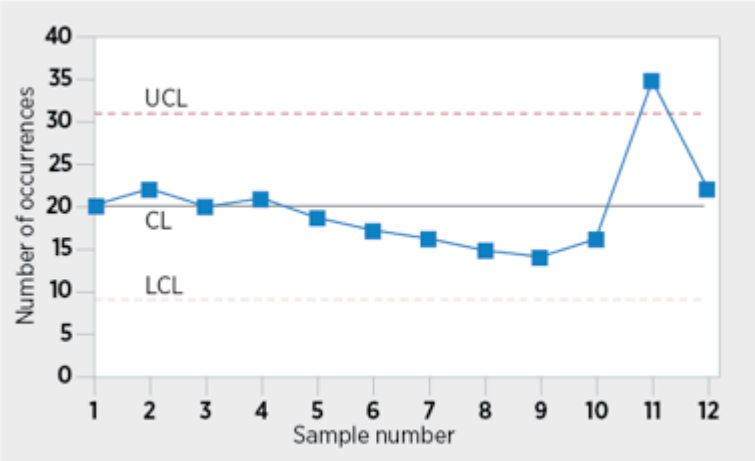

Figure 2.8.2 Example of control chart, modified from (ASQ, 2021).

3 Materials and methods

3.1 Sampling

The ABFT (n=11) were caught in the years 2018 (n=1), 2019 (n=1) and 2020 (n=9). A map of catch locations is given in figure 3.1.1. The present work loosely bases its sampling on the sampling by Balshaw et. al. The main goal of the sampling employed in this study was to investigate the distribution of the relevant substances in the edible tissue of the entire ABFT, resulting in ten different edible tissue cuts including neck and tail samples. Another factor was the economic aspect, inspiring smaller cuts taken. Figure 3.1.2 shows the schematic representation of these edible tissue cuts; 1: aggregate sample of fat, 2: neck-cut, 3: back loin cut at the tip of pectoral fin, 4: back loin cut at the base of anal fin, 5: tail-cut, 6: belly loin cut at the tip of pectoral fin, 7: ventral cut at base of the anal fin, 8; belly flap upper part in front, 9: belly flap lower part (O-toro) and 10: red muscle.

Figure 3.1.1 Map of catch locations of the sampled Atlantic bluefin tuna (*Thunnus thynnus*) in this study. Blue markers indicating male fish and red markers females.

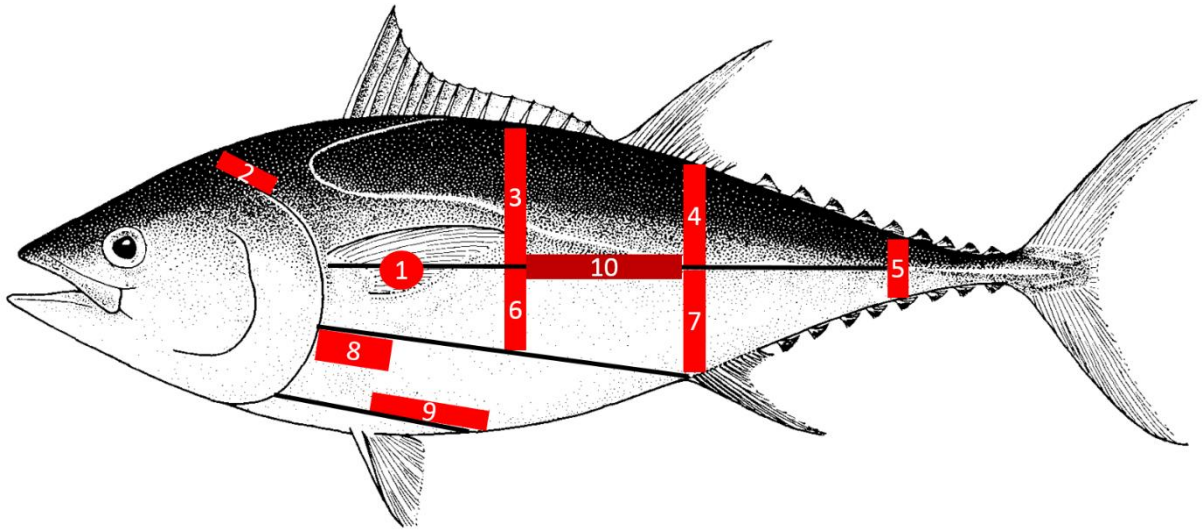

Figure 3.1.2. Schematic of the ten cuts taken of the Atlantic bluefin tuna (*Thunnus thynnus*), where 1: Aggregate sample fat, 2: neck-cut 3: back loin cut at the tip of pectoral fin, 4: back loin cut at the base of anal fin, 5: tail-cut, 6: belly loin cut at the tip of pectoral fin, 7: ventral cut at base of the anal fin, 8: belly flap upper part in front, 9: belly flap lower part (O-toro) and 10: red muscle. Modified from (FAO, 1983).

A protocol was designed to incorporate the ten edible tissue cuts, in addition to the head, guts, genetic sample from the tail and the first fin ray from the first dorsal fin. The additional samples were taken for other projects at the IMR, including but not limited to microbiology, age and species determination. Results from these analyses are still to be finalized and will not be included in this study. The protocol is attached as appendix 1 to appendix 5.

An amount of 500 grams to one kilogram was taken for all the cuts, except for the aggregate fat samples (cut one) that were lower at 200 to 300 grams. The samples were taken during the filleting process. All of the nine fish landed in 2020 were acquired through the recreational fishing project. During this project, ideally I, or a representative from the IMR would aid the sampling and transport the samples back to the laboratory. For fish caught far away from Bergen and/or had lacking freezing/storage opportunities the fishermen were guided by telephone and the aforementioned protocol was sent to them so that they could sample the fish themselves. Once the fishermen had taken the samples, they were then sent by freeze-transport to the IMR, as soon as possible. For the very last fish caught only three samples were taken, namely cuts three, five and nine due to time constraints.

Pictures of sampling done in 2019 of ABFT with cuts four and seven taken out, cut four placed on top of fish carcass, and close-up this sample provided in figure 3.1.3 and 3.1.4, respectively.

Figure 3.1.3 Picture of the Atlantic bluefin tuna (*Thunnus thynnus*) sampled at 25.09.19 with both cuts four and seven taken, and cut four placed on top of the carcass.

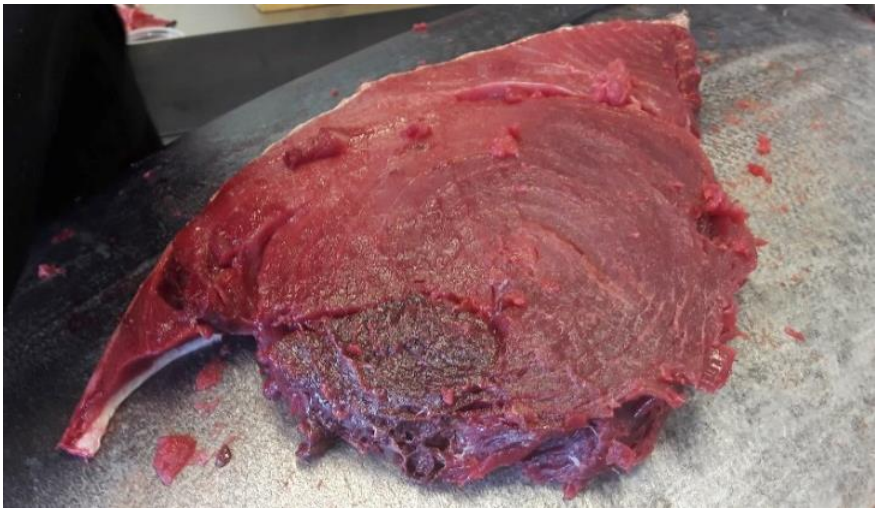

Figure 3.1.4 Close-up picture of cut four of the Atlantic bluefin tuna (*Thunnus thynnus*) sampled at 25.09.19.

After the samples were taken, they were stored at -20°C until further sample preparation was done.

3.2 Sample preparation

Table for chemicals and equipment used in the sample preparation given in table 3.2.1 and 3.2.2, respectively.

Table 3.2.1 Chemicals used in the sample preparation.

Name	Description	Provider
Liquid nitrogen for cryo-mill	Liquid Nitrogen	Nippon gases, Bergen, Norway

Table 3.2.2 Equipment used in the sample preparation.

Name	Description	Provider
Small homogenizer	Braun type 3220	Braun, Kronberg im Taunus, Germany
Medium homogenizer	Philips HR 1372	Philips, Amsterdam, Netherlands
Big homogenizer	Braun type 4200	Braun, Kronberg im Taunus, Germany
Old homogenizer	Electrolux K35	Electrolux, Stockholm, Sweden
Powerful homogenizer	Sage Kitchen Wizz BFP800	Breville, Sydney, Australia
Cryo-mill	Spex SamplePrep 6875D	Spex Methuchen, NJ

To prepare the samples for the food processor, they were thawed to about room temperature and cut into smaller pieces by hand and inspected for tendons visually. The larger tendons were removed as they would not have been eaten and would have made proper homogenization

impossible. The cut meat samples were then homogenized by food processor. Figure 3.2.1 shows a picture of the sample preparation setup.

Figure 3.2.1 Picture of sample preparation setup, showing whole sample, hand-cut sample, and food processor.

The different food processors (table 3.2.2) were chosen based on the cut being processed. This need for different processors arose since some of the samples were very small, requiring a smaller processor, and some very sinewy, requiring sharper blades. Some of the cuts were very hard to homogenize without the processor running hot, making an older, more durable one the better choice. It quickly became evident that some of the cuts were harder to homogenize properly and almost regardless of effort with cutting by hand and time in food processor they would not be completely homogenized. This was specifically the case for very fatty cuts i.e. one and nine (Figure 3.2.2), and the ones with the most tendons i.e. five and ten (Figure 3.2.3).

Figure 3.2.2 Aggregate fat sample (cut one) attempted homogenized in food processor, visibly not homogenous.

Figure 3.2.3 Red muscle sample (cut ten) attempted homogenized in food processor, visibly not homogenous.

Due to the chance of the fatty samples to boil under vacuum (see section 2.7.2), lyophilization was omitted for all samples. In an attempt to investigate a better procedure to homogenize samples, a selection of them were processed by the cryo-mill in addition to the food processor. A setup was designed to investigate the effectiveness of the cryo-mill to homogenize the samples (Figure 3.2.4).

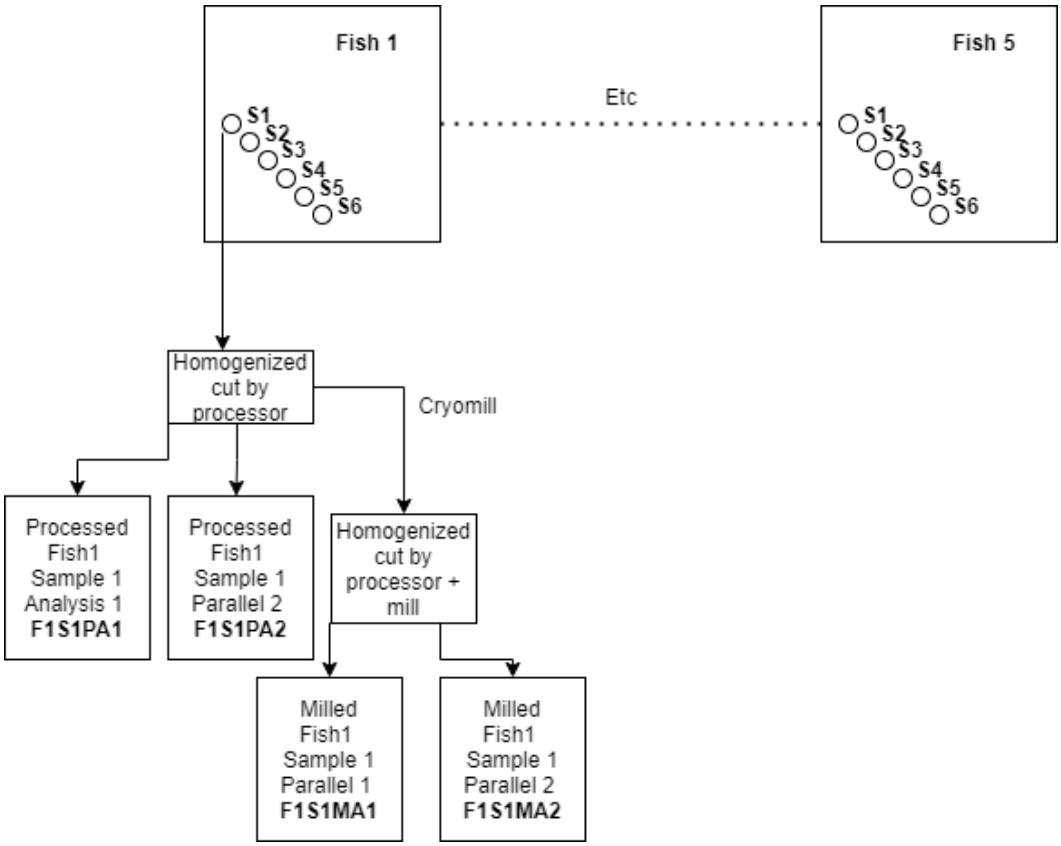

Figure 3.2.4 Cryo-mill sample setup for homogenization. Created in online resource: app.diagrams.net.

In the setup above, the samples one through six represent cuts one, three, five, seven, nine and ten, respectively. It is also shown that one sample is divided into two parallels (analysis 1 and 2, in the chart) after the initial homogenization (food processor), these are given the letter p in the chart for processed. The same sample (processed by processor) is then homogenized in the cryo-mill and divided into two parallels, again, designated m for milled. This was done for six samples, for five fish, resulting in a total of 120 samples. The reason these specific cuts were chosen was for one and nine to investigate the fatty samples, five and ten for sinewy samples, and three and seven as control samples, closer to the average filet eaten from the ABFT.

The Cryo-mill program conditions were based on recommendations from the manufacturer on similar sample matrices (Table 3.2.3). Additionally, since metals are some of the analytes in this study there was a concern that the elements from the steel rod could contaminate the samples as they are in direct contact with each other. This was investigated experimentally, internally at the IMR, and it was concluded that none of the analytes of interest in this study were at risk of contamination (unpublished data).

Table 3.2.3 Cryo-mill program conditions.

Property	Value
Precool	15/3 minutes[a]
Run time (Grind cycle length)	2 minutes
Cool time	2 minutes
Grind Cycles	3
Rate	12 cps

[a]Precool was set to 15 minutes for the first run, and 3 minutes on all subsequent runs.

Frozen samples taken from -20°C were easy to work with and got completely powdered in one attempt in the cryo-mill, except for the fatty samples. The fatty samples started to melt very quickly after being taken out of the -20°C freezer and clumped together in the milling-tube making it not entirely homogenized on the first run, requiring two runs. To mitigate this, the fatty samples were placed in a -80°C freezer overnight, in the shape of a flat disc, and then cut into pieces before

milling (Figure 3.2.5). The milling tube rods were also frozen to -80°C. This solved the issue with melting samples and allowed the fatty samples to be completely powdered in one run.

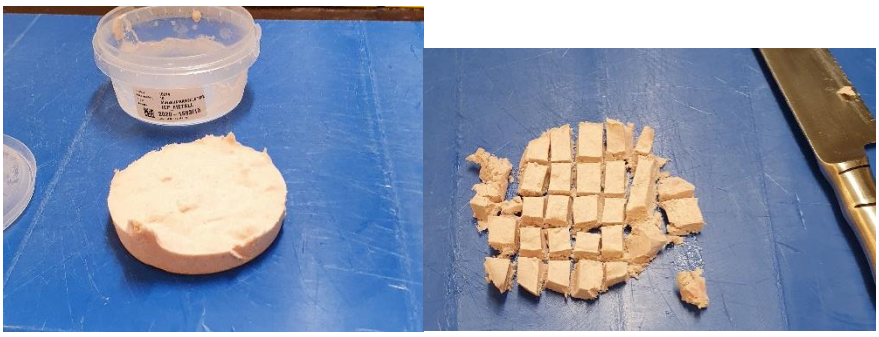

Figure 3.2.5 Picture of a fatty sample frozen into a disc shape (left panel) and cut into pieces (right panel) before cryo-milling.

3.3 Sampling mistakes and visual inspection of the samples

The samples were taken by different people, of different fish, at different localizations and at different times. This gave rise to an appreciable variance within the samples. To attempt to ensure that the samples were indeed comparable, i.e. cut one being the same for fish one and six, they were all taken pictures of at the times of homogenization as a thawed sample. The pictures were later inspected, resulting in some samples being discarded from the dataset on the visual basis of not being taken correctly. Two cuts in particular had many samples taken incorrectly. Namely, cut ten and six. Cut ten contained too much white muscle. To correct this the cuts deemed to be taken as a correct “ten’s” were named 18 (as red meat) and ten from here on refers to the red meat samples with too much fat. For cut aix several of the cuts included too much belly fat. A similar process was applied and the correct “six” samples were named 17 and the fatty ones remained as 6. Because of this the results were processed and presented for the ten original samples plus the additional two (cuts 1-10 + 17&18). For the distribution graphics presented for each contaminant, fat, and selenium the two artificial cuts 17 and 18 are attempted interpreted back into the model for a clearer visual representation and greater sample size.

3.4 Total fat determination

The total fat determination was conducted as outlined in section 2.7.3 and as per standard internal procedure at the IMR (IMR, 2020a) based on NS9402 (NS, 1994). Two parallels of each sample were analyzed for the total fat determination.

3.5 Multielement determination

The multielement determination was conducted as outlined in section 2.7.4 and as per standard internal procedure at the IMR (IMR, 2020b) based on NMKL186 (NMKL, 2007a). When preparing the samples by acid digestion, to ensure repeatability conditions, the samples were organized in a particular order. The cryo-milled samples were run in the same carousel (40 slots) as their corresponding uncryo-milled sample. This was done to ensure that as much of the sample preparation process was done equally for the samples that were to be compared when evaluating the cryo-mill. Another aspect of acid digestion is cross-contamination from very concentrated samples. Because some of the samples are very high in for example mercury, it is important to be aware of this. To mitigate cross-contamination from mercury rich samples the run order was organized so that cuts that were suspected to be low in mercury based on previous knowledge were run first. The basis for the ordering of the samples came from previously conducted studies on ABFT. The fatty samples were first analyzed followed by the fillet cuts, and lastly, the red muscle. Two parallels of each sample were analyzed for the multielement determination analysis on the ICP-MS.

3.6 MeHg determination

The MeHg determination was conducted as outlined in section 2.7.5 and as per standard internal procedure at the IMR (IMR, 2020e) based on EN16801 (NS, 2016). One parallel of each sample was analyzed for MeHg determination.

3.7 POPs determination

The POPs determination was conducted as outlined in section 2.7.6 and as per standard internal procedure at the IMR (IMR, 2020c) based on USEPA1613 (USEPA, 1994) for PCDD and PCDFs

and USEPA1668C (USEPA, 2010) for PCBs. One parallel of each sample was analyzed for the POPs determination.

3.8 Statistics

3.8.1 Anova (analysis of variance) calculations

The first statistical calculation was made to compare the difference between the samples that had been cryo-milled and their corresponding non-milled samples. The numerical basis for these calculations were the difference between parallels from select samples from multielement determination. This was done in line with the Eurachem general guide on methods and approaches concerning measurement uncertainty arising from sampling (Eurachem, 2019). The number compared in the results section is the relative standard deviation (RSD) produced for both the sampling and analytical aspect of the analysis. To attain these values the two tables were organized as shown in Table A4.14 and A4.15 in the guide. The mean was then calculated and added as a column. The difference of each value (x_i) from the mean ($\bar{x}$) was calculated and squared, providing the square of difference (formula 6).

$$Square\ of\ difference = \left(x_i - \overline{X_i}\right)^2 \quad \textbf{Formula 6}$$

The sum of square estimate of errors (SS_E) was then calculated by adding all the squared differences already calculated from formula 6 (formula 7).

$$SS\ error\ \ (SS_E) = \sum_{i=1}^{n}[(x_{i1} - \overline{X_i})^2 + \left(x_{i2} \overline{-X_i}\right)^2] \quad \textbf{Formula 7}$$

The degrees of freedom of analysis (d_{fA}) was calculated by formula 8, where N is number of samples present in study. The variance of analysis (V_A) was then calculated by dividing the SS_E by the d_{fA} (formula 9).

$$Degrees\ of\ freedom\ of\ analysis\ (df_A) = (N * 2 - N) \quad \textbf{Formula 8}$$

$$Variance\ of\ analysis\ (V_A) = \frac{SS_E}{df_A} \quad \textbf{Formula 9}$$

By squaring the variance of analysis, the standard deviation (SD) was obtained (formula 10) and lastly, the standard deviation was divided by the total mean of all analyses ($\bar{x}$) and multiplied by 100% to achieve the relative standard deviation of analysis (RSD) (formula 11).

$$Standard\ deviation\ (SD) = \sqrt{V_A}$$ ……..……..…….**Formula 10**

$$Relative\ standard\ deviation\ (RSD)(\%) = \frac{SD}{\bar{X}} * 100\%$$ ……..**Formula 11**

Similarly, for the sampling RSD, SS_E was calculated and degrees of freedom sampling (df_S) was determined (formula 12), where n is number of batches present in the study.

$$Degrees\ of\ freedom\ sampling\ (df_S) = (N * n - N)$$ …….....**Formula 12**

The variance of sampling was then decided using formula 13, by dividing the sum square error of sampling (SS_S) by degrees of freedom of sampling (d_{fS}) and subtracting that by the product of sum square error of analysis (SS_A) divided by degrees of freedom of sampling (d_{fA}).

$$Variance\ sampling\ (V_S) = (\frac{SS_S}{df_S} - \frac{SS_A}{df_A})$$ …….....**Formula 13**

The standard deviation and relative standard deviations for sampling were calculated identically to the analytical ones. The total measurement uncertainty (u_{meas}) was calculated by taking the root of the sum of the square of analytical uncertainty (u_{anal}) and the square of the sampling uncertainty (u_{samp}), formula 14.

$$u_{meas} = \sqrt{\left(u_{samp}\right)^2 + (u_{anal})^2}$$ ……..…….....**Formula 14**

3.8.2 Statistics in R

The statistics conducted in R followed the steps outlined in figure 3.8.2.1

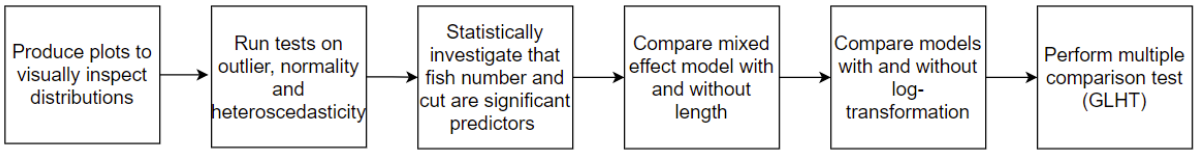

Figure 3.8.2.1 Flow chart of procedure applied in R to assess data and find best model for a given distribution. Created in online resource: app.diagrams.net

For all the distributions, except mercury and methylmercury the best model fit was the model without length and with log-transformed data. For the two mercury distributions linear mixed effect model without log-transformed data provided a better fit. In the situations where the diagnostics showed log-transformed data as a marginally better fit, the decision on whether to use log-transformation was made based on if there was a significant difference in the multiple comparison test discussed later. The specific R-code used is provided in appendix 6 to appendix 9. This was done in R version 4.0.5 in R studio. The packages used were: readxl, tidyverse, outliers, multcomp, nlme, car and lme4.

Different plots were used to assess the distribution of the different substances investigated. These plots were histograms, boxplots, QQ-plots and scatterplots (Figure 3.8.2.2). Moreover, to numerically test the dataset for outliers, normal distribution and heteroscedasticity three tests were conducted. These tests were Grubb's outlier test, Shapiro-Wilk's test for normal distribution and Fligner-Killeen test for heteroscedasticity. These tests are called in R by using grubbs.test() for Grubb's test, fligner.test() for Fligner-killeen test and shapiro.test() for Shapiro-Wilk's test.

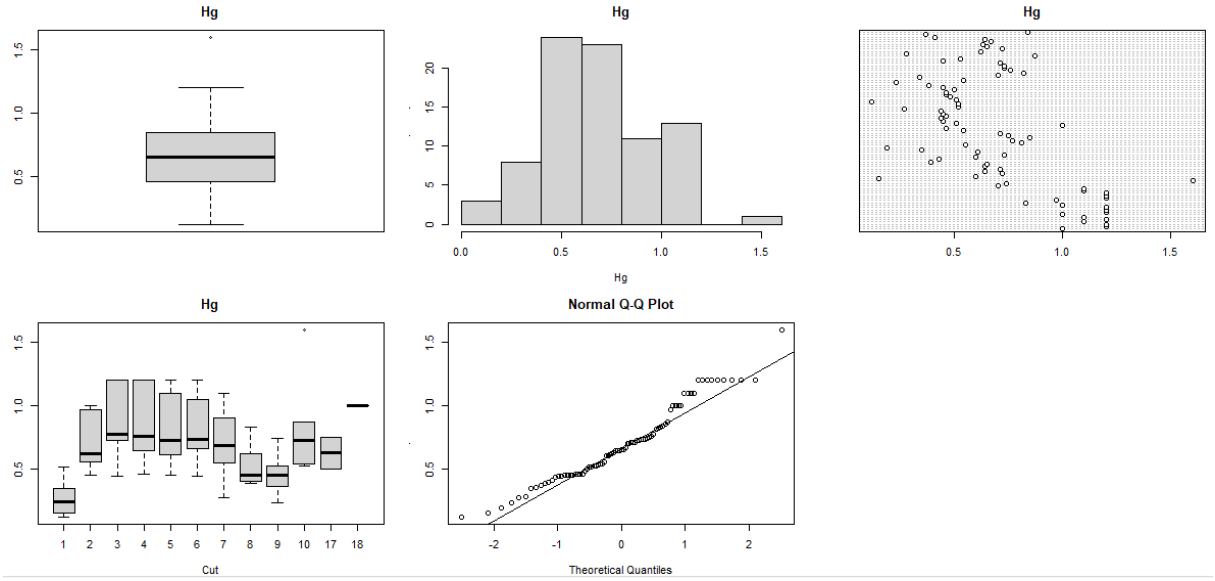

Figure 3.8.2.2 Screenshot of R-printout of the different plots (histogram, boxplots, QQ-plots, and scatterplot) used to visually inspect a contaminants' distributions.

The dataset was accepted when there were no more outliers that had to be investigated and corrected for.

When choosing the type of statistical model, the main assumption was that the data was nested (in each individual fish) as the levels of contaminants varied greatly between the fishes. This was supported by determining a statistical significance between fish ID and given contaminants. Therefore, the model chosen for each distribution was a linear mixed effect model with fish ID as the nested effect. The reason a mixed effect model is beneficial to use here is that it allows the model to account for intra-cluster correlation and therefore investigate the response of the other variables without it varying across clusters (Luke, 2017).

To compare the fit of different models against each other two types of diagnostic plots were used. The first one being the residuals vs fits plot (Figure 3.8.2.3). This is a scatterplot of residuals on the y axis and fitted values (estimated responses) on the x-axis. The plot is used to detect non-linearity, unequal errors and outliers. A scatterplot of a good model will fill three criteria. Firstly, residuals distribute evenly around the 0-line, suggesting that a linear relationship is reasonable. Secondly, the residuals form a horizontal band around 0-line, suggesting variances of error terms

are equal. Lastly, no singular residual stands out from the random pattern of the residuals, suggesting that there are no outliers (ECoS, 2018).

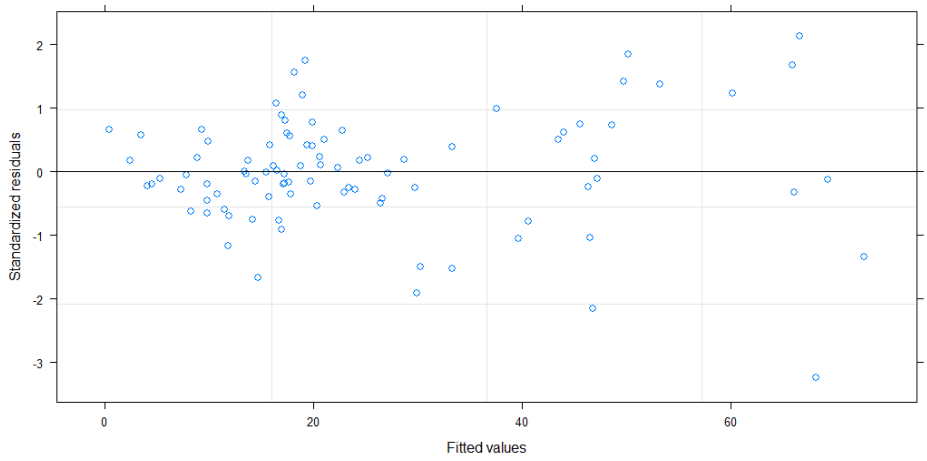

Figure 3.8.2.3 Picture of R-printout for residuals versus fitted values scatterplot.

The second plot used to compare models is the quantile-quantile plot (Q-Q) (figure 3.8.2.4). The Q-Q plot is a scatterplot using two sets of quantiles against each other. In this case the quantiles for the sample data are plotted on the y-axis versus theoretical quantiles from a normal distribution. If the points from the scatterplot follow the trend of the line y=x the assumption of normality is good (UVA, 2015). None of the distributions in this work are normally distributed, however, the Q-Q plot was still used comparatively.

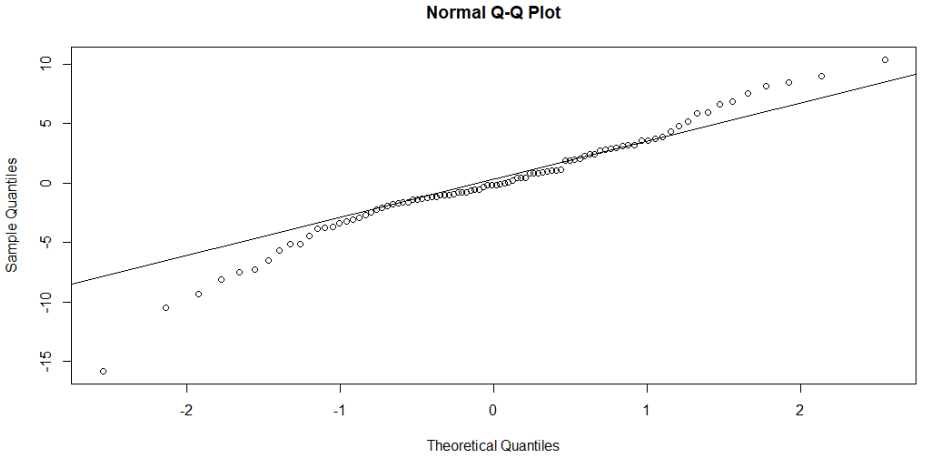

Figure 3.8.2.4 Picture of R-printout Q-Q plot with sample quantiles versus theoretical quantiles.

The Akaike information criterion (AIC) was used as the last criterion to judge the fit of the models when determining the best one. The AIC was produced by calling the function AIC(). The AIC is only a relative measurement of models, so when comparing different models the value gives a good indication how they are relative to each other, making it a useful tool. However, it does not give any information on the absolute strength of the model (Profillidis & Botzoris, 2018).

Lastly, to compare all the levels of predictor variables in the statistical models ascertained to each other a post-hoc multiple comparison test was used. In this case the Tukey HSD was used by calling the function glht(). Tukey's multiple comparison test can be used when there are more than two groups of observations which otherwise could be compared with a t-test. The test compares the difference between each pair of means with appropriate adjustment for the multiple testing (Crichton, 1999). When this quantity has been produced in R, a p value <0.01 is accepted as strongly significant, 0.01 is still significant, 0.05 still significant and 0.1 somewhat significant.

3.9 Calculations

3.9.1 Tolerable weekly intake (TWI)

The TWI is calculated by formula 15, by providing the weight of a harmful substance in the units of micrograms and dividing it by a person's body weight in kilograms. In the calculations in this study, and in general it is assumed a body weight of 70kg.

$$TWI = \frac{m_{harmful\ substance}[\mu g]}{m_{body\ weight}[kg] * t[week]} \quad \text{.....Formula 15}$$

3.9.2 Conversion of length

For one of the fish the head was severed before length could be measured and the length had to be estimated by using ICCAT's length-weight estimation table (Lombardo et al., 2019).

4 Results

4.1 Biological material

A total of eleven fish were included in this study. One fish was sampled in 2018, one in 2019, and the remaining nine in 2020. The length of the ABFT varied from 230 to 307 cm. The distribution of sex was nine males to two females (Figure 4.1.1).

Table 4.1.1 Overview of the Atlantic bluefin tuna (*Thunnus thynnus*) sampled in this study along the Norwegian coast. Including date sampled, catch location (latitude, longitude), standard fork length (cm) and sex.

Fish number	Sampling date	Catch location (Lat, Long)	Straight fork length (cm)	Sex
1	28.09.2018	60.13, 5.283	307	Male
2	25.09.2019	61.18, 4.528	250	Male
3	21.08.2020	58.08, 9.846	244	Female
4	21.08.2020	58.20, 9.665	251	Female
5	03.09.2020	62.92, 6.042	280	Male
6	03.09.2020	62.51, 5.458	252	Male
7	01.09.2020	60.69, 4.636	238	Male
8	05.10.2020	61.52, 4.383	255	Male
9	04.10.2020	60.17, 5.020	249	Male
10	09.10.2020	61.61, 4.773	250	Male
11	20.10.2020	60.73, 4.755	230	Male

4.2 Control materials and certified reference materials

Fat concentrations for the control material (fish meal) in fat determination is given in appendix 12. One control value was above 3SD. Quantified element concentrations for both certified reference materials, oyster tissue (OT) and lobster hepatopancreas (TORT) in the multielement determination is given in appendix 13 and 14, respectively. Two controls of OT were above 2SD in vanadium, one control of TORT was above 2SD in vanadium, manganese, iron and cobalt and

one control of TORT was above 2SD in iron. The sums of TEQs for PCDD/F + non-ortho PCBs and mono-ortho PCBs, and the sum of PCB6 and PBDE7 are given in appendix 15 for the control material (salmon muscle) spiked with PCDD/F and PBDE for the POPs analyses. One control was below 3SD in sum of PCDD/F + non-ortho PCB, and the other below 2SD. MeHg concentrations for the certified reference materials TORT and tuna muscle (Tuna464) are given in appendix 16. One value for TORT was below 2SD, one value for Tuna464 was above 3SD, and the remaining three Tuna464 controls were above 2SD. For the remaining controls, all values were within 2SD in all four analyses.

4.3 Cryo-mill investigation

Calculated relative standard deviations as outlined in 3.8.1 based on parallel deviations from selenium, mercury, cadmium and arsenic from the multielement determination presented in table 4.3.1, for analysis, sampling and total. These relative standard deviations show a decrease for analysis uncertainty in every element, with the biggest decrease in cadmium. The sampling RSD's all increase after milling.

Table 4.3.1 Comparison of unmilled (NCM) and milled (CM) Atlantic bluefin tuna (*Thunnus thynnus*) fillet samples using a cryo-mill. Relative standard deviations (RSD) for analysis, sampling and total measurement uncertainty, for the elements Se, Hg, Cd, and As are given.

	Analysis		**Sampling**		**Total**	
Element	NCM	CM	NCM	CM	NCM	CM
			RSD[%]			
Se	8.43	3.06	44.3	44.6	45,1	44,7
Hg	4.23	2.45	28.7	29.5	29,0	30,0
Cd	19.4	4.58	50.3	62.4	53,9	62,6
As	6.43	1.92	14.6	22.3	16,0	22,4

4.4 Analytical results

Data from all analyses for the different cuts are provided in table 4.4.1. The total fat content found was 26 ± 18% (Mean±SD). The mean selenium concentration was 1.8 ± 2.7 mg/kg WW. Mercury and methylmercury were found at concentrations of 0.72 ± 0.33 mg/kg WW and 0.76 ± 0.34 mg/kg WW, respectively. Cadmium is reported at concentrations of 0.014 ± 0.0090 mg/kg WW, and arsenic at 2.3 ± 1.3 mg/kg WW. Lastly, the POPs were found at 1.2 ± 1.1 ng/g WW TEQ, 8.0 ± 8.4 ng/g WW TEQ and 100 ± 121 ng/g WW TEQ for PCDD/PCDF, PCDD/PCDF + dl-PCB and PCB-6, respectively. Pb content was not included in this table as all values were below LoQ, where 18 samples were <0.02, and the rest <0.01 mg/kg ww. POPs were found primarily in fatty tissue, showing highest amounts in sample one and lowest in sample 18. The analytes selenium, mercury and methylmercury showed the opposite distribution to POPs, accumulating mainly in the red muscle. Cadmium had the highest content in sample 18 and the lowest in seven. Arsenic was highest in sample one, and lowest in sample three.

Table 4.4.1 Concentrations of contaminants (mercury, methylmercury, cadmium, arsenic, sum dioxins & furans (PCDD/F), sum dioxins, furans & dioxin-like PCBS(PCDD/F+dl-PCB)), sum PCB-6, fat and, selenium in the different cuts of Atlantic bluefin tuna (*Thunnus thynnus*) caught along the Norwegian coast. The values for PCDD/F, PCDD/F + dl-PCB and PCB-6 are the upper bound results. Mean value ± standard deviation and [min/max], based on wet weight, are given. The sample size (n) is also given, however, for PCDD/F, PCDD/F+dl-PCB and PCB-6 the analyses were done on a subset of six fish.

Cut	Sample size (n)	Fat [%]	Se [mg/kg WW]	Hg [mg/kg WW]	MeHg [mg/kg WW]	Cd [mg/kg WW]	As [mg/kg WW]	Sum PCDD/F [pg/g WW TEQ]	Sum PCDD/F + dl-pcb [pg/g WW TEQ]	Sum PCB-6 [ng/g WW TEQ]
1	7	67±7.9 [52/77]	0.99±0.35 [0.40/1.4]	0.19±0.090 [0.10/0.34]	0.21±0.13 [0.089/0.40]	0.019±0.0084 [0.0090/0.032]	5.3±0.86 [4.3/6.7]	2.9±2.3 [1.7/7.5]	23±15 [12/52]	310±217 [130/734]
2	10	25±5.8 [13/35]	0.96±0.27 [0.66/1.5]	0.74±0.23 [0.45/1.0]	0.83±0.27 [0.54/1.2]	0.012±0.0079 [0.0040/0.026]	2.2±0.47 [1.6/3.2]	1.3±0.93 [0.83/3.2]	7.4±5.9 [4.2/19]	86±69 [41/225]
3	11	12±5.7 [3.7/21]	1.8±0.85 [0.57/3.4]	0.86±0.27 [0.48/1.2]	0.94±0.25 [0.60/1.3]	0.011±0.0044 [0.0050/0.018]	1.3±0.33 [0.66/1.8]	0.62±0.23 [0.39/1.0]	3.3±0.98 [2.2/4.8]	34±11 [21/48]
4	10	14±7.5 [3.3/25]	1.2±0.51 [0.56/2.4]	0.84±0.30 [0.46/1.2]	0.92±0.32 [0.50/1.4]	0.0097±0.0040 [0.0040/0.015]	1.4±0.37 [0.72/2.0]	0.75±0.32 [0.36/1.2]	4.0±1.9 [2.5/7.4]	39±19 [23/70]
5	11	15±6.6 [5.2/24]	1.2±0.78 [0.76/3.5]	0.82±0.29 [0.44/1.2]	0.85±0.36 [0.22/1.4]	0.012±0.0088 [0.0030/0.035]	1.5±0.49 [0.51/2.3]	0.75±0.36 [0.44/1.4]	3.8±1.9 [2.2/7.4]	39±20 [21/76]
6	7	20±8.5 [6.6/29]	1.7±1.1 [0.76/3.6]	0.83±0.28 [0.44/1.2]	0.91±0.30 [0.58/1.4]	0.015±0.0093 [0.0040/0.030]	1.9±0.76 [0.75/3.2]	0.76±0.087 [0.66/0.82]	3.9±0.29 [3.5/4.0]	41±3.2 [38/44]
7	9	16±7.0 [3.0/23]	1.2±0.42 [0.80/2.1]	0.77±0.27 [0.45/1.1]	0.82±0.29 [0.51/1.3]	0.0093±0.0043 [0.0040/0.015]	1.4±0.36 [0.78/1.8]	0.70±0.27 [0.50/1.1]	4.0±1.7 [2.4/7.1]	40±18 [22/71]
8	8	42±11 [23/59]	0.74±0.13 [0.56/0.92]	0.56±0.18 [0.38/0.83]	0.55±0.19 [0.24/0.81]	0.013±0.0058 [0.0060/0.022]	3.5±0.74 [2.2/4.6]	2.0±1.2 [1.2/4.2]	15.±8.1 [8.9/29]	204±124 [107/417]
9	9	46±10 [26/60]	1.0±0.39 [0.64/1.8]	0.46±0.19 [0.23/0.75]	0.48±0.17 [0.32/0.74]	0.017±0.0080 [0.0080/0.032]	3.3±0.76 [1.9/4.5]	1.8±0.92 [1.2/3.6]	13±5.0 [8.7/23]	180±80 [95/328]
10	6	17±8.8 [3.5/25]	5.9±3.0 [0.89/9.9]	0.83±0.41 [0.52/1.6]	0.87±0.42 [0.59/1.7]	0.018±0.014 [0.0050/0.037]	2.0±0.47 [1.2/2.5]	0.67±0.15 [0.59/0.89]	3.5±0.60 [2.9/4.2]	37±11 [27/51]
17	3	18±4.7 [13/22]	1.4±0.65 [0.87/2.1]	0.78±0.30 [0.50/1.1]	0.70±0.21 [0.55/0.84]	0.0097±0.0025 [0.0070/0.012]	1.6±0.30 [1.3/1.9]	0.87±0.24 [0.60/1.0]	5.2±1.6 [4.2/7.0]	57±14 [47/73]
18	2	9.6±4.2 [6.6/13]	16±7.8 [10/21]	1.4±0.50 [1.0/1.7]	1.1±[a] [1.1/1.1]	0.042±0.022 [0.026/0.057]	2.7±0.50 [2.3/3.0]	0.40±0.084 [0.34/0.46]	2.6±0.33 [2.4/2.9]	29±4.1 [26/32]
Total	93	26±18 [3.0/77]	1.8±2.7 [0.40/21]	0.72±0.33 [0.10/1.7]	0.76±0.34 [0.089/1.7]	0.014±0.0090 [0.0030/0.057]	2.3±1.3 [0.51/6.7]	1.2±1.1 [0.34/7.5]	8.0±8.4 [2.2/52]	100±121 [21/734]

[a] An SD could not be calculated for MeHg cut 18 as there are only two samples and one of them does not have a MeHg value. This is due to MeHg was not conducted on the fish caught in 2018.

Illustrations of the distributions of the different substances according to the multiple comparison tests are provided in figure 4.4.1 to figure 4.4.8. Statistically different levels of contamination are indicated with different colors.

Fat was highest in the belly, with the three fatty samples being statistically similar. The neck cut, two, was at medium level and the remaining cuts contained the lowest level of fat (Figure 4.4.1).

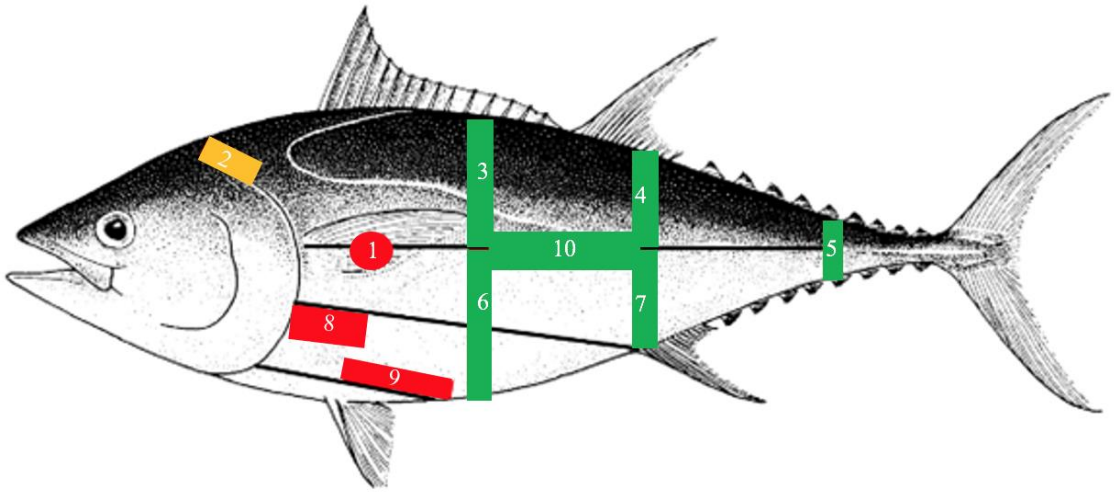

Figure 4.4.1 The distribution of fat in the different cuts of Atlantic bluefin tuna (*Thunnus thynnus*). Different colors indicate groups that are significantly statistically different from each other, with red indicating high, orange medium and green low-levels. Modified from (FAO, 1983).

Selenium showed a high level in the red muscle sample, and a low level in the remaining cuts (Figure 4.4.2).

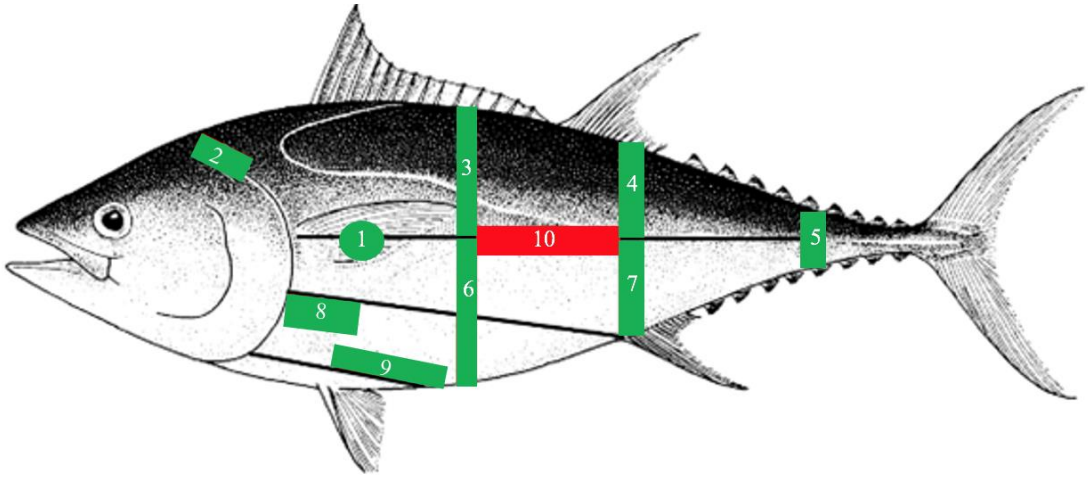

Figure 4.4.2 The distribution of selenium in the different cuts of Atlantic bluefin tuna (*Thunnus thynnus*). Different colors indicate groups that are significantly statistically different from each other, with red indicating high and green low-levels. Modified from (FAO, 1983).

Mercury showed four different levels of concentrations with the highest in red muscle, second highest in cuts two, three, four, five, six and seven, second lowest in the belly samples eight and nine, and the lowest in the aggregate fat sample, cut one (Figure 4.4.3). Methylmercury had a similar distribution, but only with two levels. High concentrations of methylmercury were found in the cuts two, three, four, five, six, seven and ten, while low concentrations were found in samples one, eight and nine (Figure 4.4.4).

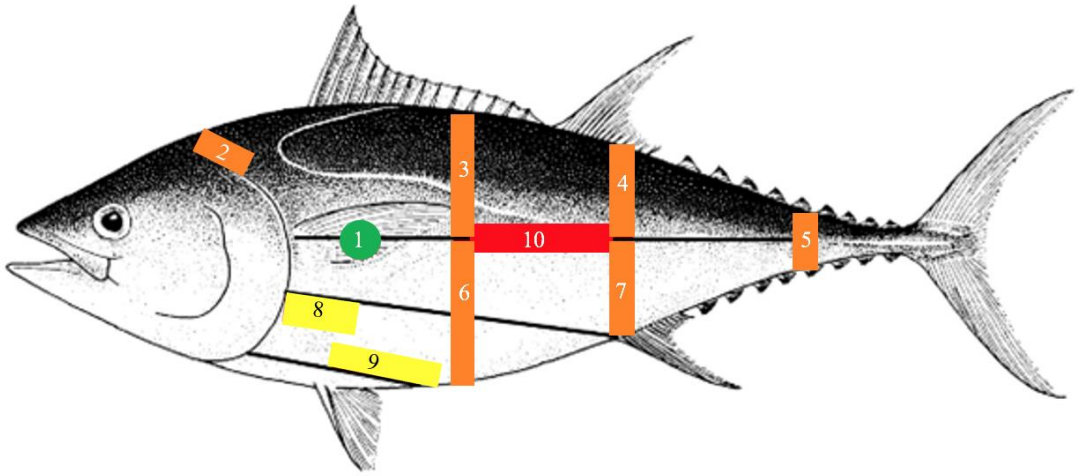

Figure 4.4.3 The distribution of mercury in the different cuts of Atlantic bluefin tuna (*Thunnus thynnus*). Different colors indicate groups that are significantly statistically different from each other, with red indicating high, orange medium-high, yellow medium-low and green low-levels. Modified from (FAO, 1983).

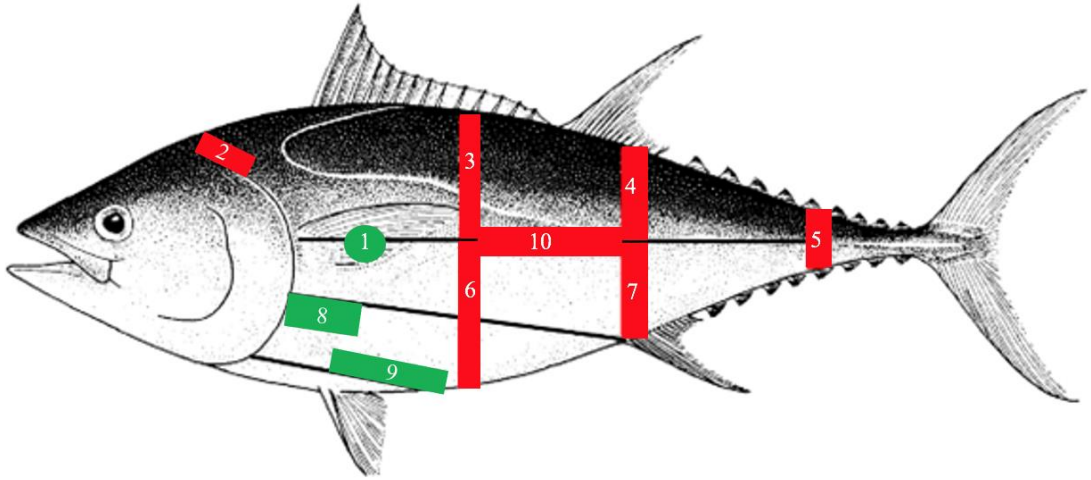

Figure 4.4.4 The distribution of methylmercury in the different cuts of Atlantic bluefin tuna (*Thunnus thynnus*). Different colors indicate groups that are significantly statistically different from each other, with red indicating high and green low-levels. Modified from (FAO, 1983).

Three different levels of cadmium were found. The highest level was found in cuts one, nine and ten. Medium level of cadmium concentrations were found in cuts eight and six, and the lowest in the remaining cuts (Figure 4.4.5).

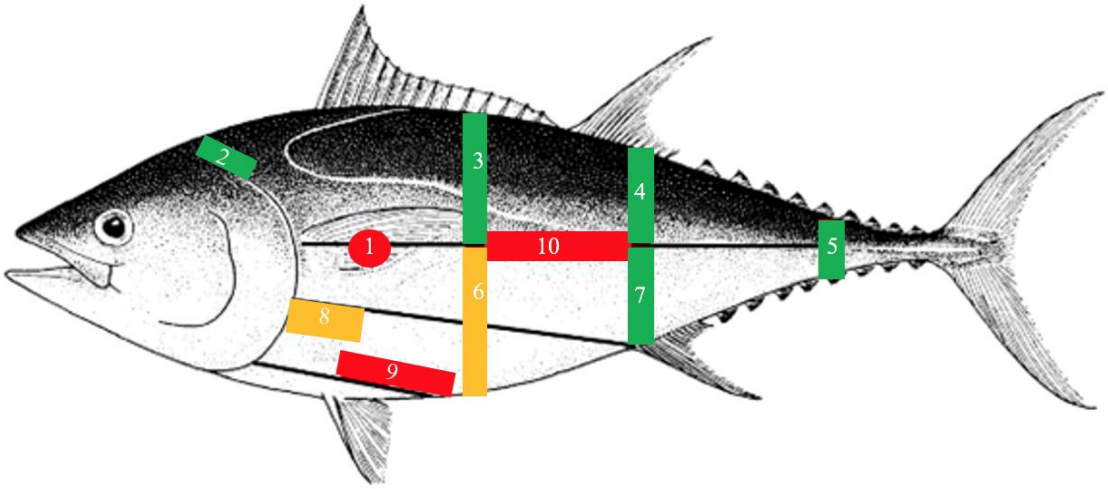

Figure 4.4.5 The distribution of cadmium in the different cuts of Atlantic bluefin tuna (*Thunnus thynnus*). Different colors indicate groups that are significantly statistically different from each other, with red indicating high, orange medium and green low-levels. Modified from (FAO, 1983).

Arsenic was the highest in the aggregate fat sample, cut one. The medium-high level was found in cuts eight and nine. Medium low level was found in cuts two, six and ten, and lowest level in cuts three, four, five and seven (Figure 4.4.6).

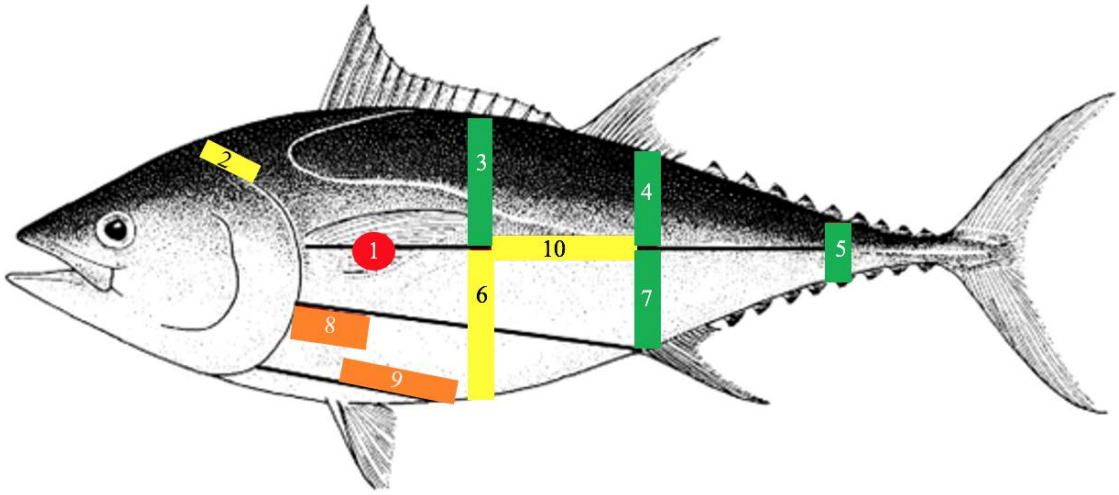

Figure 4.4.6 The distribution of arsenic in the different cuts of Atlantic bluefin tuna (*Thunnus thynnus*). Different colors indicate groups that are significantly statistically different from each other, with red indicating high, orange medium-high, yellow medium-low and green low-levels. Modified from (FAO, 1983).

The persistent organic pollutants show similar distributions to each other. The distribution of PCDD/F has three levels, with the highest in cuts one, eight and nine. The medium level was found in cut two, and the lowest in the remaining cuts (Figure 4.4.7). This is identical to the distribution of fat content. The distribution of PCDD/F + dl-PCB showed highest content in cut one, second highest in cuts eight and nine, second lowest in cut two and lowest in the remaining cuts (Figure 4.4.8).

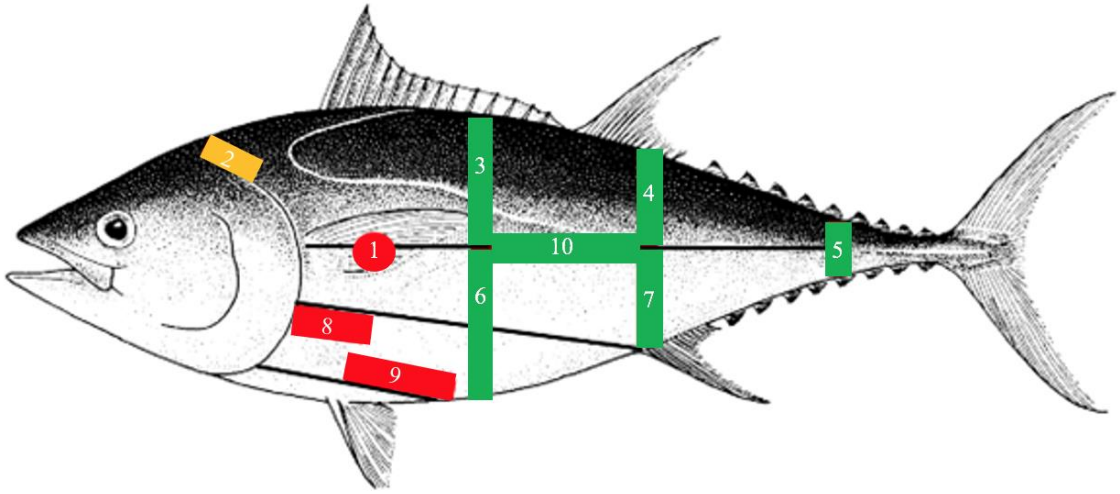

Figure 4.4.7 The distribution of PCDD/F in the different cuts of Atlantic bluefin tuna (*Thunnus thynnus*). Different colors indicate groups that are significantly statistically different from each other, with red indicating high, orange medium and green low-levels. Modified from (FAO, 1983).

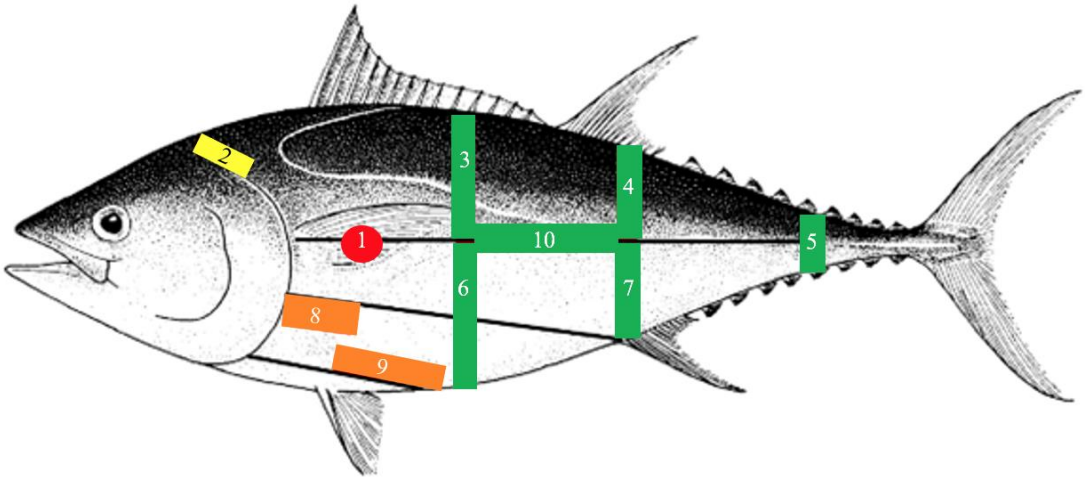

Figure 4.4.8 The distribution of PCDD/F + dl-PCB in the different cuts of Atlantic bluefin tuna (*Thunnus thynnus*). Different colors indicate groups that are significantly statistically different from each other, with red indicating high, orange medium-high, yellow medium-low and green low-levels. Modified from (FAO, 1983).

A strong negative linear relationship was found between Hg and fat (R^2=-0.45, Figure 4.4.9), while fat and PCDD/F + dl-PCBs was strongly positively correlated (R^2=0.56, Figure 4.4.10). The correlation between PCDD/F + dl-PCBs and Hg was weak (R^2=0.12, Figure 4.4.11).

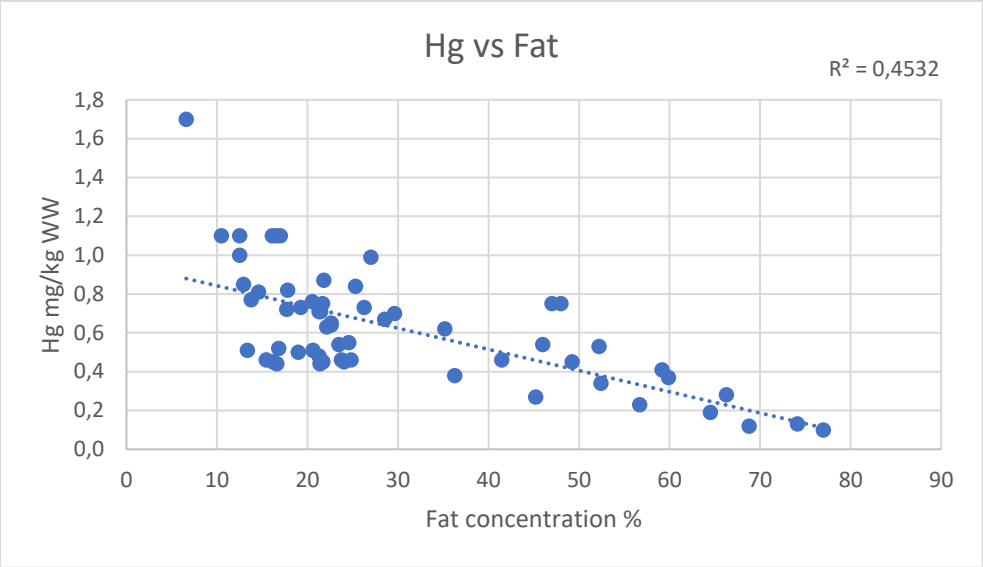

Figure 4.4.9 Correlation between mercury concentrations (mg/kg WW) and fat concentrations (%) for the six Atlantic bluefin tuna (*Thunnus thynnus*) that had POPs analyses conducted, including R^2 value.

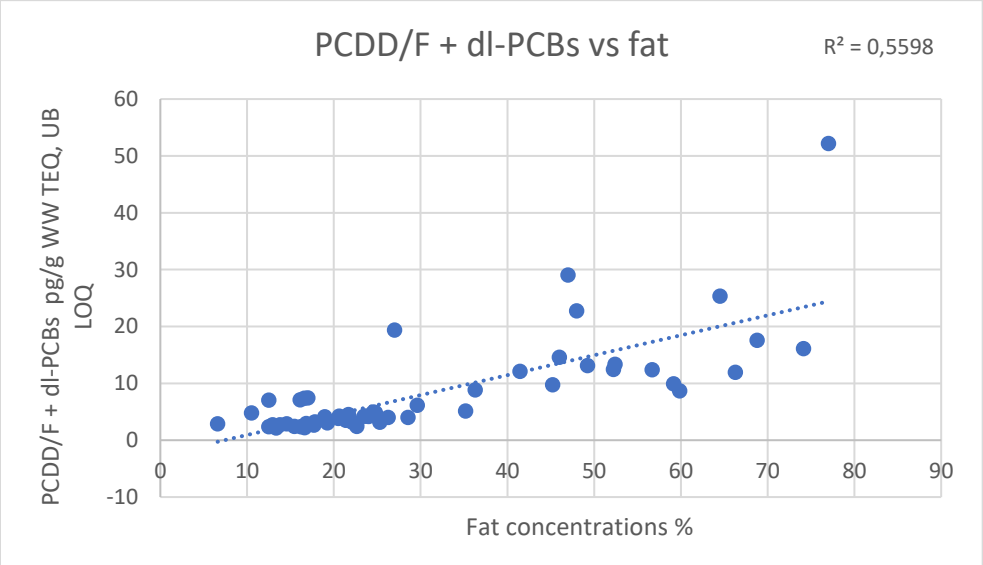

Figure 4.4.10 Correlation between PCDD/F + dl-PCBs concentrations (pg/g WW TEQ) and fat concentrations (%) for the six Atlantic bluefin tuna (*Thunnus thynnus*) that had POPs analyses conducted, including R^2 value.

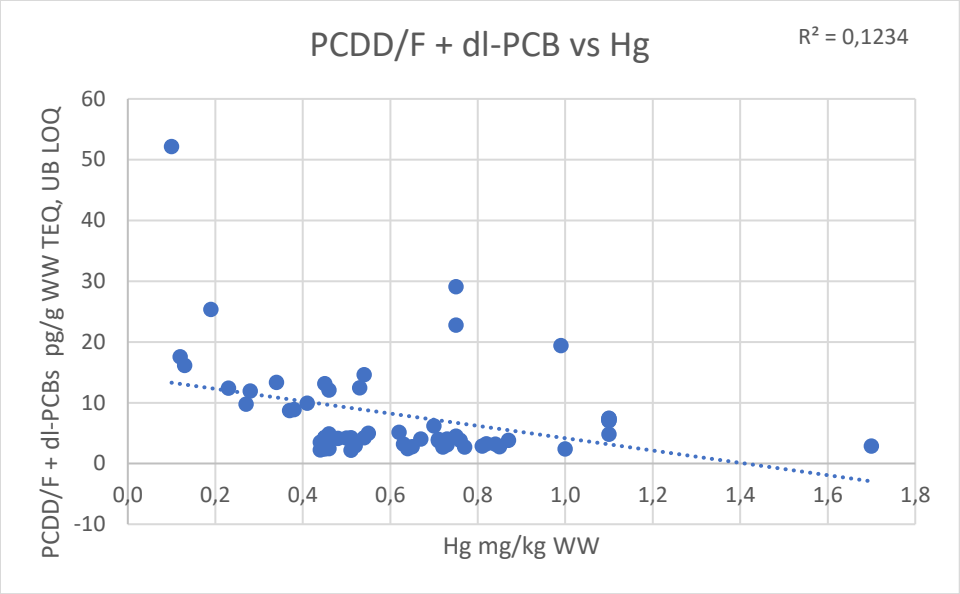

Figure 4.4.11 Correlation between PCDD/F + dl-PCBs concentrations (pg/g WW TEQ) and Hg concentrations (mg/kg WW) for the six Atlantic bluefin tuna (*Thunnus thynnus*) that had POPs analyses conducted, including R^2 value.

4.5 Food safety assessment

The amount of edible tissue needed to exceed TWI's given by JECFA and EFSA (EFSA, 2012) for each cut investigated and number of exceedances of maximum level for trade given by the European commission (EC, 2006) and CODEX (CODEX, 2018) are given in table 4.5.1. The allowed weekly intake of mercury is above 400 grams for both total mercury and methylmercury in the aggregate fat sample, and below 100 grams in the red muscle. Total mercury exceeds the maximum level more frequently, due to the lower maximum limit for trade set by the EC. The PCDD/F + dl-PCBs is the group of contaminants that both had the highest frequency of exceedances in regard to their maximum level and allows for the least amount eaten before the TWI is exceeded. Cadmium showed no exceedances of the given maximum level, and an amount above 4 kilograms has to be eaten to exceed the TWI, in the cut richest in cadmium. The molar ratio of selenium to mercury is also included. The Se:Hg molar ratio is above one for all cuts, indicating a surplus of selenium.

Table 4.5.1 Mean tolerable weekly intakes given by JECFA/EFSA, assuming a body weight of 70kg and the frequency of exceedances given in percent of the maximum level given by EC/CODEX for the different cuts of the Atlantic bluefin tuna (*Thunnus thynnus*) for mercury, methylmercury, cadmium, PCDD/F + dl-PCB. PCDD/F and PCB-6 also included showing only percentage exceedances as no TWI is available. In addition, the molar ratio of selenium to mercury is given.

Cut	Hg (g)	MeHg (g)	Cd (g)	PCDD/F	PCDD/F + dl-pcb (g)	PCB-6	Se:Hg ratio
1	599 (0%)	444 (0%)	9259 (0%)	(17%)	6.17 (100%)	(100%)	13
2	152 (0%)	110 (0%)	14831 (0%)	(0%)	19.0 (17%)	(33%)	3.3
3	130 (36%)	96.6 (20%)	15909 (0%)	(0%)	42.3 (0%)	(0%)	5.3
4	133 (40%)	99.1 (22%)	18041 (0%)	(0%)	35.0 (17%)	(0%)	3.6
5	136 (36%)	107 (20%)	14344 (0%)	(0%)	36.7 (17%)	(17%)	3.7
6	136 (29%)	99.9 (14%)	11667 (0%)	(0%)	36.3 (0%)	(0%)	5.2
7	146 (33%)	111 (25%)	18757 (0%)	(0%)	35.0 (17%)	(0%)	4.0
8	201 (0%)	165 (0%)	13462 (0%)	(20%)	9.27 (100%)	(100%)	3.6
9	244 (0%)	189 (0%)	10234 (0%)	(17%)	10.8 (100%)	(100%)	5.5
10	135 (17%)	105 (17%)	9669 (0%)	(0%)	39.6 (0%)	(0%)	18
17	143 (33%)	131 (0%)	18097 (0%)	(0%)	26.8 (33%)	(0%)	4.6
18	83.0 (50%)	83.0 (0%)	4217 (0%)	(0%)	53.0 (0%)	(0%)	29
TWI	1.6 µg/kg BW[a]	1.3 µg/kg BW[b]	2.5 µg/kg BW[b]	-	2 pg TEQ/kg BW[b]	-	-
Max level	1 mg/kg WW[c]	1.2 mg/kg WW[d]	0.1 mg/kg WW[c]	3.5 pg/g WW[c]	6.5 pg/g WW[c]	75 ng/g WW[c]	-
Total max level exceedances	22%	12%	0%	5%	37%	34%	6.4

[a] TWI given by JECFA (EFSA, 2012)

[b] TWI given by EFSA (EFSA, 2012)

[c] Maximum level given by the European Commission (EC, 2006)

[d] Maximum level given by CODEX (CODEX, 2018)

5 Discussion

5.1 Sampling

As outlined in section 2.7.1 on sampling, several sampling procedures have been utilized when investigating the distribution of contaminants in large tuna fishes. The mentioned studies have provided their sampling procedure, while others only stated that they took three independent muscle samples from each fish of about 10 g each from the dorsal area, near the back (Annibaldi et al., 2019). In the present study, samples of 11 ABFT could be obtained from the recreational tuna fishery in Norway, providing enough samples of sufficient size. The ABFT was caught at many different locations, by different fishermen using different facilities with different equipment. Consequently, this caused some challenges. The edible tissue cuts were taken during the fileting process, and when being present in person, it was difficult to maintain control for the entirety of the sampling process with several people working on the carcass. For some fish, the ABFT sampling had to be guided remotely, as fish were landed too far away to be reached within a reasonable time from Bergen and lacked proper freezing capabilities. This resulted in some samples taken inadequate in terms of mass and type of tissue included in the samples were of varying quality. Lacking freezing facilities is still a challenge and improving on this could benefit the sampling procedure. After a close examination, some of the samples had to be discarded from the dataset, even though a high quantity of samples was desirable to obtain accurate numbers on the distribution of contaminants.

Results for different contaminants in the current study (table 4.4.1), showed large variation of contents in the different cuts. Mercury concentrations ranged from 0.19 ± 0.090 mg/kg WW in cut one to 1.4 ± 0.50 mg/kg WW in cut 18, and PCDD/F + dl-PCB ranged from 23 ± 15 pg/g WW TEQ in cut one to 2.6 ± 0.33 pg/g WW TEQ in cut 18. Large variations in different fillet cuts have also been found in the studies of Piras et al., Balshaw et. al., Bosch et. al., Ando et. al. and Ross et. al(Ando et al., 2008; Balshaw et al., 2008; Bosch et al., 2016; Piras et al., 2020; Ross & Edwards, 2015). All studies found an uneven distribution of total mercury concentrations in the different cuts taken of ABFT (Piras et al., 2020). This emphasizes the need for a standardized sampling protocol.

As outlined earlier, the ABFT is an expensive fish, making the economic aspect of sampling important. To account for this it is possible to both sample smaller amounts or sample from a location on the ABFT that is less desirable for commercial use. To generate comparable data between studies in the future, sampling from the same site on the carcass is highly preferable. To arrive at one standardized cut that is representative for the contaminants is therefore desirable. As an example of a standarized cut is the Norwegian Quality Cut (NQC) for atlantic salmon. The NQC is a standardized cross section of the fish used for e.g. fat determination in Atlantic Salmon extending from the posterior of the dorsal fin to the gut (Veliyulin et al., 2005).

5.2 Sample preparation

Sample preparation was conducted as outlined in section 3.2. Initially a food processor was used which proved inadequate to obtain homogenous samples. Earlier studies (Annibaldi et al., 2019; Balshaw et al., 2008) did not elaborate on how they treated the samples before analyses were conducted, and therefore do not report any issues in this step. Due to visible inhomogeneous samples in the current study, a cryo-mill was used as an experimental step following the food processor. The cryo-mill was very effective and resulted in visibly homogenous samples of fatty and sinewy tissue (Figure 5.2.1).

Figure 5.2.1 Frozen homogenized samples in cryo-mill-tubes before milling (left panel) and slightly thawed homogenized samples after milling (right panel).

This visual impression was supported by results presented in table 4.3.1. The relative standard deviations in the analysis decrease drastically for all four elements inspected after cryo-milling, with the lowest decrease for mercury (4.2% to 2.5%) and the highest decrease for cadmium (19% to 4.6%). This suggests a smaller variation between the analysis parallels, due to improved homogenization. The sampling uncertainty increases for all four elements. The increase in relative standard deviation for sampling in selenium and mercury are deemed insignificant, both increasing by less than one percent. This might be attributed to the fact that selenium and mercury are more evenly distributed throughout the different cuts investigated in this comparison. Conversely, arsenic showed an increase in sampling RSD (15% to 22%), possibly due to it being more unevenly distributed throughout the cuts, and this difference becomes more pronounced when the analysis parallels have a smaller variance. For cadmium sampling uncertainty increased from 50% to 62%. The cadmium concentrations measured are low. Therefore, similarly to arsenic, when the variations between parallels is reduced, the difference between the different cuts is thought to increase. However, whether the sampling uncertainty has any merit to investigate in this manner for the given dataset can be discussed, as the values for contaminants differ significantly between the different cuts. Due to the high variation between the cuts, a high sampling uncertainty is not alarming, but rather expected. If anything, the high uncertainty in sampling further emphasizes the importance of a clear sampling protocol.

To my knowledge, this is the first study to investigate the effect of cryo-milling on fish samples. As ascertained in this study, the relative standard deviations are generally lower for the milled samples than for the samples prepared without the cryo-mill. Earlier results obtained at the IMR used to assess potential metal contamination as outlined in section 3.2, support this. The cryo-mill effectively improved the homogenization. Due to small amounts weighed in for several analyses, proper homogenization of sample-matrices is very important to obtain accurate and reliable results.

For both the multielement and MeHg determination, an amount of 0.3-0.5g of wet material was weighed into 15mL quartz or plastic tubes. The sample needed to be introduced at the bottom of the tube to ensure that it was entirely immersed in the acid or base. This was a challenging task as the samples were sticky and the amount of sample was small. Furthermore, the diameter of the test tube was narrow making it difficult to maneuver the sample well into the tube, without having it adhere to the walls of the tube above the acid or base. The cryo-milled samples were significantly

easier to work with at this point of the sample preparation than their unmilled equivalent, but the issue of samples sticking to the top of the tube was still present. Using a method that uses a larger sample amount or figuring out how to freeze-dry the fatty samples, are two possible avenues to solve this. When preparing samples for fat and POPs analyses, these issues were not encountered. This is likely explained by the use of a larger amount of sample.

5.3 Assessment of control material and certified reference material

For the fat determination one value for the control material exceeded 3SD. This would normally result in a reanalysis of the entire batch, however this exceedance was caused by a pipetting error. Therefore the batch was a approved based on the other parallel of control and parallel deviations between the samples. With only one control outside 3SD, caused by human error, fat determination showed good precision. For multielement determination one control for OT was above 2SD in vanadium for both parallels in the one batch. In the same batch TORT exceeded 2SD in one parallel for vanadium, manganese and cobalt, and iron in both parallels. This batch was accepted as these elevated levels were close to the "true" certified values for the reference materials. With all other results for both reference materials being withing 2SD, multielement determination showed good precision and trueness. For the POPs determination the control material was incorrectly spiked and results for the sums of PCDD/F + non-ortho PCBs and sum PBDE7 cannot be compared to the internally ascertained mean. The two batches were still accepted based on the values for PCBs which are naturally present in the control material. For the MeHg determination one value for TORT was below 2SD, but the mean between the two parallels of TORT was acceptable. Tuna464, however was higher than 3SD in one control, and higher than 2SD in the rest. A possible explanation for this was that the spike solution used had gone bad. The high MeHg values were replicated by another analyst with both the old and a new spike solution, meaning the issue was not with the spike solution, and the MeHg values were accepted for both batches.

5.4 Assessment of the analyses

For the two analyses where samples were analyzed in parallels (two parallel test portions are weighed into separate tubes from the same test sample), parallel deviations were encountered. Parallel deviations occur when the difference between parallels reaches an unacceptable level. The

accepted levels between parallels are defined by the analysis method in question. If the difference between parallels exceeds the given level, the analytical result will not be approved. The lower the detected concentration of analyte, the higher the accepted parallel deviation. Table 5.4.1 presents the accepted deviations between parallels for total fat determination at the IMR (IMR, 2020a).

Table 5.4.1 Accepted deviations (%) between parallels for total fat determination for levels low, medium and high based on concentration given in grams total fat per 100 grams of sample (IMR, 2020a).

Level	g/100g	Accepted difference %
Low	0.1-5	10
Medium	5-15	6
High	15-100	4

For the multielement determination a difference of 10% between parallels is accepted if the value for the analyte is higher than ten times the LoQ, and 25% if the value is less than ten times then LoQ, but more than the LoQ.

The number of samples that had to be reanalyzed due to parallel deviation were eight and 11, for fat and multielement determination, respectively. For the multielement determination, however, some of the samples that had to be reanalyzed had acceptable results from their cryo-milled equivalent. This both reduced the work in preparing samples anew for reanalyzes and further underlined the importance of proper homogenization.

In most samples the measured concentrations of MeHg exceeded the concentration of total mercury. This systematic difference has also historically been observed internally at the IMR. In practical terms, this cannot occur. The content of one chemical specie cannot exceed the total content of all species together. However, due to total mercury content and methylmercury content being determined by two different analytical methods, both having a measurement uncertainty associated with them, this is explicable. Tables 5.4.2 and 5.4.3 list measurement uncertainties in three levels based on analyte concentrations for the analyses of MeHg and Hg from multielement determination, respectively.

Table 5.4.2 Measurement uncertainty (%) for MeHg determination for levels low, medium and high based on analyte concentration given in nanogram analyte per gram sample (IMR, 2020e).

Level	ng/g	Measurement uncertainty (%)
Low	3-30	35
Medium	30-200	25
High	200-5300	20

Table 5.4.3 Measurement uncertainty (%) for mercury in multielement determination for levels low, medium and high based on analyte concentration given in milligrams analyte per kilogram sample dry weight (IMR, 2020b).

Level	mg/kg DW	Measurement uncertainty (%)
Low	0.005-0.05	70
Medium	0.05-0.5	25
High	0.5-4.6	20

The MeHg and Hg contents in most of the samples were within the medium or high uncertainty levels, resulting in a measurement uncertainty of 25% and 20% for each method, respectively. The total measurement uncertainty for both determinations can be calculated by taking the square root of the sum of the squared individual uncertainties. This is the simplified calculation of the law of error propagation which neglects correlations or assumes variables to be independent. Given that the result for both analyses fall in the same level, the total uncertainty is 28% for medium and 35% for high levels. A total of eight samples exceeded the interval given by the total measurement uncertainty. The samples that showed the highest deviations between MeHg and Hg were samples that were discarded based on visual inspection, due to inhomogeneity or wrong tissue type taken. Based on expert judgement by the analyst on instrumental stability (judged using raw data from instrument response to assess e.g. peak shape and control charts) and inherent weakness when weighing in such small sample amounts, none of these samples were selected to be reanalyzed based on the ratio of MeHg to total Hg.

5.5 Distributions between cuts

Fat was distributed as expected for teleosts (Table 4.4.1 and Figure 4.4.1), with most fat stored in the belly region (cut eight and nine) and the least in the red muscle (cut ten and 18). Due to varying sampling (see section 2.7.1) and different methods for determining fat content/lipid content in different studies, comparing results between studies is complex. Moreover, most of the studies conducted on tuna species sampled smaller or farmed fish, making the comparison to the wild, large fish investigated in the present study challenging. Balshaw et. al. (Balshaw et al., 2008), determined lipid concentration in farmed SBFT by use of Soxhlet extractor and diethyl ether as solvent, in individuals of 16 to 42 kg. They found that the O-toro sample, chu-toro sample and akami sample had lipid contents of 33 ± 5%, 20 ± 5% and 5 ± 2%, respectively. These samples can be compared to the present study's cut nine (46 ± 10%), six (20 ± 8.5%) and four (14 ± 7.5%). The observed fat content is very high compared to fish in general (Olagunju et al., 2012). A high fat content is considered beneficial for human health (outlined in section 2.5.1). It is suggested that the high fat values found in this study are due to factors such as the strongest/largest swimmers of ABFT make the migration this far north. This has been shown by Boge (Boge, 2019). The fat content in fish is often varying with season. The fish were caught during the months of August, September and October, following the breeding months of May to August (Teo et al., 2007). Goñi et. al. (Goñi & Arrizabalaga, 2010) showed a clear correlation between length and fat content in albacore and bluefin tuna. They also show an increase in fat content through the months of August, September and October.

Selenium showed only a statistically significant higher level in cut ten (Table 4.4.1 and Figure 4.4.2). However, there was also an appreciable variation between the other cuts. The fatty cuts had the lowest concentrations of 0.74 – 1.0 mg/kg, while the fillet cuts generally being higher e.g, cut six with 1.7 mg/kg. Kljaković-Gašpić et.al. (Kljaković-Gašpić & Tičina, 2021), found concentrations of 15 ± 5.2 mg/kg in red muscle, 1.9 ± 0.48 mg/kg in white muscle behind the head, 1.5 ± 0.32 mg/kg in white muscle from middle dorsal part and 1.6 ± 0.40 mg/kg in white muscle from the tail. This corresponds to this studies' 16 ± 7.8 mg/kg in cut 18, 0.96 ± 0.27 mg/kg in cut two, 1.8 ± 0.85 mg/kg in cut three and 1.2 ±0.78 mg/kg in cut five. These numbers underline that red muscle contains the highest concentrations of selenium, often by a factor of ten.

Mercury and methylmercury were distributed as expected, accumulating primarily in the protein rich tissue (Table 4.4.1, Figure 4.4.3 and Figure 4.4.4), with their aforementioned strong affinity for thiol groups, and even stronger affinity for the selenohydryl group (Sugiura et al., 1978). Methylmercury showed a different distribution than total mercury. Both mercury and methylmercury showed highest levels in cut ten, this was statistically similar to all other filet cuts for methylmercury, except for the fatty samples (cut one, eight and nine). Mercury however, had four levels with the highest concentration in cut ten, and the lowest in the aggregate fat sample, cut one. The two belly samples that were low in methylmercury had medium-low levels of mercury, and the remaining filet cuts had medium-high levels. Considering that methylmercury concentrations are higher than total mercury in all samples except 17 and 18, this difference in distribution is possibly attributed to methodological differences. Kljaković-Gašpić et.al (Kljaković-Gašpić & Tičina, 2021) found total mercury levels of 1.9 ± 0.76 mg/kg in red muscle, 1.4 ± 0.45 mg/kg in white muscle behind the head, 1.3 ± 0.52 mg/kg in white muscle from middle dorsal part and 1.4 ± 0.48 mg/kg in white muscle from the tail of ABFT. These samples can be compared to 1.4 ± 0.50 in cut 18, 0.74 ± 0.23 in cut two, 0.86 ± 0.27 in cut three and 0.82 ± 0.29 in cut five. Both studies, suggest a distribution with red meat being appreciably richer in mercury and the lean white muscle samples lower and very similar to one another, and fatty white muscle with the lowest concentrations. Kljaković-Gašpić et.al however, found higher concentrations of mercury in smaller ABFT caught in the Adriatic sea. Other studies report concentrations of: 0.23 ± 0.05 mg/kg to 0.36 ± 0.02 mg/kg in farmed southern bluefin tuna of 16 to 42 kg (Balshaw et al., 2008), 0.49 ± 0.037 mg/kg to 0.72 ± 0.029 mg/kg in cultured pacific bluefin tuna of 22 to 62 kg (Ando et al., 2008), 0.88 ± 0.30 mg/kg to 0.72 ± 0.23 mg/kg in wild yellowfin tuna of 29 to 51 kg (Bosch et al., 2016), 1.7 ± 0.6 mg/kg in wild Atlantic bluefin tuna of 45 ± 26 kg (Annibaldi et al., 2019) and 0.96 ± 0.39 mg/kg to 0.53 ± 0.21 mg/kg in wild Atlantic bluefin tuna of 127 to 320 kg (Piras et al., 2020), comparable to the present study.

An assessment of the food safety aspect of mercury and methylmercury is given in table 4.5.2. The mercury content in the measured samples exceeds the maximum level for trade of 1 mg/kg WW in 22% of the cases. The percentage of exceedances does not take measurement uncertainty into account. A consumption of 83 grams red muscle (cut 18) and 599 grams of pure fat (cut one) would fulfill the TWI at 1.6 µg/kg BW for a person of an assumed body weight of 70kg. These are the

two most extreme cases. For the suggested representative fillet sample (cut five), a consumption of 136 grams fulfills the TWI, and it exceeds the maximum level for trade in 36% of the cases. The National Health Services in Great Britain (NHS) recommended a tuna portion of 140g per meal (NHS, 2018). Following the data from sample five, a person weighing 70 kilograms could eat one tuna meal weekly, in regards to the TWI given by JECFA (EFSA, 2012). As outlined in section 2.5.2, selenium can counteract the toxic effects of mercury, and a ratio of or above 1 (Se:Hg) has been suggested to be protective (Kljaković-Gašpić & Tičina, 2021). The Se:Hg ratios are above one in all cuts (Table 4.5.1), stating an excess of selenium. E.g. sample five having a ratio of 3.7. Kljaković-Gašpić et.al found ratios of 22 ± 8.5 in red muscle, 3.7 ± 1.5 in white muscle behind the head, 3.2 ± 1.2 in white muscle from middle dorsal part and 3.1 ± 0.92 in white muscle from the tail. This is comparable to the corresponding ratios in similar cuts in the present study of 29, 3.3, 5.3 and 3.7, respectively. The TWI set by EFSA is lower at 1.3 µg/kg BW (EFSA, 2012), than the one by JECFA. The methylmercury concentration is arguably more relevant when assessing food safety as it is the most toxic among the mercury compounds (Hong et al., 2012). Codex gives a higher maximum level for trade of methylmercury at 1.2 mg/kg WW (CODEX, 2018) compared to the European Commission's on total mercury at 1.0 mg/kg WW (EC, 2006). The European Commission has reserved itself from setting a maximum level for trade on methylmercury. Following the value set by Codex, it would be allowed for more of the samples to be sold for consumption. However, the European Commission implements legislation, and therefore it is their maximum trade level for trade of total mercury that is enforced.

Lead was observed at levels below limit of quantification (0,030 mg/kg dw (IMR, 2020b)). Similar results were found by Núñez et. al. (Núñez et al., 2018) in yellowfin tuna and albacore tuna (fresh and packaged in cans or on glass). Storelli et. al. report 0.10 ± 0.03 mg/kg in wild Atlantic bluefin tuna muscle. Due to lead not being found at significant levels, its toxicity is considered negligible.

Cadmium showed an ambiguous distribution compared to the other investigated contaminants (Table 4.4.1 and Figure 4.4.5). Cadmium appears at high levels both in the fatty tissue of cut one and nine, and in the red muscle, of cut ten. The highest value of cadmium is observed in cut 18 at 0.042 ± 0.022 mg/kg suggesting a higher rate of accumulation in red muscle, similar to mercury. This can possibly be explained by cadmium usually being bound to sulfhydryl group-containing protein (Bernhoft, 2013). The present study reports a mean of 0.014 ±0.0090 mg/kg. Girolametti

et. al. (Girolametti et al., 2021) investigated potential toxic elements in wild and farmed ABFT, following the same sampling procedure as Annibaldi (Annibaldi et al., 2019). They reported concentrations of 0.014 ± 0.006 mg/kg and 0.021 ± 0.020 mg/kg for wild and farmed fish, respectively. Storelli et. al. investigated accumulation of mercury, cadmium, lead and arsenic in bluefin tuna from the Mediterranean Sea (Storelli et al., 2005). They reported cadmium a concentration of 0.02 ± 0.01 mg/kg, similar to the findings in the present study.

An assessment of the food safety aspect of cadmium is given in table 4.5.2. Cadmium concentrations determined in this study are significantly below the maximum level for trade of 0.1 mg/kg WW, showing no exceedances in any sample. Cut 18, containing the highest amount of cadmium allows for 4.2 kg consumed before exceeding the TWI. Cadmium toxicity is thus considered negligible.

Arsenic accumulated most in the fatty tissue (Table 4.4.1 and Figure 4.4.6), showing the highest levels in the aggregate fat sample, of cut one. The second highest concentrations were found in cuts eight and nine, second lowest in cuts two, six and ten and lowest in the remaining samples. This distribution might be explained by arsenic being present as both water soluble and lipid soluble arsenic species. Taleshi et. al. reported an approximate even distribution between these two in sashimi tuna (Taleshi et al., 2010). The mean concentration found in this study of total arsenic was 2.3 ± 1.3 mg/kg. This is consistent with other studies reporting 2.6 ± 1.5 mg/kg (Storelli et al., 2005) and 3.8 ± 2.2 mg/kg (Núñez et al., 2018).

The food safety aspect of arsenic has not been evaluated as there is no current TWI set. There previously was set a TWI for arsenic at 15 µg/kg BW (FAO, 1989). This was removed in 2011 however, as it was evaluated as not being health protective since no safe level of arsenic exposure could be established (FAO, 2011). As most of the arsenic found in fish is in its organic form, arsenic toxicity is considered negligible (Francesconi & Kuehnelt, 2004).

The persistent organic pollutants PCDD/F and PCDD/F + dl-PCBs show a clear accumulation in the fatty tissue (Table 4.4.1, Figure 4.4.7 and Figure 4.4.8), as these substances are characteristically lipophilic (Moser & McLachlan, 2001). There was a small variation between the two groups with and without dioxin-like PCBs, with PCDD/F showing high levels in cuts one, eight and nine. PCDD/F + dl-PCBs had the highest levels in cut one, and second highest in eight

and nine. Both distributions then had the neck sample, cut two, as a level above the remaining fillet cuts. It is important to be mindful of which version of the TEF factors is used when comparing numbers reported in the literature since there are different versions from both 1998 and 2005. Kawakami et. al (Kawakami et al., 2010), using the 2005 factors, report concentrations of 0.13 pg/g to 0.42 pg/g in akami, 0.8 pg/g to 1.2 pg/g in chu-toro and 2.0 pg/g to 2.7 pg/g in O-toro for PCDD/F in three wild bluefin tuna. They also report 1.0 pg/g to 2.1 pg/g, 5.0 pg/g to 7.2 pg/g and 12 pg/g to 23 pg/g in the same cuts for PCDD/F + dl-PCBs. These results are within the same range as reported in the present study. Padula et. al. (Padula et al., 2008), using the 1998 factors, investigated POPs in wild and farmed Australian SBFT. They reported low numbers of 0.27 pg/g in wild and 0.61 pg/g in farmed tuna. The southern bluefin tuna investigated in that study however, had a low lipid content at 0.9% for wild and 11% for farmed fish, providing a possible explanation.

Table 4.5.2 includes an assessment of the food safety aspect of dioxins, furans with and without dioxin-like PCBs. The PCDD/F's only show exceedances of the maximum level for trade in the fatty samples of cuts one, eight and nine with 17%, 20% and 17%, respectively. When the dioxin like PCBs are included however, they are the group that exceed the maximum level most frequently. They also allow for the smallest amount of tissue eaten before exceeding the TWI of 2 pg TEQ/kg BW. In the worst case, for pure fat (cut one), only 6.2 grams of tissue can be eaten weekly before exceeding this threshold. Furthermore, the concentrations of PCDD/F + dl-PCBs are above the maximum level for trade of 6.5 pg/g WW (given in EC1881/2006 latest consolidated version) in all cases for the fatty cuts one, eight and nine. In total, 37% of the measurements exceeded the maximum level for trade, which is the highest frequency of any contaminant investigated here. **PCB-6** showed similar levels of exceedances as PCDD/F + dl-PCBs (Table 4.5.2) with concentrations shown in table 4.4.1. As for dioxins, furans and dioxin like PCBs, PCB-6 surpass the maximum level for trade set at 75ng/g in all cases for the fatty samples, cuts one, eight and nine. This suggests that it is the PCB portion that contributes most to the sum of PCDD/F + dl-PCBs.

The statistical models for the distributions did not benefit significantly from including length as a predictor. This is unexpected, as it has been proved for other tuna species that individuals are proven to accumulate contaminants as they grow. Studies show a positive correlation between mercury content and length e.g. in yellowfin tuna (Ordiano-Flores et al., 2011) and in three

different tuna species (Adams, 2004). A possible reason for this is that the ABFT investigated in the present study did not vary greatly in length. The weights were not recorded in this study as the ABFT were caught far offshore, and big enough balances were not available at sea. The fish were often gutted on the way to land, making weighing each individual difficult.

5.6 Suggested sampling

The present study attempted to arrive at a convenient sampling procedure resulting in the most representative results. Piras (Piras et al., 2020) postulates that for Hg analysis a composite sample of white meat may give the most accurate representation of mercury levels in ABFT. Producing such a sample of a large fish is however costly and time consuming. Piras further concludes, in agreement with Balshaw (Balshaw et al., 2008) that an anterior portion of the upper loin could serve as representative for the average mercury contencentration in white muscle tissue. However, due to the large variation within the different muscles/fillets of ABFT, it is difficult to establish one sample that represents the distribution in all muscle parts for all the investigated contaminants well. Based on the current data, it is therefore suggested to take three samples to obtain an accurate view of contaminant concentrations within the muscle/fillet of ABFT. Cut one, extremely rich in fat is proposed as a worst case representative for contaminants that accumulate in lipid-rich tissue, mainly the persistent organic pollutants. The second sample proposed is cut five, as a representative for the average fillet, and the main portion of the tuna eaten. Cut five is poroposed due to it being statistically similar to the other lean fillet samples in almost all distributions. The representability of sample five is supported by Ando et. al. showing that the tail sample was statistically similar in mercury content to all other cuts investigated except for the ventral frontal sample, with a lower mercury content (Ando et al., 2008). Moreover, cut five is economically favorable, being a less attractive commercial cut. This cut is often taken at the fish processing plant before trade to visually examine the fat content and quality of the fish. The last sample proposed is cut ten, for the lean, red muscle. Cut ten would serve as a worst case representative for contaminants that acculamate in protein-rich tissue, mainly mercury. This is also in accordance with Codex, suggesting sampling muscle from the tail for fish above 10 kg with a value of above 10 USD/kg in their discussion paper on methylmercury in fish (Codex, 2021).

As mentioned, it is preferable to reduce the amount of samples while still being representative. Given enough data, it might be possible to determine models/conversion factors e.g. based on cut five to estimate the distribution of the contaminants for the other cuts, and thereby the whole fillet of ABFT. The relationship between fat and mercury and fat and POPs for the six fish that had POPs analyses were investigated (Figure 4.4.9 and 4.4.10). Significant correlations between fat and mercury ($R^2 = 0.45$) and fat and POPs (R2 =0.56) were found. This suggests that fat might be a good predictor for these contaminants. Using fat as a predictor for the contaminants is economically beneficial as it is a cheap and quick analysis to conduct. The relationship between mercury and POPs for the same six fish (Figure 4.4.11) was weaker ($R^2 = 0.12$). The sample size is low for these relationships, and extreme singular values might skew them. It is therefore advised to continue investigating the distribution of these contaminants in ABFT when establishing a representative sampling procedure and models that predict the distributions.

5.7 ABFT as food

Considering table 4.5.2 it is evident that the POPs are the contaminants that allows the least amount of tissue eaten before exceeding the TWI. This is exemplified in cut 18, containing the highest levels of mercury and lowest levels of POPs. Consuming 83 grams of cut 18, would be enough exceed the weekly tolerable intake for mercury, but a meal of 53 grams would be enough to exceed the TWI for PCDD/F + dl-PCBs. This underlines that even though mercury is present in high concentrations and its toxicity should be taken seriously, POPs are even more limiting. Some of the cuts contain high concentrations of POPs and are above the maximum level, making them unsuitable for trade. This is the case for cuts one, eight and nine, exceeding the maximum level allowed for POPs in all samples from all fish. Other cuts like four, five and 18 exceeded the maximum level for trade for mercury in 40%, 36% and 50% of the samples, respectively. The most representative view on the majority of the eaten tissue is given by the average fillet sample, cut five. Cut five exceeded the TWIs for mercury given by JECFA, and EFSA and POPs at an amount of 136 grams, 107 grams and 37 grams tissue consumed, respectively. Moreover, cut five's mercury concentration exceeded the maximum level in 36% of the fish, methylmercury concentration in 20% of the fish and POPs concentration in 17% of the fish. One hundred and forty grams of meat is assumed as an ordinary amount of tuna meat in a dinner (NHS, 2018). A person weighing 70 kg would exceed the TWI on POPs almost four times if 140 grams of cut five was

consumed. When considering mercury alone it is possible to recommend a different number of weekly servings of tuna fillets considering their different mercury content. This is done by Balshaw et. al., suggesting two additional weekly serving of o-toro or one additional weekly serving of chu-toro in comparison to akami (Balshaw et al., 2008). Due to the low TWI of POPs they exceed this level at small concentrations, making different serving recommendations based on cut taken infeasible. When discussing the possible amount of consumed tuna tissue before exceeding the TWI it is important to note that the TWI accounts for all exposure to a toxicant. This means that if a person would eat ABFT in amounts right below the TWI for a given contaminant, but also ate other foods that contained the same contaminant, they would exceed the TWI. Therefore, caution is advised even when following the TWIs.

Annibaldi et al. show greater concentrations of mercury in wild than farmed tuna (Annibaldi et al., 2019). This is expected as they are exposed to more contaminants in the wild diet than in the farmed, controlled diet. Thus, farming tuna might contribute to provide tuna tissue with lower amounts of contaminants for human consumption. However farming ABFT in Norway is not established.

As discussed earlier, ABFT is a good source of unsaturated fatty acids and the essential trace element selenium, in addition to tunas often being rich in vitamin D and B12 (WebMD, 2021). However, as extensively discussed, ABFT are also a source of accumulated contaminants. The benefits versus the risks of eating ABFT is compared below. Typically, between the threshold of adequacy for nutrients and the maximum safe dose for contaminants is where the “window of benefit” is located (Thomsen et al., 2021). The two contaminants that are of concentrations that limit intake are mercury and PCDD/F + dl-PCBs. Thomsen et. al. found that in 106 risk benefit assessments of fish and other seafood the most frequently included beneficial components were polyunsaturated fatty acids, and selenium. The most commonly included hazardous components were dioxins, dioxin-like PCBs and methylmercury (Thomsen et al., 2021), consistent with this study. Cut five allows for 37 grams eaten regarding its TWI on POPs. Assuming the fish meat portion of a sashimi piece is 15 grams, a person weighing 70kg could eat a little more than two pieces weekly. As mentioned earlier, the TWI factors in all exposure to a contaminant, meaning eating 37 grams of ABFT sample five, no other food containing PCDD/F and dl-PCBs can be consumed to stay beneath the threshold. The TWI for PCDD/F + dl-PCB is 2 pg/kg bodyweight,

which was set in 2018. The TWI is set as low as it is to protect against adverse effects on semen quality, amongst other things. The toxicity of the most harmful dioxin-like PCBs may be overestimated however, and European Food Safety Authority's expert Panel on Contaminants in the Food Chain (CONTAM) would support a review of the toxic equivalent factors for both dioxins and dioxin-like PCBs (EFSA, 2018).

6 Conclusion and future perspectives

The aim of the study was to investigate the distribution of contaminants as well as fat and selenium in individual ABFTs. This was performed by sampling 11 ABFT in the years 2018, 2019 and 2020, off the Norwegian coast. When preparing the samples, challenges were encountered during the homogenization process of the samples, primarily in the fatty samples and sinewy samples. A cryo-mill was successfully used to improve the homogenization of the selected samples.

Four analyses were conducted on the samples. The total fat content was determined at 26 ± 18% in all samples investigated in ABFT. Selenium concentrations were 1.8 ± 2.7 mg/kg WW. Total mercury and methylmercury were determined at 0.72 ± 0.33 mg/kg WW and 0.76 ± 0.34 mg/kg WW, respectively. Lead was under the limit of quantification and its distribution was not possible to assess. Cadmium was found at 0.014 ± 0.0090 mg/kg WW, and Arsenic at 23 ± 1.3 mg/kg WW. The POPs were of the concentrations 1.2 ± 1.1 pg/g, 8.0 ± 8.4 pg/g and 100 ± 121 ng/g for PCDD/F, PCDD/F + dl-PCB and PCB-6, respectively. The investigated substances all distributed themselves throughout the ABFT carcass as expected. The concentrations of most of the contaminants were comparable to other studies conducted on ABFT or other tuna species. The persistent organic pollutants were high however, possibly explained by the high fat content. Fat showed a significant negative correlation to mercury (R^2=0.45) and a significant positive correlation to POPs (R^2=0.56).

It was desired to reduce the number of samples taken, and it was possible to suggest reducing this from ten to three. The suggested cuts are, the aggregate fat sample (cut one), the tail sample (cut five) and the red muscle sample (cut ten).

Mercury and POPs represent the two toxicities of concern in the edible tuna tissues investigated. In the tail sample (cut five), an amount of 136 grams can be eaten before exceeding the TWI for mercury (1.6 µg/kg BW) and it surpassed the maximum level for trade (1.0 mg/kg WW) in 36%

of the fish investigated. POPs allow for less tuna eaten, in all samples. In cut five specifically, 37 grams of tissue fills the TWI for POPs (2 pg TEQ/kg BW) and 17% of the fish were above the maximum level for trade (6.5 pg/g WW). The molar ratio of selenium to mercury was above one in all samples, indicating a surplus.

Future perspectives

Suggested further studies include working on a homogenization procedure that efficiently homogenizes all sample matrices presented by the ABFT. Evaluating the nutrient content of ABFT to be able to better assess risks and benefits of ABFT as food, is desirable. Also, continuing to sample and analyze ABFT for contaminants to get a broader knowledge of the contaminant load. These numbers from the contaminant analyses can further be used to establish models that predict values for the entire ABFT from one sample. It is recommended to investigate if fat content could be a reliable predictor for contaminants, and if so, establish a model that predicts values for contaminants. Similarly, investigate if PCB6 is a good indicator for total PCDD/F + dl-PCB content, and if so, establish a model that can predict the total POPs concentrations from PCB6.

7 References

ABCNews (2006). Giant Tuna Sells for Record $173,600. Retrieved 30.09.2021 from https://abcnews.go.com/International/story?id=81767&page=1.

Abu-Samra, A., Morris, J. S., & Koirtyohann, S. (1975). Wet ashing of some biological samples in a microwave oven. *Analytical Chemistry, 47*(8), 1475.

Adams, D. H. (2004). Total mercury levels in tunas from offshore waters of the Florida Atlantic coast. *Marine pollution bulletin, 49*(7), 659.

Ajsuvakova, O. P., Tinkov, A. A., Aschner, M., Rocha, J. B., Michalke, B., Skalnaya, M. G., Skalny, A. V., Butnariu, M., Dadar, M., & Sarac, I. (2020). Sulfhydryl groups as targets of mercury toxicity. *Coordination chemistry reviews, 417*, 213343.

Albert, C. M., Campos, H., Stampfer, M. J., Ridker, P. M., Manson, J. E., Willett, W. C., & Ma, J. (2002). Blood levels of long-chain n–3 fatty acids and the risk of sudden death. *New England Journal of Medicine, 346*(15), 1113.

Ando, M., Seoka, M., Nakatani, M., Tsujisawa, T., Katayama, Y., Nakao, M., Tsukamasa, Y., & Kawasaki, K.-i. (2008). Trial for quality control in mercury contents by using tail muscle of full-cycle cultured bluefin tuna (*Thunnus orientalis*). *Journal of food protection, 71*(3), 595.

Annibaldi, A., Truzzi, C., Carnevali, O., Pignalosa, P., Api, M., Scarponi, G., & Illuminati, S. (2019). Determination of Hg in farmed and wild atlantic bluefin tuna (*Thunnus thynnus* L.) muscle. *Molecules, 24*(7), 1273.

Artioli, G., & Angelini, I. (2010). *Scientific methods and cultural heritage: an introduction to the application of materials science to archaeometry and conservation science*: Oxford University Press.

ASQ (2021). CONTROL CHART. Retrieved 30.09.2021 from https://asq.org/quality-resources/control-chart.

Azad, A. M., Frantzen, S., Bank, M. S., Nilsen, B. M., Duinker, A., Madsen, L., & Maage, A. (2019). Effects of geography and species variation on selenium and mercury molar ratios in Northeast Atlantic marine fish communities. *Science of The Total Environment, 652*, 1482.

Balshaw, S., Edwards, J. W., Ross, K., & Daughtry, B. (2008). Mercury distribution in the muscular tissue of farmed southern bluefin tuna (*Thunnus maccoyii*) is inversely related to the lipid content of tissues. *Food Chemistry, 111*(3), 616.

Bernhoft, R. A. (2013). Cadmium toxicity and treatment. *The Scientific World Journal, 2013*.

BiteSizeBio (2016). A Gas Chromatography System. Retrieved 30.09.2021 from https://bitesizebio.com/28687/carrying-gas-chromatography/.

Blanchard, W. (2011). Inductively Coupled Plasma. Retrieved 30.09.2021 from https://commons.wikimedia.org/w/index.php?curid=27531915.

Block, B. A., Dewar, H., Blackwell, S. B., Williams, T. D., Prince, E. D., Farwell, C. J., Boustany, A., Teo, S. L., Seitz, A., & Walli, A. J. S. (2001). Migratory movements, depth preferences, and thermal biology of Atlantic bluefin tuna. *Science, 293*(5533), 1310.

Boge, E. (2019). *The return of the Atlantic bluefin tuna to Norwegian waters.* (Thesis, MSc). Depat. biol. sci., The University of Bergen, 1-84.

Bosch, A. C., O'Neill, B., Sigge, G. O., Kerwath, S. E., & Hoffman, L. C. (2016). Mercury accumulation in Yellowfin tuna (*Thunnus albacares*) with regards to muscle type, muscle position and fish size. *Food Chemistry, 190*, 351.

Carey, F. G. (1973). Fishes with warm bodies. *Scientific American, 228*(2), 36.

Cattaneo-Vietti, R., Cappanera, V., Castellano, M., & Povero, P. (2015). Yield and catch changes in a Mediterranean small tuna trap: a warming change effect? *Marine Ecology, 36*(2), 155.

CDC (2009). Mercury. Retrieved 30.09.2021 from https://www.cdc.gov/biomonitoring/pdf/Mercury_FactSheet.pdf.
CDC (2015). Alara - As Low As Reasonably Achievable Retrieved 30.09.2021 from https://www.cdc.gov/nceh/radiation/alara.html.
Chapman, E. W., Jørgensen, C., & Lutcavage, M. E. (2011). Atlantic bluefin tuna (*Thunnus thynnus*): a state-dependent energy allocation model for growth, maturation, and reproductive investment. *Canadian Journal of Fisheries and Aquatic Sciences, 68*(11), 1934.
Chavoshani, A., Hashemi, M., Amin, M. M., & Ameta, S. C. (2020). *Micropollutants and challenges: emerging in the aquatic environments and treatment processes*: Elsevier.
Chou, C.-H., & Harper, C. (2007). *Toxicological profile for arsenic*. Atlanta, Georgia, USA: Agency for Toxic Substances and Disease Registry.
Codex (2007). *Codex Alimentarius Commission: Procedural Manual. 17 edition*. Rome, Italy: Food and Agriculture Organization of the United Nations.
CODEX (2018). CODEX COMMITTEE ON CONTAMINANTS IN FOODS 12th Session.
Codex (2021). DISCUSSION PAPER ON METHYLMERCURY IN FISH.
CONTAM (2012). Scientific Opinion on the risk for public health related to the presence of mercury and methylmercury in food. *Efsa Journal, 10*(12), 2985.
Cook-Botelho, J., Bachmann, L., & French, D. (2017). Steroid hormones. In *Mass Spectrometry for the Clinical Laboratory* (pp. 205): Elsevier.
Crichton, N. (1999). Information point: tukey multiple comparison test. *Journal of Clinical Nursing, 8*, 299.
Donohue, J. M., & Abernathy, C. O. (1999). Exposure to inorganic arsenic from fish and shellfish. In *Arsenic Exposure and Health Effects III* (pp. 89-98): Elsevier.
Druon, J.-N., Fromentin, J.-M., Hanke, A. R., Arrizabalaga, H., Damalas, D., Tičina, V., Quílez-Badia, G., Ramirez, K., Arregui, I., & Tserpes, G. (2016). Habitat suitability of the Atlantic bluefin tuna by size class: An ecological niche approach. *Progress in Oceanography, 142*, 30.
DSP-Systems (2021). Fully Automated Sample Preparation System for POPs Analysis GO-EHT. Retrieved 24.04.2021 from https://www.dspsystems.eu/wp-content/uploads/2019/12/Brochure-DSP-GO-EHT.pdf.
EC (1993). Council Regulation (EEC) No 315/93 of 8 February 1993 laying down Community procedures for contaminants in food. *Official Journal of the European Union, 37*(13/02), 1.
EC (2006). Commission Regulation (EC) No 1881/2006 of 19 December 2006 setting maximum levels for certain contaminants in foodstuffs. *Official Journal of the European Union, 364*.
ECoS (2018). Residuals vs. Fits Plot. Retrieved 30.09.2021 from https://online.stat.psu.edu/stat462/node/117/.
EFSA (2012). Mercury in food – EFSA updates advice on risks for public health. Retrieved 30.09.2021 from https://www.efsa.europa.eu/en/press/news/121220.
EFSA (2018). Dioxins and related PCBs: tolerable intake level updated. Retrieved 30.09.2021 from https://www.efsa.europa.eu/en/press/news/dioxins-and-related-pcbs-tolerable-intake-level-updated.
Endo, T. (2013). *Special Report: Serving Japanese Food to the World, Aided by the Health Conscious Boom*. Retrieved from Jetro.go.jp:
EPA (2007). Method 3051A microwave assisted acid digestion of sediments, sludges, soils, and oils. *Zeitschrift für Analytische Chemie, 111*, 362.
EPA (2009). Persistent Organic Pollutants: A Global Issue, A Global Response. Retrieved 27.09.2021 from https://www.epa.gov/international-cooperation/persistent-organic-pollutants-global-issue-global-response.
Eurachem (2014). The Fitness for purpose of analytical methods 2nd Edition.

Eurachem (2019). Measurement uncertainty arising from sampling A guide to methods and approaches, 2nd Edition.
FAO (1983). FAO Fisheries Synopsis No. 125, Volume 2.
FAO (1989). *Evaluation of certain food additives and contaminants: thirty-third report of the Joint FAO*: World Health Organization.
FAO (2011). Evaluation of certain contaminants in food Seventy-second report of the Joint FAO/WHO Expert Committee on Food Additives. *World Health Organization technical report series*(959), 1.
FAO (2021). Cultured Aquatic Species Information Programme: *Thunnus thynnus* (Linnaeus, 1758). Retrieved 30.09.2021 from http://www.fao.org/fishery/culturedspecies/Thunnus_thynnus/en.
Faroon, O., Ashizawa, A., Wright, S., Tucker, P., Jenkins, K., Ingerman, L., & Rudisill, C. (2013). *Toxicological profile for cadmium*. Atlanta, Georgia, USA: Agency for Toxic Substances and Disease Registry.
Fisher, J. F. (2003). *Elemental mercury and inorganic mercury compounds: human health aspects* (9241530502). Atlanta, Georgia, USA.
Francesconi, K. A., & Kuehnelt, D. (2004). Determination of arsenic species: a critical review of methods and applications, 2000–2003. *Analyst, 129*(5), 373.
Frieden, E. (1985). New perspectives on the essential trace elements. *Journal of Chemical Education, 62*(11), 915.
Fromentin, J.-M., Bonhommeau, S., Arrizabalaga, H., & Kell, L. T. (2014). The spectre of uncertainty in management of exploited fish stocks: The illustrative case of Atlantic bluefin tuna. *Marine Policy, 47*, 8.
Fromentin, J.-M., & Powers, J. E. (2005). Atlantic bluefin tuna: population dynamics, ecology, fisheries and management. *Fish and Fisheries, 6*(4), 281.
Fromentin, J.-M., & Ravier, C. (2005). The East Atlantic and Mediterranean bluefin tuna stock: looking for sustainability in a context of large uncertainties and strong political pressures. *Bulletin of Marine Science, 76*(2), 353.
Galuardi, B., Royer, F., Golet, W., Logan, J., Neilson, J., & Lutcavage, M. (2010). Complex migration routes of Atlantic bluefin tuna (*Thunnus thynnus*) question current population structure paradigm. *Canadian Journal of Fisheries and Aquatic Sciences, 67*(6), 966.
Garelick, H., Jones, H., Dybowska, A., & Valsami-Jones, E. (2009). *Arsenic pollution sources*. Summerfield, North Carolina, USA.
Genchi, G., Sinicropi, M. S., Lauria, G., Carocci, A., & Catalano, A. (2020). The effects of cadmium toxicity. *International journal of environmental research and public health, 17*(11), 3782.
Girolametti, F., Annibaldi, A., Carnevali, O., Pignalosa, P., Illuminati, S., & Truzzi, C. (2021). Potential toxic elements (PTEs) in wild and farmed Atlantic bluefin tuna (*Thunnus thynnus*) from Mediterranean Sea: Risks and benefits for human consumption. *Food Control, 125*, 108012.
Godt, J., Scheidig, F., Grosse-Siestrup, C., Esche, V., Brandenburg, P., Reich, A., & Groneberg, D. A. (2006). The toxicity of cadmium and resulting hazards for human health. *Journal of Occupational Medicine Toxicology, 1*(1), 22.
Goñi, N., & Arrizabalaga, H. (2010). Seasonal and interannual variability of fat content of juvenile albacore (*Thunnus alalunga*) and bluefin (*Thunnus thynnus*) tunas during their feeding migration to the Bay of Biscay. *Progress in Oceanography, 86*(1-2), 115.
Graham, J. B., & Dickson, K. A. (2001). Anatomical and physiological specializations for endothermy. *Fish physiology, 19*, 121.
Gutleb, A. C., Arvidsson, D., Örberg, J., Larsson, S., Skaare, J. U., Aleksandersen, M., Ropstad, E., & Lind, P. M. (2010). Effects on bone tissue in ewes (*Ovies aries)* and their foetuses exposed to PCB 118 and PCB 153. *Toxicology letters, 192*(2), 126.
Guzzi, G., & La Porta, C. A. (2008). Molecular mechanisms triggered by mercury. *Toxicology, 244*(1), 1.

Hitchcock, R. T. (2004). *Radio-frequency and microwave radiation*: AIHA.
Hong, Y.-S., Kim, Y.-M., & Lee, K.-E. (2012). Methylmercury exposure and health effects. *Journal of Preventive Medicine and Public Health, 45*(6), 353.
Horiguchi, H., Oguma, E., Sasaki, S., Miyamoto, K., Ikeda, Y., Machida, M., & Kayama, F. (2004). Dietary exposure to cadmium at close to the current provisional tolerable weekly intake does not affect renal function among female Japanese farmers. *Environmental Research, 95*(1), 20.
Hutton, M. (1983). Sources of cadmium in the environment. *Ecotoxicology and environmental safety, 7*(1), 9.
Hutton, M., & Meema, K. M. (1987). Human Health Concerns of Lead, Mercury, Cadmium and Arsenic. In *Lead, mercury, cadmium, and arsenic in the environment* (pp. 53-68).
Hyman, M. (2004). *The impact of mercury on human health and the environment.* Paper presented at the Tulane Univeristy School of Public Health and Tropical Medicine. General Meeting. Tulane Univeristy, New Orleans.
ICCAT (2008). Report from ICCAT stock assessment meeting madrid.
ICCAT (2010). Report from ICCAT stock assessment meeting madrid.
ICCAT (2017). International Commission for the Conservation of Atlantic Tunas, Basic texts 6th revision.
IMR (2020a). Metode 091 Fett bestemmelse, etylacetat metode.
IMR (2020b). Metode 197 Multielement bestemmelse med induktivt koblet plasma-massespektrofotometri (ICP-MS) etter våtoppslutning i mikrobølgeovn.
IMR (2020c). Metode 292 Dioxin, furan, PCB og PBDE.
IMR (2020d). Metode 377 Tørrstoffinnhold ved frysetørking.
IMR (2020e). Metode 390 Metylkvikksølvbestemmelse v/isotopfortynning, GCICPMS.
IMR (2021). Oppslutning med UltraWave og UltraClave Prøveopparbeiding til metode nr. 197 og nr. 382.
Inczédy, J., Lengyel, T., Ure, A. M., Gelencsér, A., & Hulanicki, A. (1997). *Compendium of analytical nomenclature 3rd edition*: Hoboken: Blackwell Science.
ISO (2004). International Vocabulary of Basic and General Terms in Metrology (VIM) 3rd edition.
ISO (2017). ISO/IEC 17025:2017 - General requirements for the competence of testing and calibration laboratories.
Jaishankar, M., Tseten, T., Anbalagan, N., Mathew, B. B., & Beeregowda, K. N. (2014). Toxicity, mechanism and health effects of some heavy metals. *Interdisciplinary toxicology, 7*(2), 60.
JHSPH (2021). U-Shaped Dose-Response. Retrieved 30.09.2021 from http://ocw.jhsph.edu/index.cfm/go/imageLib:il.viewImageDetails/resourceID/ADC04CCA-B540-A552-B574C6772C66D5AC/browseTopic/General%20Public%20Health/topicID/9/.
Jones, K. C., & De Voogt, P. (1999). Persistent organic pollutants (POPs): state of the science. *Environmental Pollution, 100*(1-3), 209.
Juberg, D. R., Kleiman, C. F., & Kwon, S. C. (1997). Position paper of the American Council on Science and Health: lead and human health. *Ecotoxicology Environmental Safety, 38*(3), 162.
Julshamn, K., Nilsen, B. M., Frantzen, S., Valdersnes, S., Maage, A., Nedreaas, K., & Sloth, J. J. (2012). Total and inorganic arsenic in fish samples from Norwegian waters. *Food Additives and Contaminants: Part B, 5*(4), 229.
Kawakami, H., Amakura, Y., Tsutsumi, T., Sasaki, K., Iketsu, A., Inasaki, M., Kubota, E., & Toyoda, M. (2010). Correlation of fat content and dioxins, total mercury and methyl mercury levels in tuna. *Shokuhin eiseigaku zasshi. Journal of the Food Hygienic Society of Japan, 51*(5), 258.
Kljaković-Gašpić, Z., & Tičina, V. (2021). Mercury and selenium levels in archive samples of wild Atlantic bluefin tuna from the Mediterranean Sea. *Chemosphere, 284*, 131402.
Lajunen, L. (2007). *Spectrochemical analysis by atomic absorption and emission*: Royal Society of Chemistry.

Lehnherr, I., Louis, V. L. S., Hintelmann, H., & Kirk, J. L. (2011). Methylation of inorganic mercury in polar marine waters. *Nature Geoscience, 4*(5), 298.
Lombardo, F., Gioacchini, G., Pappalardo, L., Baiata, P., Candelma, M., Pignalosa, P., & Carnevali, O. (2019). DETERMINATION OF LENGTH-WEIGHT EQUATION APPLICABLE TO ATLANTIC BLUEFIN TUNA (*THUNNUS THYNNUS*) IN THE MEDITERRANEAN SEA. *Collective Volumes of Scientific Papers ICCAT, 75*(6), 1392.
LOVDATA (1969) International Convention on the Conservation of Atlantic Tunas, 14-05-1966 nr 21 Multilateral C.F.R.
Luke, S. G. (2017). Evaluating significance in linear mixed-effects models in R. *Behavior research methods, 49*(4), 1494.
Luo, H., Cheng, Q., & Pan, X. (2020). Photochemical behaviors of mercury (Hg) species in aquatic systems: A systematic review on reaction process, mechanism, and influencing factor. *Science of The Total Environment, 720*, 137540.
Martin, S., & Griswold, W. (2009). Human health effects of heavy metals. *Environmental Science and Technology briefs for citizens*(15), 1.
MARUNAKA (2020). Retrieved 19.09.2020 from http://www.marunaka-net.co.jp/.
Mason, L. H., Harp, J. P., & Han, D. Y. (2014). Pb neurotoxicity: neuropsychological effects of lead toxicity. *BioMed research international, 2014*.
Mather, F. J., Mason, J. M., & Jones, A. C. (1995). Historical document: life history and fisheries of Atlantic bluefin tuna. NOAA Technical Memorandum NMFS-SEFSC. *370*, 165.
Mindess, S. (2019). *Developments in the Formulation and Reinforcement of Concrete*. University of British Columbia, Vancouver, BC, Canada: Woodhead Publishing.
Mohrig, J. R., Hammond, C. N., & Schatz, P. F. (2010). *Techniques in organic chemistry*: Macmillan.
Moser, G. A., & McLachlan, M. S. (2001). The influence of dietary concentration on the absorption and excretion of persistent lipophilic organic pollutants in the human intestinal tract. *Chemosphere, 45*(2), 201.
NHS (2018). Fish and shellfish nutrition. Retrieved 30.09.2021 from https://www.nhs.uk/live-well/eat-well/fish-and-shellfish-nutrition/.
NMKL (2007a). NMKL 186 Trace elements - As, Cd, Hg, Pb and other elements. Determination by ICP-MS after pressure digestion.
NMKL (2007b). NMKL Procedure 9 Evaluation of method bias using certified reference materials.
NOAA (2019). Fishing Gear: Purse Seines. Retrieved 30.09.2021 from https://www.fisheries.noaa.gov/national/bycatch/fishing-gear-purse-seines.
NRC (2000). *Toxicological effects of methylmercury*. Washington (DC), USA: National Academies Press.
NS (1994). NS9402 Atlantisk laks Måling av farge og fett.
NS (2016). EN16801 Næringsmidler Bestemmelse av elementer og deres kjemiske forbindelser Bestemmelse av metylkvikksølv ved isotop fortynning GC-ICP-MS i næringsmidler av marin opprinnelse.
Núñez, R., García, M. Á., Alonso, J., & Melgar, M. J. (2018). Arsenic, cadmium and lead in fresh and processed tuna marketed in Galicia (NW Spain): Risk assessment of dietary exposure. *Science of The Total Environment, 627*, 322.
Økland, H. M., Stoknes, I. S., Remme, J. F., Kjerstad, M., & Synnes, M. (2005). Proximate composition, fatty acid and lipid class composition of the muscle from deep-sea teleosts and elasmobranchs. *Comparative Biochemistry and Physiology Part B: Biochemistry and Molecular Biology, 140*(3), 437.
Olagunju, A., Muhammad, A., Bello, S., Mohammed, A., Mohammed, H. A., & T Mahmoud, K. (2012). Nutrient Composition of Tilapia zilli, Hemi-synodontis membranacea, Clupea harengus and

Scomber scombrus Consumed in Zaria. *World Journal of Life Sciences and Medical Research, 2*(1), 16.
Ordiano-Flores, A., Galván-Magaña, F., & Rosiles-Martínez, R. (2011). Bioaccumulation of mercury in muscle tissue of yellowfin tuna, *Thunnus albacares*, of the eastern Pacific Ocean. *Biological Trace Element Research, 144*(1), 606.
Padula, D. J., Daughtry, B. J., & Nowak, B. F. (2008). Dioxins, PCBs, metals, metalloids, pesticides and antimicrobial residues in wild and farmed Australian southern bluefin tuna (*Thunnus maccoyii*). *Chemosphere, 72*(1), 34.
Pearson-Scott-Foresman (2010). Illustration of basic seine net. Retrieved 30.09.2020 from https://commons.wikimedia.org/w/index.php?curid=10348700.
PerkinElmer (2011). The 30-Minute Guide to ICP-MS.
Piras, P., Bella, A., Cossu, M., Fiori, G., Sanna, A., & Chessa, G. (2020). A representative sampling of tuna muscle for mercury control. *Italian Journal of Food Safety, 9*(4).
Prichard, E., & Barwick, V. (2007). *Quality assurance in analytical chemistry* (Vol. 25): John Wiley & Sons.
Profillidis, V. A., & Botzoris, G. N. (2018). *Modeling of transport demand: Analyzing, calculating, and forecasting transport demand*: Elsevier.
Ralston, N. V., Ralston, C. R., Blackwell III, J. L., & Raymond, L. J. (2008). Dietary and tissue selenium in relation to methylmercury toxicity. *Neurotoxicology, 29*(5), 802.
Ravier, C., & Fromentin, J.-M. (2001). Long-term fluctuations in the eastern Atlantic and Mediterranean bluefin tuna population. *ICES Journal of Marine Science, 58*(6), 1299.
Rayman, M. P. (2012). Selenium and human health. *The Lancet, 379*(9822), 1256.
Rodriguez-Marin, E., Ortiz, M., De Urbina, J. M. O., Quelle, P., Walter, J., Abid, N., Addis, P., Alot, E., Andrushchenko, I., & Deguara, S. (2015). Atlantic bluefin tuna (*Thunnus thynnus*) biometrics and condition. *Public Library of Science, 10*(10).
Rodríguez-Ezpeleta, N., Díaz-Arce, N., Walter III, J. F., Richardson, D. E., Rooker, J. R., Nøttestad, L., Hanke, A. R., Franks, J. S., Deguara, S., & Lauretta, M. V. (2019). Determining natal origin for improved management of Atlantic bluefin tuna. *Frontiers in Ecology and the Environment, 17*(8), 439.
Rooker, J. R., Alvarado Bremer, J. R., Block, B. A., Dewar, H., De Metrio, G., Corriero, A., Kraus, R. T., Prince, E. D., Rodríguez-Marín, E., & Secor, D. H. (2007). Life history and stock structure of Atlantic bluefin tuna (*Thunnus thynnus*). *Reviews in Fisheries Science & Aquaculture, 15*(4), 265.
Ross, K., & Edwards, J. (2015). Spatial variation in the mercury concentration of muscle myomeres in steaks of farmed southern bluefin tuna. *Foods, 4*(2), 254.
Sandroni, V., & Smith, C. M. (2002). Microwave digestion of sludge, soil and sediment samples for metal analysis by inductively coupled plasma–atomic emission spectrometry. *Analytica Chimica Acta, 468*(2), 335.
Sharma, H., Rawal, N., & Mathew, B. B. (2015). The characteristics, toxicity and effects of cadmium. *International journal of nanotechnology and nanoscience, 3*, 1.
Storelli, M., Giacominelli-Stuffler, R., Storelli, A., & Marcotrigiano, G. (2005). Accumulation of mercury, cadmium, lead and arsenic in swordfish and bluefin tuna from the Mediterranean Sea: a comparative study. *Marine pollution bulletin, 50*(9), 1004.
Sugiura, Y., Tamai, Y., & Tanaka, H. (1978). Selenium protection against mercury toxicity: high binding affinity of methylmercury by selenium-containing ligands in comparison with sulfur-containing ligands. *Bioinorganic Chemistry, 9*(2), 167.
Taleshi, M. S., Edmonds, J. S., Goessler, W., Ruiz-Chancho, M. J., Raber, G., Jensen, K. B., & Francesconi, K. A. (2010). Arsenic-containing lipids are natural constituents of sashimi tuna. *Environmental science & technology, 44*(4), 1478.

Tangen, M. (2009). The Norwegian fishery for Atlantic bluefin tuna. *Collective Volumes of Scientific Papers ICCAT, 63*(1), 79.
Taylor, N. G., McAllister, M. K., Lawson, G. L., Carruthers, T., & Block, B. A. (2011). Atlantic bluefin tuna: a novel multistock spatial model for assessing population biomass. *Public Library of Science, 6*(12).
Teo, S. L., & Block, B. A. (2010). Comparative influence of ocean conditions on yellowfin and Atlantic bluefin tuna catch from longlines in the Gulf of Mexico. *Public Library of Science, 5*(5).
Teo, S. L., Boustany, A., Dewar, H., Stokesbury, M. J., Weng, K. C., Beemer, S., Seitz, A. C., Farwell, C. J., Prince, E. D., & Block, B. A. (2007). Annual migrations, diving behavior, and thermal biology of Atlantic bluefin tuna, Thunnus thynnus, on their Gulf of Mexico breeding grounds. *Marine Biology, 151*(1), 1.
Thomas, R. (2001). A beginner's guide to ICP-MS. *Spectroscopy, 16*(4), 38.
Thomsen, S. T., Assunção, R., Afonso, C., Boué, G., Cardoso, C., Cubadda, F., Garre, A., Kruisselbrink, J. W., Mantovani, A., & Pitter, J. G. (2021). Human health risk–benefit assessment of fish and other seafood: a scoping review. *Critical Reviews in Food Science and Nutrition*, 1.
Truzzi, C., Annibaldi, A., Illuminati, S., Antonucci, M., Api, M., Scarponi, G., Lombardo, F., Pignalosa, P., & Carnevali, O. (2018). Characterization of the fatty acid composition in cultivated atlantic bluefin tuna (*Thunnus thynnus* L.) Muscle by gas chromatography-mass spectrometry. *Analytical Letters, 51*(18), 2981.
USEPA (1994). USEPA1613 Tetra- through Octa-Chlorinated Dioxins and Furans by Isotope Dilution HRGC/HRMS .
USEPA (2010). USEPA1668C Chlorinated Biphenyl Congeners in Water, Soil, Sediment, Biosolids, and Tissue by HRGC/HRMS .
UVA (2015). Understanding Q-Q Plots. Retrieved 30.09.2021 from https://data.library.virginia.edu/understanding-q-q-plots/.
Van den Berg, M., Birnbaum, L. S., Denison, M., De Vito, M., Farland, W., Feeley, M., Fiedler, H., Hakansson, H., Hanberg, A., & Haws, L. (2006). The 2005 World Health Organization reevaluation of human and mammalian toxic equivalency factors for dioxins and dioxin-like compounds. *Toxicological Sciences, 93*(2), 223.
Veliyulin, E., van der Zwaag, C., Burk, W., & Erikson, U. (2005). In vivo determination of fat content in Atlantic salmon (*Salmo salar*) with a mobile NMR spectrometer. *Journal of the Science of Food and Agriculture, 85*(8), 1299.
Vockley, J. (2013). Organic Acidemias and Disorders of Fatty Acid Oxidation. In *Emery and Rimoin's Principles and Practice of Medical Genetics* (pp. 1-33): Elsevier.
Waalkes, M. P. (2003). Cadmium carcinogenesis. *Mutation Research/Fundamental and Molecular Mechanisms of Mutagenesis, 533*(1-2), 107.
Wardle, C., Videler, J., Arimoto, T., Franco, J., & He, P. (1989). The muscle twitch and the maximum swimming speed of giant bluefin tuna, *Thunnus thynnus* L. *Journal of fish biology, 35*(1), 129.
WebMD (2021). Health Benefits of Tuna. Retrieved 30.09.2021 from https://www.webmd.com/diet/health-benefits-tuna#1.
Webster, D. (2011). The irony and the exclusivity of Atlantic bluefin tuna management. *Marine Policy, 35*(2), 249.
White, S. S., & Birnbaum, L. S. (2009). An overview of the effects of dioxins and dioxin-like compounds on vertebrates, as documented in human and ecological epidemiology. *Journal of Environmental Science Health, Part C, 27*(4), 197.
Wilschefski, S. C., & Baxter, M. R. (2019). Inductively coupled plasma mass spectrometry: introduction to analytical aspects. *The Clinical Biochemist Reviews, 40*(3), 115.

Zhang, R., Wilson, V. L., Hou, A., & Meng, G. (2015). Source of lead pollution, its influence on public health and the countermeasures. *International Journal of Health, Animal Science and Food Safety, 2*(1).

8 Appendix

Prøvetakingsprotokoll for makrellstørje fanget langs norskekysten 2020 for å undersøke forskjellige mattrygghetsaspekter.

Prøvetakingsprosedyre

Prøver tas fra fisken uten skinn som vist på andre side.

Viktig å dokumentere lengde!

Innvollene i sin helhet skal bevares.

1: Ren fettprøve tatt rett under skinnet til fisken. Denne kan tas som vist på bildet, eller andre steder der dere finner mye fett.

2: Nakkekjøtt fra den ene siden av hodet.

På prøvene 3-7 er det viktig å kutte hele veien ned til beinet, slik at prøven blir et «tverrsnitt» av

fisken. Det er ofte hensiktsmessig å fjerne fiskeskjellene med en skarp kniv for å klare å kutte gjennom

skinnet. Tykkelse ca. 2-3cm.

3: Ryggprøve på tuppen av brystfinnen.

4: Ryggprøve under bakre ryggfinne.

5: Prøve nær halen. **Viktig at denne inneholder kjøtt og ikke bare sener.**

6: Mageprøve på tuppen av brystfinnen.

7: Mageprøve på basen til analfinnen.

8: Mageprøve øvre del av bukregion under brystfinne.

9: Mageprøve nedre del av bukregion over bukfinnen.

10: Rød muskelprøve mellom tverrsnittene 3/6 og 4/7.

Oversikt over de 10 prøvene er vist i bilde 1.

Hodet skal bevares. Når hodet kappes av er det viktig å kappe noe opp på hodet slik at hjernen og otolitter følger med.

Første finnestråle på ryggfinnen.

Appendix 1 Protocol sent to fishermen when guiding remotely, page 1.

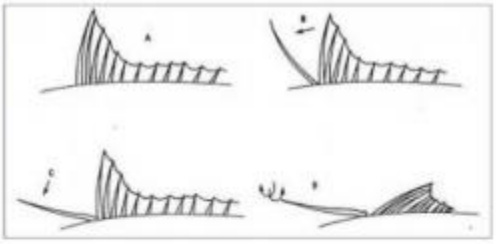

Genetikkprøve fra halen (1x1cm stor).

Det blir totalt 14 prøver, de 10 nummererte, innvoller, hodet, finnestråle og genetikkprøve fra halen. Det er viktig at prøvene er av en viss størrelse. Et godt referansepunkt er kjøttstykket som er vist på bilde 3, helst 400g+.

Dersom en representant fra havforskningsinstituttet ikke er til stede skal alle prøvene bli pakket i individuelle poser og merkes med deres prøvenummer (1-10), eller navn på prøve (f.eks innvoller/finnestråle). Prøvene skal deretter fryses og følgeskjema fylles ut. **Transport av prøver ordnes gjennom havforskningsinstituttet** som også vil dekke eventuelle kostnader iht. emballasje.

Appendix 2 Protocol sent to fishermen when guiding remotely, page 2.

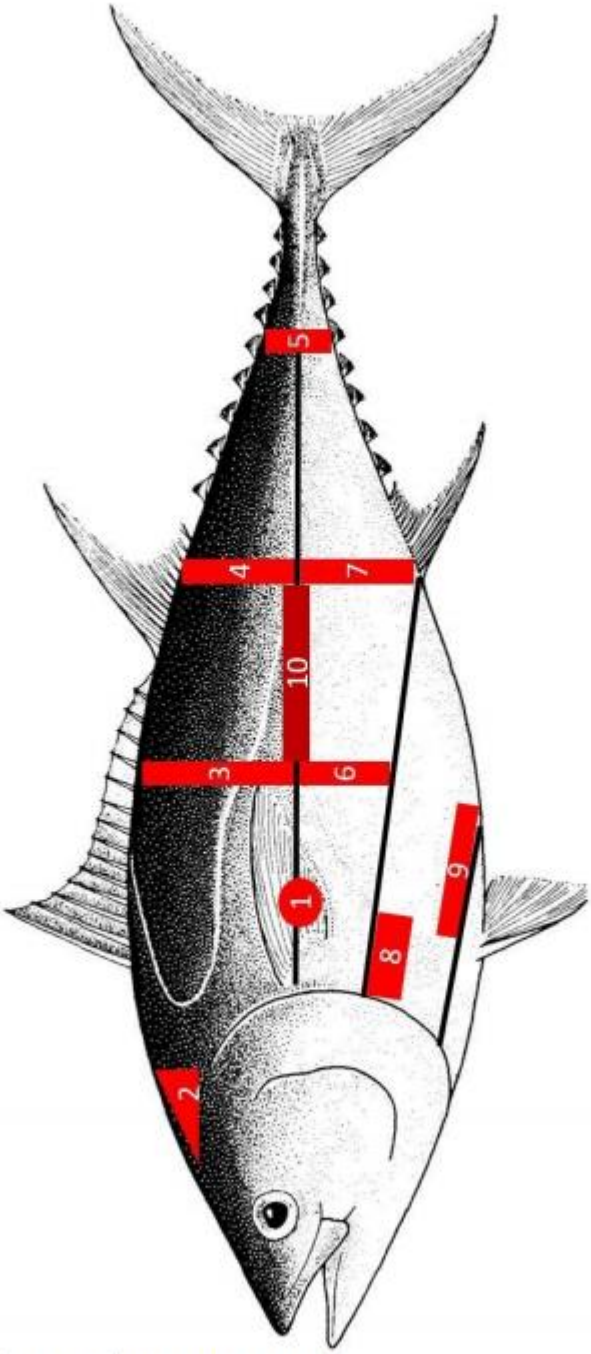

Bilde 1 Skjema over de 10 nummererte prøver.

Appendix 3 Protocol sent to fishermen when guiding remotely, page 3.

Bilde 2 Prøve 9 tatt, nederst på fisken, og prøve 8 påbegynt der skjellene er skrapt av.

Appendix 4 Protocol sent to fishermen when guiding remotely, page 4.

Bilde 3 Begge prøver 4 og 7 tatt, hvor en av dem ligger oppå fisken.

Bilde 4 Prøve 3, 6, 4, 7, 8 og 9 tatt.

Appendix 5 Protocol sent to fishermen when guiding remotely, page 5

```
par(mfrow = c(2,3), mar =c(4,3,3,2))
Box_Hg<-boxplot(Hg, main = "Hg")
Hist_Hg<-hist(Hg, main = "Hg")
Dot_Hg<-dotchart(Hg, main = "Hg")
Box_Hg_H<-boxplot(Hg~Cut,main="Hg")
qqnorm(Hg)
qqline(Hg)
```

Appendix 6 R-code used to produce diagnostic plots.

```
ST_Hg<-shapiro.test(Hg)
GT_Hg<-grubbs.test(Hg,type=10,opposite=FALSE,two.sided=FALSE)
FT_Hg<-fligner.test(Hg ~ Cut, Tuna_2)
```

Appendix 7 R-code used to perform outlier-tests.

```
lme_Fat<-lme(Fat~Cut,random=~+1|Fish_Nr,data=Tuna, na.action=na.omit)
lme_Fat2<-lme(Fat~Cut+Length,random=~+1|Fish_Nr,data=Tuna, na.action=na.omit)
plot(lme_Fat)
residuals_lme_Fat<-resid(lme_Fat)
qqnorm(residuals_lme_Fat)
qqline(residuals_lme_Fat)
AIC(lme_Fat)
plot(lme_Fat2)
residuals_lme_Fat2<-resid(lme_Fat2)
qqnorm(residuals_lme_Fat2)
qqline(residuals_lme_Fat2)
AIC(lme_Fat2)
```

Appendix 8 R-code used to produce the models and produce plots to compare them.

```
lme_Hg_mc<-glht(lme_Hg_s, linfct=mcp(Cut='Tukey'))
Resultat_Hg<-summary(lme_Hg_mc)
```

Appendix 9 R-code used to produce and plot multi factor comparison.

```
Linear mixed-effects model fit by REML
  Data: Tuna
       AIC       BIC   logLik
  -53.8329 -20.31062 40.91645

Random effects:
 Formula: ~+1 | Fish_Nr
        (Intercept)   Residual
StdDev:   0.2521976 0.09922472

Fixed effects:  Hg ~ Cut
                Value  Std.Error DF   t-value p-value
(Intercept) 0.3007224 0.08529584 71  3.525639   7e-04
Cut2        0.4217112 0.04951239 71  8.517286   0e+00
Cut3        0.5620049 0.04887006 71 11.499984   0e+00
Cut4        0.5267112 0.04951239 71 10.637967   0e+00
Cut5        0.5201867 0.04887006 71 10.644282   0e+00
Cut6        0.4788653 0.05462179 71  8.766928   0e+00
Cut7        0.4825888 0.05042653 71  9.570136   0e+00
Cut8        0.2361147 0.05201688 71  4.539194   0e+00
Cut9        0.2282775 0.05062604 71  4.509092   0e+00
Cut10       0.6285019 0.05595212 71 11.232853   0e+00
Cut17       0.5350183 0.07003683 71  7.639099   0e+00
Cut18       0.9792722 0.08207111 71 11.931997   0e+00
```

Appendix 10 R-printout of the model established for the distribution of total mercury with cut as predictor and individual fish as nested effect.

```
Linear mixed-effects model fit by REML
  Data: Tuna
       AIC      BIC    logLik
  46.30164 72.20371 -9.150821

Random effects:
 Formula: ~+1 | Fish_Nr
        (Intercept)  Residual
StdDev:   0.3676504 0.2008304

Fixed effects:  PCDD_F_dl_PCB_L ~ Cut
                 Value Std.Error DF    t-value p-value
(Intercept)  2.9837377 0.1710261 42  17.446091   0e+00
Cut2        -1.1651871 0.1159495 42 -10.049091   0e+00
Cut3        -1.8195784 0.1159495 42 -15.692852   0e+00
Cut4        -1.6760590 0.1159495 42 -14.455077   0e+00
Cut5        -1.7267962 0.1159495 42 -14.892657   0e+00
Cut6        -1.4108765 0.1447484 42  -9.747097   0e+00
Cut7        -1.6691493 0.1159495 42 -14.395484   0e+00
Cut8        -0.4307883 0.1222248 42  -3.524558   1e-03
Cut9        -0.4664492 0.1159495 42  -4.022865   2e-04
Cut10       -1.5626137 0.1311253 42 -11.916951   0e+00
Cut17       -1.5812133 0.1447484 42 -10.923876   0e+00
Cut18       -2.3520263 0.1686491 42 -13.946274   0e+00
```

Appendix 11 R-printout of the model established for the distribution of PCDD/F + dl-PCB (using log-transformed values) with cut as predictor and individual fish as nested effect.

Appendix 12 Determined fat concentrations (g/100g) for the control material (fish meal) for fat determination, compared to the ascertained mean at the IMR. Samples were run in nine batches, with two parallels of controls.

Date	Parallel	Fat g/100g
14/12-20	1	25
14/12-20	2	25
16/12-20	1	26
16/12-20	2	25
17/12-20	1	26
17/12-20	2	25
18/12-20	1	28[a]
18/12-20	2	26
06/01-21	1	25
06/01-21	2	25
07/01-21	1	25
07/01-21	2	25
08/01-21	1	25
08/01-21	2	25
08/01-21	1	25
08/01-21	2	26
13/01-21	1	26
13/01-21	2	26
	Mean	26
	2SD	1.4
	2RSD	5.6
IMR	Mean	25
	2SD	1.3

[a]Values outside 3SD.

Appendix 13 Determined element concentrations (mg/kg WW) for the certified reference material oyster tissue (OT) for multielement determination, compared to the ascertained mean at the IMR. Samples were run in four batches, with two parallels.

	Element concentration (mg/kg WW)												
Date	**20/11/2020**	**20/11/2020**	**23/11/2020**	**23/11/2020**	**26/01/2021**	**26/01/2021**	**15/03/2021**	**15/03/2021**				**IMR**	
Paralell	1	2	1	2	1	2	1	2	**Mean**	**2SD**	**2RSD**	**Mean**	**2SD**
V	0.54	0.55	0.54	0.53	0.56	0.54	0.60[a]	0.61[a]	0.56	0.060	11	0.54	0.050
Cr	0.40	0.35	0.39	0.34	0.38	0.38	0.40	0.52	0.40	0.11	28	0.38	0.15
Mn	17	17	17	17	17	17	18	19	17	1.3	7.3	17	1.4
Fe	189	190	189	186	189	186	203	203	192	14	7.3	188	16
Co	0.34	0.34	0.34	0.33	0.34	0.34	0.36	0.36	0.34	0.021	6.2	0.34	0.030
Ni	0.90	0.88	0.93	0.89	0.95	0.92	0.98	0.99	0.93	0.081	8.8	0.93	0.14
Cu	64	64	64	64	65	64	66	65	64	1.6	2.5	62	7.5
Zn	1393	1392	1376	1385	1400	1391	1353	1334	1378	46	3.3	1339	141
As	7.5	7.6	7.6	7.6	7.7	7.7	7.9	7.8	7.7	0.28	3.7	7.5	0.63
Se	2.1	2.0	2.0	2.0	2.1	2.1	2.1	2.1	2.1	0.089	4.4	2.1	0.22
Mo	0.19	0.17	0.19	0.18	0.19	0.18	0.19	0.19	0.19	0.015	8.2	0.18	0.020
Ag	0.55	0.56	0.56	0.60	0.59	0.60	0.59	0.60	0.58	0.042	7.2	0.59	0.060
Cd	2.5	2.5	2.5	2.5	2.5	2.5	2.6	2.5	2.5	0.052	2.1	2.5	0.21
Hg	0.030	0.030	0.030	0.030	0.030	0.030	0.030	0.030	0.030	0	0	0.030	0.010
Pb	0.31	0.31	0.31	0.31	0.31	0.31	0.29	0.28	0.30	0.024	7.8	0.30	0.030

[a]Values outside 2SD.

Appendix 14 Determined element concentrations (mg/kg WW) for the certified reference material lobster hepatopancreas (TORT) for multielement determination, compared to the ascertained mean at the IMR. Samples were run in four batches, with two parallels.

Element concentration (mg/kg WW)													
Date	**20/11/2020**	**20/11/2020**	**23/11/2020**	**23/11/2020**	**26/01/2021**	**26/01/2021**	**15/03/2021**	**15/03/2021**				**IMR**	
Parallel	1	2	1	2	1	2	1	2	**Mean**	**2SD**	**2RSD**	**Mean**	**2SD**
V	9.0	8.9	8.5	9.0	8.8	8.9	9.8	10[a]	9.1	1.0	11	8.9	0.88
Cr	1.9	1.8	1.8	1.8	1.9	1.8	2.0	2.1	1.9	0.22	12	1.9	0.43
Mn	14	14	13	14	13	13	15	15[a]	14	1.4	10	14	1.2
Fe	166	163	157	162	158	161	176[a]	178[a]	165	16	9.5	159	15
Co	1.0	1.0	0.98	1.0	1.0	1.1	1.1	1.1[a]	1.1	0.093	8.9	1.0	0.090
Ni	4.7	4.7	4.7	4.7	4.9	4.9	5.0	5.1	4.8	0.36	7.4	4.7	0.62
Cu	431	425	423	441	435	437	441	454	436	20	4.5	450	40
Zn	132	129	128	131	126	129	121	123	127	7.6	6.0	126	13
As	67	66	66	68	66	67	67	68	67	1.5	2.3	65	5.7
Se	11	11	11	11	10	11	10	10	11	0.37	3.5	11	1.1
Mo	3.6	3.5	3.5	3.6	3.5	3.5	3.7	3.7	3.6	0.20	5.6	3.6	0.32
Ag	2.7	3.0	2.4	2.3	2.3	2.3	2.5	2.3	2.5	0.50	20	2.8	2.6
Cd	42	41	41	42	40	40	39	40	41	1.6	4.0	41	4.0
Hg	0.27	0.27	0.25	0.26	0.27	0.26	0.26	0.26	0.26	0.014	5.4	0.27	0.040
Pb	0.21	0.20	0.20	0.21	0.20	0.20	0.18	0.17	0.20	0.028	14	0.20	0.030

[a]Values outside 2SD.

Appendix 15 Determined sum TEQ PCDD/F + non-ortho PCBs (pg/g), sum TEQ mono-ortho PCBs (pg/g), sum PCB6 (pg/g) and sum PBDE7 (ng/g) for the control material spiked freeze-dried salmon muscle for POPs determination, compared to the ascertained mean at the IMR. Samples were run in two batches, with one parallel.

Date	**18/01/2021**	**20/01/2021**				**IMR**	
Parallel	1	2	Mean	2SD	2RSD	Mean	2SD
SUM TEQ PCDD/F + n-o-PCB (pg/g)	35[a]	37[b]	36	2.8	7.9	43	2.5
SUM TEQ m-o-PCB (pg/g)	0.070	0.070	0.070	0	0	0.070	0.0030
SUM PCB6 (pg/g)	11985	11826	11906	225	1,9	11221	802
SUM PBDE7 (ng/g)	9.3	9.3	9.3	0.070	0.76	9.7	0.43

[a]Below 3SD
[b]Below 2SD

Appendix 16 Determined methylmercury concentrations (ng/g) for the certified reference materials lobster hepatopancreas (TORT) and tuna muscle (Tuna464) for methylmercury determination, compared to the ascertained mean at the IMR. Samples were run in two batches, with two parallels.

Date	**22/02-21**		**23/02-21**					**IMR**	
	1	2	1	2	Mean	2SD	2RSD	Mean	2SD
TORT	109[a]	147	133	134	131	32	24	130	18
Tuna 464	5527[b]	5589[b]	5586[b]	5604[c]	5577	68	1.2	5115	324

[a]Below 2SD
[b]Above 2SD
[c]Above3SD